FAKULTAT FÜR MEDIZIN

INSTITUT FÜR MEDIZINISCHE MIKROBIOLOGIE, IMMUNOLOGIE UND HYGIENE

DER TECHNISCHEN UNIVERSITÄT MÜNCHEN

Clinical multi-parameter purification of human central memory T cells for adoptive therapy

Vollständiger Abdruck der von der Fakultät für Medizin der Technischen Universität zur Erlangung des akademischen Grades eines Doktors der Naturwissenschaften genehmigten Dissertation

Jeannette Bet

Vorsitzender: Univ.-Prof. Dr. P. A. Knolle

Prüfer der Dissertation: 1. Univ.-Prof. Dr. D. Busch

                                 2. Univ.-Prof. Dr. M. Groll

Publications:

Bet, J. et al. *Direct ex vivo clinical-grade multi-parameter purification and characterization of human central memory T cells for adoptive therapy*
(manuscript in preparation)

Parts of this thesis were previously published:

Stemberger, C., Dreher, S., Tschulik, C., Piossek, C., **Bet, J**., Yamamoto, T. N., Schiemann, M., Neuenhahn, M., Martin, K., Schlapschy, M., Skerra, A., Schmidt, T., Edinger, M., Riddell, S. R., Germeroth, L., Busch, D. H. *Novel serial positive enrichment technology enables clinical multiparameter cell sorting.* PLoS One, 2012. **7**(4): p. e35798.[1]

Nauerth, M., Weissbrich, B., Knall, R., Franz, T., Dossinger, G**., Bet, J**., Paszkiewicz, P. J., Pfeifer, L., Bunse, M., Uckert, W., Holtappels, R., Gillert-Marien, D., Neuenhahn, M., Krackhardt, A., Reddehase, M. J., Riddell, S. R., Busch, D. H. (2013). "TCR-Ligand koff Rate Correlates with the Protective Capacity of Antigen-Specific CD8+ T Cells for Adoptive Transfer." Sci Transl Med **5**(192): 192ra187.[2]

Dossinger, G., Bunse, M., **Bet, J**., Albrecht, J., Paszkiewicz, P. J., Weissbrich, B., Schiedewitz, I., Henkel, L., Schiemann, M., Neuenhahn, M., Uckert, W., Busch, D. H. (2013). "MHC multimer-guided and cell culture-independent isolation of functional T cell receptors from single cells facilitates TCR identification for immunotherapy." PLoS One **8**(4): e61384.[3]

Contents

1. Summary

Background: Adoptive transfer of primary or genetically modified T cells is a promising treatment for malignant or chronic infectious diseases. Inefficient engraftment, limited persistence and protectivity of *in vitro* expanded cells often still impair therapeutic success. Different T cell subpopulations (for example central memory and effector memory) are not equally suitable for patient treatment, and optimal functionality and longevity of transferred cells are crucial for therapeutic efficacy. Recent studies indicate that antigen-specific central memory T cells are capable of giving rise to long-term persistent T cell responses and have an excellent safety profile. Therefore, this T cell subset seems to have clear advantages for adoptive immunotherapy. However, direct isolation of central memory T cells was so far hampered by the lack of clinical multi-parameter selection platforms.

Results: We developed a three-step serial magnetic selection procedure based on the fully reversible *Strep*tamer technology targeting $CD3^+$, $CD62L^+$ and $CD45RA^-$ central memory T cells. We established isolation of human central memory T cells in a closed system using equipment and consumables that have been previously approved for clinical use and present a GMP-compliant protocol to manufacture purified T cell products for the use in patients. We validated phenotype and function of purified subsets, which can then be used directly for adoptive transfer or further modified *in vitro*. We have further tested new tools for a faster purification of central memory T cells e.g. a column for the removal of reagents.

Conclusion: We demonstrate that central memory T cells can be purified to high purities and with high yields under GMP-compliant conditions using a fully reversible serial enrichment procedure. This procedure can in principle be adapted to select cell subsets based on any constellation of cell surface markers, and may provide a means of ensuring more defined T cell products for adoptive cellular therapy.

2. List of Abbreviations

AIDS	acquired immunodeficiency syndrome
APC	antigen presenting cells
ATMP	advanced therapeutic medicinal product
CAR	chimeric antigen receptor
CD	cluster of differentiation
CDR	complementarity determining region
CMV	cytomegalovirus
CTL	cytotoxic T lymphocyte
DC	dendritic cell
DLI	donor lymphocyte infusion
EBV	Epstein-Barr-virus
FACS	fluorescent activated cell sorting
GMP	good manufacturing practice
GvHD	graft-versus-host disease
HIV	human immunodeficiency virus
HLA	human leukocyte antigen
hr/hrs	hour/hours
IFNγ	interferon gamma
IL-2	interleukin-2
mAb	monoclonal antibody
MACS	magnetic-activated cell sorting
MHC	major histocompatibility complex
min	minute/minutes
nm	nanometer
PBL	peripheral blood lymphocyte
PBMC	peripheral blood mononucleated cell
PCR	polymerase chain reaction
PE	phycoerythrin
PI	propidium iodide
rpm	rounds per minute
ScFv	single-chain variable fragment
T_{CM}	central memory T cell

TCR	T cell receptor
T_E	effector T cell
T_{EM}	effector memory T cell
T_{EMRA}	effector memory CD45RA-positive T cell (terminally differentiated)
TIL	tumor-infiltrating lymphocyte
T_{REG}	regulatory T cell
T_{SCM}	memory stem cell (T cell)

Logical operators

| + | set union |
| ∩ | intersection / cut set |

3. Introduction

3.1 T cell-mediated immunity

T cells are part of the adaptive immune system. The highly specific recognition of a large spectrum of ligands encoded or expressed by different pathogens is a unique feature of adaptive immunity in contrast to innate immunity [4]. Another hallmark of adaptive immunity is the ability to generate a life-long immunologic memory through formation of memory B and T cells, which protect individuals upon clearance of infection or following vaccination [5, 6]. Both, the adaptive and innate branch of the immune system, cooperate in a complex network of interactions. The immunological role of T cells is multilayered and involves both effector and regulatory functions. T cells patrol tissues in search of infected or degenerated cells and in the optimal case destruct those cells or control the activity of other immune cells. The immune system has evolved side-by-side with pathogens, the cause of infections, and is therefore highly adapted to protect the host through various specialized mechanisms. The infusion of a patient with specific T cells has meanwhile developed into a very promising treatment for some virus infections. Similarly, a protective but less well understood role is assigned to T cells in the context of malignant diseases. Although certain subsets of T cells have been described that infiltrate the tumor microenvironment and support tumor growth, the exploitation of anti-tumor immunity through adoptive transfer of tumor-reactive effector T cells is regarded as a potentially curative therapy for some cancers. Some important parameters that determine persistence and functionality of infused T cells are believed to be cell-intrinsic features linked to the cell phenotype. Therefore, the efficacy of T cell-based therapies might be improved by understanding the differential role of T cell subsets and by developing strategies to efficiently purify well-defined cell populations.

3.1.1 Antigen-recognition and function of T cells

T and B lymphocytes- are equipped with specialized receptors capable of binding an enormous variety of ligands. The T and B lymphocyte antigen receptors are generated during their development by somatic recombination, a gene rearrangement process through which defined gene fragments are nearly randomly combined from different gene sets [7]. Thus, a broad repertoire of diverse immune receptors is produced.

T cell receptors (TCRs) are heterodimeric cell surface structures, usually consisting of membrane-anchored α and β subunits. The major histocompatibility complex (MHC) is capable to present short

peptide fragment (8-12 amino acids) derived from protein degradation. TCRs recognize peptide-MHC complexes as their ligand. Thereby, recognition of both the peptide fragment as well as the relevant MHC molecule is required for T cell activation, and is termed MHC restriction [8].

Two main groups of functionally distinct T cells are characterized by the class of MHC molecules that they recognize. **CD8$^+$** T cells usually recognize epitopes presented by MHC class I molecules, which are expressed in all tissues on all nucleated cells. **CD4$^+$** T cells recognize antigen in the context of MHC class II molecules, which are expressed in a more restricted manner by professional antigen presenting cells of the innate and adaptive immune system, namely dendritic cells (DCs), macrophages, and B cells. The structure and generation of peptide-MHC complexes is similar but not identical for the two classes of MHC. The most important difference is the origin of the presented peptide, which they display on the cell surface. Peptides presented by MHC molecules originate either from the cytosol (MHC class I) or from vesicles with content taken up from the extracellular space (MHC class II) [9]. Therefore, CD8$^+$ T cells mainly take over the role of inspecting the content of nucleated cells and thus detect foreign proteins of viruses and intracellular pathogens as well as mutated proteins in cancerous cells. However, exceptions from these strict presentation pathways have been reported. Under defined circumstances, presentation of extracellular antigens by MHC class I as well as MHC class II presentation of cytosolic antigen can play an essential role in generating a potent T cell response.

CD8$^+$ and CD4$^+$ molecules function as co-receptors of the TCR. By co-binding to the same MHC molecule as the respective TCR, they enhance T cell binding and signaling. Mature CD4$^+$ and CD8$^+$ T lymphocytes also differ in their effector functions. CD4$^+$ T cells, also termed T helper cells, control the activity and maintenance of other immune cells. They induce maturation and activation of B cells or innate immune cells, for example. However, some CD4$^+$ T cells with cytotoxic activity have also been reported [10]. A substantial fraction of CD8$^+$ cells on the other hand are predestined to become cytotoxic effectors capable of killing target cells upon activation [11] (see chapter 3.1.3 for a detailed description of T cell cytotoxicity).

3.1.2   T cell development

Like all blood cells, T lymphocytes arise from multipotent hematopoietic stem cells in the bone marrow. During their development, they undergo rigorous positive and negative selection events in the thymus. Selection of T cells is based on their respective TCR. This is essential both to ensure a repertoire of T cells capable of binding to self-MHC and delete potentially harmful cells that might attack healthy tissue. Roughly 95% of T cells do not withstand thymic selection. During positive selection, TCRs are screened for their capability to bind self-MHC within a defined affinity range. Those that do not bind sufficiently to self- MHC die by neglect [12]. Subsequent negative selection compels T cells that respond too strongly to self-MHC into apoptosis in order to delete potentially

autoreactive cells. After thymic selection, mature T lymphocytes become part of the lymphatic system and bloodstream as naïve T cells, which continually circulate through the lymphatic tissues in the search for foreign antigen. Their state is defined as naïve until activation through the first encounter with their cognate peptide-MHC complex.

At least two different signals are necessary to activate naive T cells. This process is called 'priming'. 'Signal one' is the binding of the peptide-MHC complex through the TCR. 'Signal two' is determined by the ligation of co-stimulatory molecules of the B7 protein family through co-stimulatory receptors of which CD28 is best characterized. Furthermore, secreted cytokines, often termed "signal three" are needed for the expansion phase of an immune response.

3.1.3   The course of a T cell-mediated immune response

The innate immune system is generally the first branch to respond to pathogen encounter resulting in activation of antigen presenting cells (APCs) which leads to initiation of the adaptive immune response. A typical T cell-mediated immune response can be subdivided into three consecutive phases: priming, expansion, and contraction. Initiation takes place when activated professional APCs provide the cognate TCR epitope plus co-stimulation to a naïve pathogen-specific cell (priming). With the support of secreted cytokines, rapid clonal expansion and differentiation into effector cells is initiated upon repetitive encounter with the respective antigen.

Driven by cytokines, activated T cells can give rise to thousands of daughter cell bearing identical pathogen-specific TCRs (expansion phase). The expanding clones together guarantee a large pool of effector cells, usually reaching a peak in cell numbers around 7-10 days after initial antigen encounter. Subsequently, many of these cells undergo apoptosis upon clearance of the infection, leaving only a small fraction of pathogen-specific long-living memory T cells (contraction phase). Clonal expansion and consecutive contraction are closely linked to differentiation into subsets with distinct function (chapter 3.1.5).

Once developed into effector cells, T cells respond to antigen without strict dependency on co-stimulatory signals just by triggering of the T cell receptors [13-15]. Activated $CD4^+$ T cells provide help to B cells for the differentiation into antibody producing plasma cells. $CD8^+$ T cells combat infected cells through formation of close contacts with their respective target cell [16, 17]. Effector proteins of $CD8^+$ T cells, which are released at the site of interaction with the target cell, are, for example, perforin and proteins of the granzyme family. Perforin multimerizes to form a lytic pore in the target cell membrane. Through these pores, protein degrading granzymes as well as ions and water can enter and ultimately lyse the target cell. Beyond that, other, perforin-independent mechanisms of target cell killing have been described: the induction of apoptosis upon binding of the receptor Fas-ligand (CD178) to the Fas molecule (CD95). Furthermore, a pathway of cell-mediated death distinct from Fas receptor-induced apoptosis is known to be activated by the antimicrobial protease granulysin

[18]. Besides these mechanisms, direct effector functions of cytokines, such as antiviral effects of interferons, have been described [19, 20]. CD8^{+} T cells play a particularly important role in the control of viral infections. However, not all viruses can enter and infect dendritic cells, the most specialized cells in priming of T cells directly. Therefore, dendritic cell mediated cross-priming ensures activation of virus-specific cytotoxic T cells by presentation of extracellular antigens through MHC class I. This mechanism is a requirement for the induction of cytotoxic immunity through all peptide-based vaccinations and plays a particularly important role in engaging tumor immunity against most tumors, some of which can impair dendritic cell function [21-23].

Taken together, the role of T cells is to patrol the tissues, to kill pathogen infected cells or cancer cells (CD8^{+}) upon activation, or they help to augment or dampen the activity of other components of the immune system in response to a specific antigen (CD4^{+}). T cells are essential for sustained protection, which gets altered during (therapeutic) suppression of the immune system or in some immune deficiencies. Patients suffering from the acquired immune deficiency syndrome (AIDS), which destroys CD4+ T cells, have a higher prevalence for some cancers, e. g. lung cancer [24]. Further, individuals without a functional T cell compartment because of a genetic disorder often suffer from severe bacterial, viral, or fungal infections [25]. Similarly, upon allogeneic hematopoietic stem cell transplantation, recovery of a functional T cell system can take many months and therefore infections or reactivation of latent chronic infections can cause severe disease [26-28]. In line with this, long term suppression of the immune system to avoid rejection of organ transplants is associated with an increase in cancer incidence, for example following kidney transplantation [29].

3.1.4   T cell subset differentiation

T cell differentiation is associated with changes in phenotype, metabolism, life-span, proliferative capacity, and function. How and when fate decisions are made and how subsets differentiate has been thoroughly investigated throughout the last decades. It has been shown that a single naïve T cell precursor is capable of giving rise to all antigen-experienced subsets, namely effector, central memory, and effector memory T cells [30, 31]. For the diversification of T cells out of naïve precursor T cells, different models have been suggested. According to the linear differentiation model, naïve T cells develop first into effector T cells, a subset of which then continue to develop into memory T cells. The model of progressive differentiation on the other hand describes a differentiation progressing from slowly proliferating memory subsets to rapidly proliferating subsets with decreased differentiation plasticity. Corresponding to the latter model, differentiation largely depends already on early signals, postulating that memory T cells might already be detectable during an immune response before the contraction phase [32, 33]. There is indeed evidence for the occurrence of memory T cells based on lineage markers as early as day 4 in infections of mice with *Listeria monocytogenes* [34]. Furthermore, T cells of the memory compartment represent an earlier stage of differentiation than their effector

counterparts. Presumably, central memory T cells (T_{CM}) are generated very early from naïve precursors during the course of an infection before the effector memory compartment is established [35]. Similarly, an early stage of differentiation for the memory compartment in contrast to the effector compartment has been stated, when patients with infections with persistent viruses were monitored [36]. Only recently some groups have shed light on the kinetics of differentiation on a single-cell level, providing strong evidence that naïve precursor cells can give rise to subsets that are associated with a high capacity for self-renewal validated by serial transplantation of donor-derived cells [37]. Central memory precursor cells, which arise early from naïve T cells followed by effector memory and effector precursors, uniquely reveal the capacity to differentiate into all but naïve subsets and are associated with a high capacity for self-renewal, which is verified by adoptive transfer of single cells and *in vivo* fate mapping of single cells [38, 39].

Recently, a multi-potent pool of memory stem cells (T_{SCM}) characterized by an even less differentiated phenotype among memory cells and increased proliferative capacity and survival has been described in mice and later in humans. Human T cells with a T_{SCM} phenotype were found within a T cell compartment which is characteristic for naïve T cells but have phenotypic and functional properties distinct from those of naïve or memory T cells like high expression of CD95, increased proliferation capacity, and more efficient reconstitution of immunodeficient hosts [40-42]. Furthermore, in a pre-clinical study in a humanized mouse model, T_{SCM} mediated superior anti-tumor responses [41]. Compared with other memory T cell subsets, T_{SCM} conferred superior immune responses against tumors and better proliferative capacity upon adoptive transfer in mice [42]. Like naïve T cells, T_{SCM} were found to be capable of differentiating into T_{CM}, $T_{EM,}$ and T_E subsets as well as maintaining themselves by homeostatic proliferation. Although T_{SCM} were further hypothesized to be responsible for the maintenance of the memory T cell pool based on these findings, it remains unverified whether this memory subset arises in T cell responses to every antigen, like other memory subets. However, serial adoptive transfer experiments on the single-cell level and subsequent re-expansion of single T_{CM}-derived T cells has led to the revelation of true stemness for an epitope-specific immune response in the T_{CM} compartment [43]. Therefore repetitive transfusion of single cells of the T_{CM} pool over three generations of mice was conducted revealing that the T_{CM} subset possesses essential traits of regular tissue stem cells. These findings challenge the suggested role of the T_{SCM} subset as a source for sustaining long-term memory. These findings have tremendous impact on the development of new therapies, especially adoptive T cell therapy, through identification of most suitable candidates for adoptive transfer to provide a durable and functionally diverse immune response. The functional attributes associated with stem cell-like memory T cells, high proliferative capacity and continuous self-renewal, can be most suitable for the adoptive transfer of low numbers of T cells with long-term *in vivo* survival. Thus, re-transfers of short-term effector cells could be avoided [44].

Particularly naïve and central memory T cells, which reveal highest capacity of diversification, have been thoroughly investigated for their *in vivo* behavior upon adoptive transfer. Both subsets have been

shown to possess the ability to fully reconstitute the whole subset diversity of the T cell compartment [45, 46].

Along this line, the *in vivo* survival of T_{CM}s upon adoptive transfer has been investigated and proven to be superior to the one of T_{EM}s (and T_{ES}) in animal models and patients, and has proven more successful for T_{CM} [47-50].

Memory T cells change the expression of many surface molecules as they differentiate from naïve T cells. Some of these surface markers are expressed differentially between the two memory subsets T_{CM} and T_{EM}. Changes occur mainly in the surface molecules L-selectin (CD62L) and CD45. While naïve T cells exclusively express the RA splice variant of the tyrosine phosphatase CD45 (CD45RA), memory cells are mostly found to express the variant CD45RO. Molecules of the CD45 family act by modulating signaling in T cells. Further, T_{CM}s can be phenotypically segregated from T_{EM} subsets by the characteristic expression of the markers CCR7 and CD62L (lymph node homing receptor). The combination of both characteristics allows discrimination of short-lived effector T cells from naïve, effector memory and central memory T cells [51, 52]. Thus, the surface molecules CD45RO and CCR7 (or CD62L) together with a T cell marker (either CD3 or CD4 and CD8) can strictly segregate T_{CM} from all other subsets.

The abovementioned findings argue that T_{CM} can be of superior quality for adoptive T cell therapy (see chapter 3.2.4) [32]. **Fig. 1.1** illustrates chosen aspects of T cell differentiation with respect to their grade of differentiation and phenotype. It is obvious that precisely defined, functional subsets can only be characterized by a combination of at least two markers.
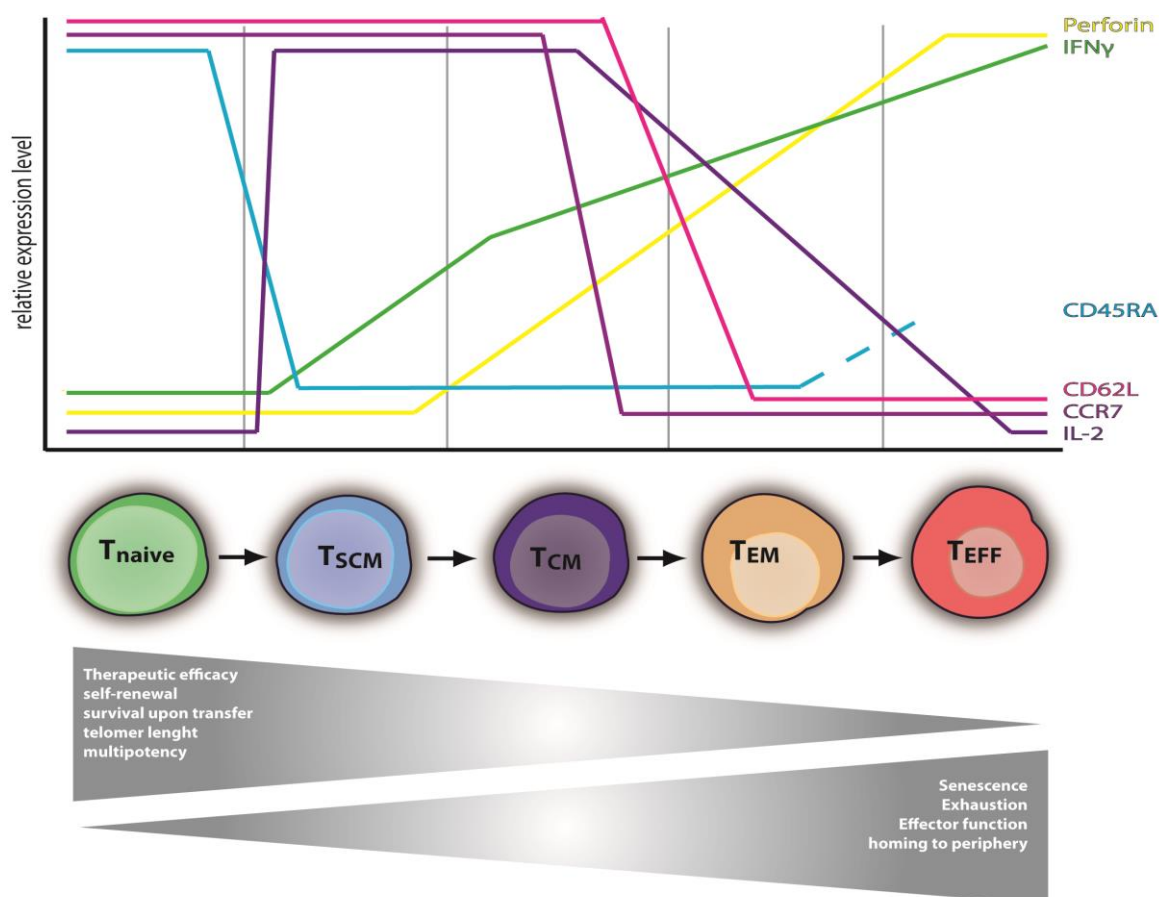
Fig. 1.1: Changes in phenotype and characteristics during T cell differentiation.

The relative expression levels of classical effector proteins (perforin and IFNγ), homing receptors (CCR7 and CD62L), the signaling molecule CD45RA and Interleukin-2 are displayed dependent on the grade of T cell differentiation [36]. The progressive differentiation model is represented in the order of T cell subsets. With regard to the characteristics of less differentiated T cell subsets, aspects like self-renewal and multipotency are believed to be associated with higher therapeutic efficacy.

3.1.5 Distinct immunological roles of T cell subpopulations

As previously described, we distinguish at least between naïve, effector, effector memory, and central memory T cell subsets, all of which can be associated with distinct activation requirements and a characteristic phenotype composed of a combination of cell surface markers suggesting a division of labor between the subsets. Compared to naïve T cells, memory subsets are maintained at higher frequencies, have been shown to respond to a specific antigen or epitope without the requirement for co-stimulation and interact more efficiently with dendritic cells in *in vitro* cultures [52-55].

Effector T cells are associated with one or multiple immediate effector functions and a relatively short lifespan in the absence of specific antigen. Survival of these cells is dependent on the availability of antigen-dependent signals and cytokines [56]. Memory subsets are long-lived and are maintained mainly by cytokines. Central memory T cells can be distinguished from effector memory T cells as follows: CD45RO+ CD62L+ T cells (all T cells are CD3+) are referred to as central memory T cells,

whereas CD45R0$^+$ CD62L$^-$ CD3$^+$ cells are defined as effector memory T cells. These subpopulations can be found in the CD4$^+$ and in the CD8$^+$ T cell pool alike. Based on differential expression of the homing receptor CD62L, there are two subpopulations of long-lived T cells, which can survive long-term without antigen re-encounter: **effector memory T cells (CD62L low)** on the one hand respond to an eventual antigen re-encounter very rapidly without the need for prior clonal expansion or differentiation and preferentially reside in non-lymphoid "peripheral" tissues. **Central memory T cells (CD62L high)** preferentially migrate to lymphoid organs such as lymph nodes and spleen, where they search for their specific antigen. In particular, central memory T cells proliferate vigorously upon antigen re-encounter and upon further differentiation provide a rapid source for newly generated effector and memory T cell subsets.

The contribution of effector memory and central memory T cells in long-lasting protective immunity may differ depending on the pathogen. For example, it has been reported that long-lasting protection against the fast-replicating intracellular pathogen *Listeria monocytogenes (L.m.)* strongly depends on the presence of antigen-specific effector memory T cells at the time point of infection; recruitment of newly generated effector cells from central memory T cells seems to take too long. Nevertheless, it has been observed that robust recall responses could be obtained originating from previously induced *L.m.*-specific central memory T cells, suggesting that this T cell compartment serves as a source for robust recall expansion providing large numbers of armed effector cells [48]. Thus, it is assumed that effector memory T cells are crucial for the control of fast-replicating pathogens. On the other hand, persisting protection against slowly-replicating pathogens like Cytomegalovirus (CMV) can be reconstituted by adoptive transfer of central memory derived T cells in various animal models. In a study in non-human primates, antigen-specific CD8+ effector T cell clones derived from isolated CMV-specific T$_{EM}$ or T$_{CM}$ subsets were cultured for 8 weeks and adoptively transferred. While T$_{EM}$-derived clones survived for only a short duration, failed to home to lymphoid organs, and did not reacquire phenotypic characteristics of memory T cells, T$_{CM}$-derived clones persisted long-term after transfer, migrated to niches of T cell memory, reacquired their respective phenotypic properties, and responded to antigen challenge [47].

3.1.6   The role of T cells in controlling malignant diseases

Adaptive cellular immunity is a potent effector arm of the immune system, which is also able to combat cancer cells [57]. Three mechanisms collectively termed immunoediting have been described that mark the interaction -that is control and shaping of malignant cells- between T cell immunity and tumor growth: (1) Elimination: immunosurveillance suppresses tumor outgrowth. (2) Equilibrium: control of tumor cell mass by immune cells. (3) Escape: outgrowth of a selected part as a result of co-evolution between immune system and tumor development [58].

Direct evidence of the protective role of T cells towards tumors was derived from animal experiments. Tumors in immunodeficient (lacking T cells) and wild-type mice were chemically induced and the presence or absence of T cells was found to be critical for tumor outgrowth after induction. A publication in 1964 reported already that the transfer of lymphocytes could inhibit outgrowth of a chemically induced sarcoma in the rat [59].

Evidence for immunoediting was conclusively conducted when tumors from immunodeficient mice were found to be more immunogenic compared to tumors outgrown in wild-type mice [60, 61]. Furthermore, in immunodeficient mice, some malignancies like carcinogen-induced sarcomas, occurred faster and with an increased incidence with respect to wildtype mice with a normal immune system [62]. These findings provide direct evidence for the shaping of tumor immunogenicity under the pressure of the immune system. Tumor growth in an immunocompetent individual can proceed very slowly over decades in humans resulting in an expanding tumor with reduced immunogenicity and/or the ability to escape or suppress the immune system. Higher cancer incidences, e.g. lung cancer, are also associated with the occurrence of acquired immunodeficiency (AIDS) in patients [24]. Co-localization of T lymphocytes and tumor cells and infiltration of tumor sites by lymphocytes provide more insights into the role of T cells in malignant diseases: among cancer patients, clinical prognoses often are significantly better when tumor-associated lymphocytes occur within the tumor, so-called tumor-infiltrating lymphocytes (TILs). TILs have become clinically relevant prognostic markers in many cancers including colorectal cancer, gastric cancer, urothelial carcinoma, ovarian cancer and breast cancer. Not all tumor-associated immune cells correlate with a positive prognosis though and a growing number of immune escape mechanisms have been described, for example the recruitment of immune suppressor cells to the tumor site, an immune-inhibiting tumor microenvironment or other mechanisms that lead to either accumulation of immune cells associated with a negative prognosis for patients or the escape from being recognized by beneficial immune cells. Remarkably, factors like CD8+ T cell frequency, T_{REG} phenotype and ratio between subsets of lymphocyte determine in several samples over good or poor prognosis. Some TIL compositions of cell types might be associated with suppression of micrometastasis in patients [63-68]. Once again, different roles are attributed to subsets of T lymphocytes and ongoing research is producing more insights into their functional interaction.

3.2 Adoptive T cell therapy

The far-reaching immunologic function of T cells can be transferred from one individual to another by a strategy termed 'adoptive T cell transfer' which harnesses the regenerative potential, protective re-expansion and effector cell differentiation of T cells. T cells isolated from the patient can be expanded and/or manipulated *in vitro* and re-infused into the patient. This strategy is termed autologous transfer of T cells as opposed to the allogeneic approaches, where the T cell donor is distinct from the patient. Adoptive therapy is a form of immune therapy, which is curably applied to treat chronic diseases like some viral infections and certain cancers (transfer of cytotoxic T cells) [69] as well as Graft-versus-host disease (GvHD) (transfer of immunosuppressive T_{REGS}) [70, 71]. Adoptive T cell therapy has been explored in clinical trials for over two decades now. The following section will cover early developments in the field of adoptive T cell therapy, selected clinical trials using various antigen-specific T cells as well as giving an overview on further developments and demands including the composition of such T cell products for therapeutic applications and mechanisms to increase safety.

3.2.1 Early developments in adoptive cellular therapy

3.2.1.1 *Donor lymphocyte infusion*

The first cornerstone in adoptive T cell therapy has been laid even before the existence of T cells was discovered, with the first bone marrow transplantation following sublethal whole body irradiation in 1959: three grafts from their respective identical twins where transplanted to patients suffering from leukemia. The grafts were transplanted from the patients' respective twin donors to the patients as a procedure designed to heal the leukemia which resulted in the remission of the leukemia for up to 6 months [72]. Unfortunately, the leukemia relapsed in all patients. A different approach consisting in the transfer of stem cells between HLA identical individuals that was initially designed to reconstitute the patient's immune cells after intense chemoradiotherapy resulted in high success rates as a treatment for hematological malignancies [73]. Up to the present, although it is associated with many possible complications, the described procedure termed allogeneic hematopoietic stem cell transplantation (HSCT) is the most commonly applied form of adoptive immunotherapy and is used as a standard treatment for hematological malignancies. T lymphocytes, which naturally occurred as part of the graft and which were therefore transplanted along with the graft, could later be identified as the responsible element mediating an anti-tumor effect in patients and the term graft-versus-leukemia effect (GvL effect) was coined describing this effect.

Nonetheless, this remarkable anti-leukemic effect is just one side of a two-faced medal. On the downside, severe cases of graft-versus-host disease (GvHD) occurred, a T cell-mediated allo-reactive

effect found in form of pathology in skin, gut, liver, lung and bone marrow. Analysis of leukemia relapse rates showed a 2.5 times lower incidence of relapse in allogeneic-marrow recipients with GvHD than in recipients without it stressing the association of both the GvL and the GvHD effect [74]. The *in vitro* depletion of T cells from the stem cell graft prior to transplantation has been tried with success to increase safety by reducing the risk of GvHD for non-autologous settings [72]. Comparison of patients who received transplants with or without prior T cell depletion again showed a higher risk of tumor recurrence in the T-cell depleted group. [75]. In a GvHD mouse model, Chen et al. succeeded in identifying naïve T cells as the mainly responsible subset for GvHD. Thus, dissection of GvL from GvHD could potentially be accomplished by depletion of the naïve subset [76]. Taken together, infusion of T cells along with the stem cell graft increases the anti-tumor effect drastically and has meanwhile become standard in allogeneic settings where donor and patient are distinct despite the risk of severe GvHD. For this form of treatment, T lymphocytes are obtained from the stem cell donor. The procedure is termed donor lymphocyte infusion (DLI) and can be seen as an early form of adoptive T cell therapy [77]. Thus, transplantation of donor T cells along with an allogeneic hematopoietic stem cell graft provided clinical proof that donor-derived immune cells can respond to host tumor cells after bone marrow transplantation in leukemia patients. Further investigations revealed that this effect is mainly T cell-mediated and T cells isolated from transplanted patients were shown to have tumor-specific activity. Further investigation revealed an important role for minor histocompatibility antigens as targets in some settings responsible for GvL which is a milestone in beginning to dissect GvL from GvHD [78].

3.2.1.2 *Tumor-infiltrating lymphocytes*

A breakthrough in adoptive cellular therapy (ACT) was made when Rosenberg et al. showed in 1986 that infusion of naturally occurring tumor-infiltrating lymphocytes (TILs) induced tumor remission in a remarkable fraction of mice, a result that could so far not be achieved by transfer of cultured lymphocytes [79]. Soon, the first T cells with known specificity for tumor-associated antigens (TAAs) from tumor infiltrates could be isolated. In that way, tumor infiltrates were harnessed as a source for T lymphocytes that are specific for tumor antigens and were therefore recruited to the tumor site.

Subsequently, TIL therapy was combined with administration of high doses of intravenous IL-2 [80] and innovative lymphodepleting regimens; a strategy, which has been proven successful in about 50% of melanoma patients enrolled in a study in 2002 [81, 82]. Especially lymphodepleting preconditioning of recipients showed improved clinical effects presumably in consequence of depletion of immunosuppressive regulatory T cells or other subsets possibly competing with donor cells for cytokines and antigen-presenting cells [83, 84]. It is still unclear whether TAA-specific T cells, which as auto-antigens also underlie tolerance providing mechanisms, contribute to the tumor protective capacity assigned to TILs. In addition, TILs often show signs of exhaustion such as limited

functionality, self-renewal and proliferation due to chronic antigen exposure [85]. However, clinical results were not always reproducible and highly diverse between studies [86, 87].

Consequently, attempts to transfer TILs with a defined anti-tumor specificity were conducted by stimulation of TILs with antigens obtained from tumor biopsies. Cells were co-cultivated with tumor cells to selectively grow out tumor-specific cells from the cell culture. Surprisingly, those cultured TILs could not yield better clinical results so far [88].

3.2.1.3 Transfer of antigen-specific T cells

For the treatment of chronic viral infections, adoptive transfer of T cells with defined antigen specificity proved very effective. In 1992, for the first time, cytomegalovirus (CMV)-specific CD8^{+} T cell clones were successfully transferred to patients upon *in vitro* propagation. All patients had previously undergone allogeneic bone marrow transplantation and suffered from an increased risk of CMV reactivation, a life-threatening disease in immunocompromised people. Infusion of donor-derived CMV-specific CTLs reconstituted protective immunity against CMV reactivation [89]. Other studies using CTLs specific for antigens of EBV [90] and HIV [91] have provided further evidence for the efficacy, persistence and safety of adoptively transferred virus-specific T cell clones. Newer data indicate that low numbers of transferred T cells can already be sufficient to confer protective immunity towards CMV in recipients of allogeneic stem cell transplantation [92, 93]. For the last two decades, adoptive transfer of antigen-specific T cells has yielded promising results for chronic viral infections and some tumors, especially when the number of host cells competing for cytokines was reduced by lymphodepletion [81]

For the treatment of malignant diseases, advances in adoptive T cell therapy are needed. Since our knowledge on tumor-associated antigens (TAAs) has vastly improved, efforts were made to expand and transfer cells with known antigen specificity. Nonetheless, it is still difficult to isolate high-avidity tumor-specific T cells and gain access to suitable TCRs directed against these self-antigens [94]. Self-antigen specific T cells with high avidity are usually deleted in the thymus by negative selection (central tolerance). Because of the sometimes extremely low frequencies or complete absence of tumor-specific T lymphocytes in the patients and low *in vivo* response rates of such cells [95], it was sought to generate T cells of a defined specificity by genetic redirection of specificity. There are two principle strategies to impose a defined specificity on T cells: transgenic TCRs or synthetic CARs. Both strategies rely on the discovery of suitable target antigens.

A prerequisite of transgenic TCRs is the isolation of cDNA sequences for TCR α and β chains for the transduction of T cells with viral vectors. TCR gene sequences are usually obtained from tumor-reactive T cells e.g. upon isolation from tumor-infiltrating lymphocytes. Novel, MHC multimer-based single cell sorting and single cell PCR amplification enables the isolation of TCR sequences directly

ex vivo, e.g. from peripheral blood without the need for tissue biopsies or long expansion procedures *in vitro* [3].

The design and development of anti-tumor CARs requires the gene sequence of a single chain variable fragment (scFv) derived from a tumor antigen-specific antibody. Thus, the discovery of suitable tumor antigens is a prerequisite for obtaining TCRs or CARs of defined tumor-specificity for T cell therapies.

As a source for T cells, the reasonable approach was to use peripheral blood mononucleated cells (PBMCs) containing all functional subsets of T cells in contrast to using surgically removed tumor infiltrates containing partly functionally impaired T cells. Furthermore, not all tumors have lymphocyte infiltrates and are therefore not accessible by TIL-based approaches.

3.2.2   Genetically re-directed T cells for adoptive immunotherapy

The first report of genetically engineered T cells adoptively transferred to patients with metastatic melanoma originates from Morgan et al. in 2006: a transgene encoding the TCR which recognizes the melanoma-specific tumor antigen MART-1 was retrovirally introduced into peripheral blood lymphocytes (PBLs) that were expanded and adoptively transferred to patients with metastatic melanoma. 2 of 15 patients responded by complete tumor remission. Furthermore, adoptively transferred cells could be detected up to 20 months post transfer [96]. This was the first evidence in patients that tumor recognition can be established *de novo* in lymphocytes via introduction of a transgenic TCR. Transgenic TCRs are generally expressed in the same cell compartment as native TCRs. Therefore, mispairing of endogenous and transgenic TCR chains can occur, creating unpredictable and potentially toxic specificities [97]. Various strategies have been developed to overcome this problem [98]. An inherent limitation of TCR gene therapy is the HLA-restricted nature of antigen recognition by TCRs. TCRs recognize antigen in the context of a human leukocyte antigen (HLA) molecule, which is the human analogue to the MHC molecule. Often, through genomic instability, tumors escape the immune system by acquisition of escape mechanisms such as manipulation of antigen processing and antigen presentation to T cells or down-regulation of HLA class I altogether [99]. In such settings it could be beneficial to target tumor stromal cells, which are vital for sustaining tumor growth. Stromal cells are also less prone to immune escape because of their higher genetic stability compared with tumor cells. In addition, stromal cells are known to cross-present exogenous antigens on MHC class I molecules, a process which allows targeting tumor epitopes on stromal cells with re-directed T cells [21, 100]. Modifications in vectors and amino acid sequence enable the expression of TCRs in T cells at high levels. So far, a number of clinical trials have demonstrated the efficacy of TCR transgenes in adoptive T cell transfer. Two recent studies treating patients with metastatic melanoma or synovial cell carcinoma yielded clinical response rates of 28% and 79% [101-103].

3.2.3   Chimeric antigen receptor-engineered T cells

Another strategy to redirect tumor or other specificity of T cells is independent of HLA presentation: chimeric antigen receptors (CARs). The relative resistance of CARs towards a number of immune evasion mechanisms involving peptide processing and HLA expression renders them an attractive alternative to transgenic TCRs. CARs are artificial one-peptide chain antigen receptors usually containing intracellular and trans-membrane domains derived from TCRs (CD3ζ domain) and the antigen-specific fragment of an immunoglobulin (single-chain variable fragment). Thus, the CAR molecule combines HLA-independent antigen recognition (taken from immunoglobulins) with intrinsic effector functions and signaling of T cells in a single fusion protein [104]. As a result, CAR-transduced T cells are equipped with an antigen-specificity in addition to their native TCR. Structurally, CARs are built with a Fc hinge region as spacer domain between single-chain variable fragment (ScFv) and transmembrane domain, thus enabling increased expression levels through dimerization. According to a general classification, first generation CARs carry no additional co-stimulatory molecules in the intracellular signaling domain. Second generation CARs have either CD28, CD27, 41BB or OX40 as co-stimulatory domains and third generation CARs carry a combination of at least two co-stimulatory domains. It has been demonstrated that insertion of the co-stimulatory domain CD28 [105] or CD27 [106] in the CAR molecule results in increased persistence and anti- tumor effect of transferred T cells. For 41BB and CD80, it has been shown that constitutive expression of these co-stimulatory ligands on tumor-infiltrating T cells can lead to enhanced anti-tumor activity [107]. Unlike engineered TCRs, CARs are artificial molecules and potentially confer immunogenicity. Advances in design will be necessary to completely eliminate this problem. Second and third generation CARs with increased co-stimulation have yielded dramatic impact in the field of adoptive therapy of patients with hematologic malignancies. [108, 109]. In these trials, T cells were engineered to express CARs specific for the lineage-specific antigens CD19 or CD20, both of which are overexpressed in the respective B cell malignant diseases that patients suffered from. In other studies, CARs directed against the CE7R and GD2, both tumor antigens of neuroblastoma, have been tested demonstrating clinical responses in some cases [110, 111].

It is now more and more accepted that effective clinical response rates are associated with *in vivo* engraftment and persistence of transferred T cells as well as migration to the respective tumor sites [112, 113]. It is therefore of particular interest to conduct trials comparing the *in vivo* persistence of transferred cells. Functional subsets of the T cell compartment, however, are not equally suitable to achieve the desired *in vivo* persistence and migratory capacity. Following the discovery of diverse differentiation properties of T cell subsets, it is now appreciated that some subsets are superior in terms of their capacity to persist and reconstitute functional immunity upon transfer.
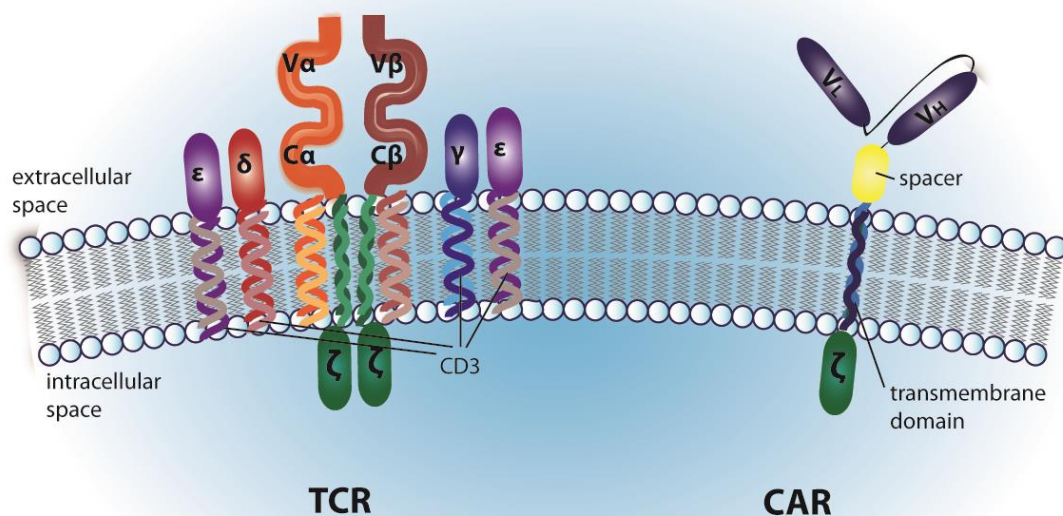
Fig. 1.2: The structure and organization of T cell receptor (TCR) and chimeric antigen receptor (CAR).

Organization of extracellular, transmembrane and intracellular domains of TCR/CD3 complex and CAR. TCRs are heterodimers which are associated with the extra- and intracellular subunits of CD3 (γ-ζ). ζ is a signaling domain which is also used in chimeric antigen receptor for the same purpose. In contrast, V_H and V_L are antibody-derived. Therefore, CARs can recognize antigenic structures in their native form while TCRs recognize small peptide fragments presented in a binding groove of major histocompatibility (MHC) molecules.

3.2.4 Finding the ideal T cells for adoptive therapy

Application of lymphodepleting regimens along with infusion of T cells has demonstrated increased persistence of T cells and as a consequence increased antitumor efficacy. Nevertheless, clinical results often lack efficacy and persistence, even when very high numbers of T cells are administered to patients. Retrospective analysis correlated in vivo persistence with therapeutic outcome. One obvious parameter is the lack of uniformity in given T cell products, which, in most trials, underlie large variation [114]. Therefore, it appears consequent to isolate T cells of a defined specificity **and** with optimal characteristics regarding longevity and safety. One strategy is the selection of an ideal subset of T cells with the intrinsic capacity for long-term survival upon transfer along with the ability to give rise to potent effector responses and to infiltrate sites of infection or tumor tissue. However, the ideal subset for successful and sustained persistence of adoptively transferred T cells is still controversially discussed, and may depend on the clinical indication. As described in detail in chapter 3.1.6, the less differentiated central memory T cell subset, characterized by longer telomeres, the general capacity for self-renewal and differentiation, expression of homing receptors and secretion of growth factors,

revealed better persistence both in non-human primates and in patients [47, 49, 115]. In recent CAR-engineered T cell studies, retrospective analysis for the T_{CM} content positively correlates with objective clinical responses. Since started in 2005, the trend of selecting a subset of T cells for adoptive transfer has been increasingly adopted [116]. It has been clearly shown that T cells transferred at early stages of differentiation confer superior anti-tumor efficacy. In mouse models, the anti-tumor response of naïve T cells could exceed the response of T_{CM} [45, 50, 116, 117]. In contrast to T_{CM}s, naïve T cells are of unknown and potentially harmful specificity and are therefore believed to be the main mediators for graft-versus-host toxicities in allogeneic transplantation [118]. A means of ensuring a pre-defined T cell specificity is the selection of virus-specific T cell clones for introduction of a transgene, thus generating bi-specific cells of defined specificity [119]. It has been shown in a clinical trial applying CAR-transduced T cells targeting neuroblastoma that, indeed, bi-specific T cells persisted longer than CAR-specific T cell clones lacking virus specificity and therefore have a shortage of co-stimulation through engagement of their natural epitope [111]. Thus, it seems relevant to this field to develop a selection protocol for isolation of long-lived antigen-experienced memory T cells.

Most recent attempts in ACT aim at further dissecting the role of CD8$^+$ and CD4$^+$ T cells in adoptive transfer settings to find the optimal composition of a functional cell product.

It could be demonstrated that purified CD8+ TILs were in principle sufficient to mediate tumor regression [69]. However, when infusion of CD8+ enriched TILs was compared to infusion of unselected TILs, the CD8+ enriched T cells were not more potent therapeutically [120]. Furthermore, it has been demonstrated that in some cases CD8$^+$ cytotoxic T cells even rely on CD4$^+$ T cell help to infiltrate virus-infected tissue [121]. In contrast, complete remission in a melanoma patient has been observed upon transfer of tumor-specific CD4$^+$ T cell clones alone [122]. The selection of suitable CD4$^+$ subsets however might depend on further distinction of subsets of the CD4$^+$ compartment since not only different subsets of T helper cells but also regulatory T cells, which might dampen an immune response, constitute the CD4$^+$ compartment. The first pre-clinical studies attempting to pre-select a defined composition of naïve and memory CD4$^+$ and CD8$^+$ T cells and examine their *in vivo* behavior are currently conducted. Preliminary data on persistence and therapeutic efficacy of genetically modified tumor-reactive human T cells in immunodeficient Nod/Scid/gc−/− mice with engrafted tumors confirmed a distinct behavior and efficacy of defined compositions of subsets of CD4+ and CD8+ T cells. Lowest numbers of transferred CD19-CAR T cells were capable of eradicating tumors in these mice [123].

The definition of an ideal T cell subset for adoptive therapy may therefore be extended to not only one subset of cytotoxic T cells but to a combination of subsets of both functional T cell types (CD4$^+$ and CD8$^+$).

3.3   Purification of T cell populations

3.3.1   Methods for human T cell isolation

T lymphocytes can be visualized and isolated by a number of methods. The common base of visualization and separation methods is the labeling of cell-surface proteins (antigens) with specific probes, ultimately distinguishing labeled from unlabeled cells.

Components of the cell surface to be labeled are on the one hand phenotypic markers characterizing functional subsets of T cells e.g. CD4; CD8, adhesion molecules, αβTCR etc. and on the other hand the respective TCR for its specificity. Moreover, the number of parameters that can be addressed by cell sorting is constantly expanding and includes not just surface antigens but also intracellular proteins, DNA, cell viability just to name a few.

The separation of cells out of a heterogeneous mixture of cells or directly from the blood is referred to as cell sorting. In general, there are two major technologies available for cell sorting: the fluorescence activated cell sorting (FACS) where light emission by fluorescent dyes is detected and magnetic-activated cell sorting (MACS), which harnesses the behavior of magnetic and para-magnetic particles in a magnetic field [124]. Magnetic particles have to be specifically bound to the cell surface and magnetically labeled cells can be retained in a magnetic field either directly using tubes, bags or flasks or indirectly using magnetic columns, depending on the nature and size of magnetic particles. Sorting by FACS however requires a more sophisticated fluidics and electronic appliance for the purpose of charging droplets –containing the scattered single cells- to be charged and electrostatically deflected from a stream.

Independent of the technology, there are two general strategies for isolation of a desired target population: target cells can be isolated either by positive or by negative enrichment. Positive enrichment is the selection of labeled cells for downstream applications, whereas in negative enrichment unwanted cells are labeled leaving the unlabeled target cells behind for further use. Each strategy is associated with specific advantages. Positive enrichment yields better purities of the target population and can, therefore, be applied even for very small target populations. Negatively enriched cells are obtained as so-called untouched cells without the risk for activation or damaging of the target cells but not all target populations can be accessed by negative enrichment [125].

For FACS and MACS, the enrichment strategy can be either positive or negative depending on the availability of reagents. For negative enrichment, also non-magnetic fluorescent-independent strategies have been developed e.g. unwanted cells are cross-linked to red blood cells, and subsequently separated from the target cells by density gradient centrifugation [126, 127]. All these technologies are based on the principle of specific antigen-binding mediated either by monoclonal antibodies specific for phonotypic markers or by particular TCR ligands, since by the sole means of monoclonal antibody labeling it is not possible to visualize and separate T cells based on their TCR specificity. The

groundwork for visualization and isolation of T cell specificity has been laid by Altman et al., who for the first time made soluble peptide-MHC tetramers that stably bind to the respective TCRs and can be combined with fluorescent or magnetic labels [128].
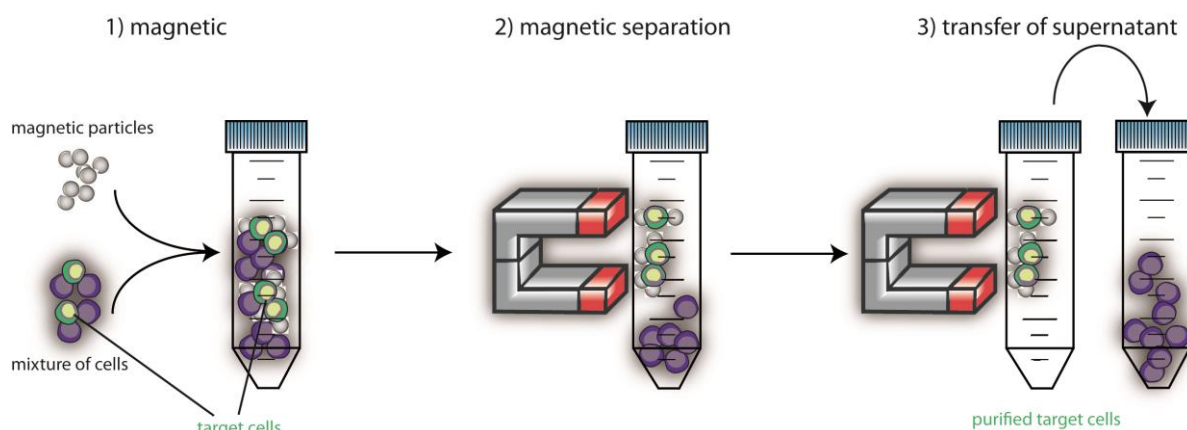

Fig. 1.3: Positive cell selection using magnetic microbeads and a strong hand-held permanent magnet.

1) A mixture of cells is mixed with specific labeling microbeads to magnetically label a desired target fraction. 2) In a strong magnetic field, labeled cells are held back. 3) Unlabeled cells can be transferred in a separate tube. Washing of the cells improves the purity of the target cell population.

3.3.2   Comparison of different strategies for cell separation

The negative enrichment strategy can in principle target cells that are characterized by one or a combination of two or more markers depending on the nature of the cell mixture and the availability of antibodies. Purities of the target cell population, however, are significantly lower compared to positively enriched populations. Positive enrichment can target cells characterized by more than one markers currently mainly with FACS, which works with parallel detection of different dyes at the same time. Positive MACS enrichment can only be conducted with one specificity at a time, since cells are either magnetic (labeled) or not (unlabeled). Since the labels remain stably bound to the cell surface, clinical use of both technologies depends on the availability of clinically approved labeling reagents at present. Especially for fluorescent dyes, the nature of the reagents poses regulatory issues and is suspected to be associated with immunogeneicity. Another issue with FACS sorting is the limitation that most sorters cannot be transferred into a closed, sterile system.

However, the advantages of magnetic cell selection over FACS are: (i) less training of personnel is required, since protocols are easier to follow and time of labor is shorter, (ii) the method enables fast high-throughput sorts and cell numbers can be scaled up without a direct correlation to the required sorting time, (iii) recovery rate of target cells exceeds those of other isolation methods since the need for specialized equipment can be minimized, (iv) magnetic selection can be performed in an affordable closed system, a feature that is mandatory in good manufacturing practice, (v) the first

magnetic selection reagents are in clinical use for ten years now and second-generation reagents are easier to receive approval for by the regulatory authorities.

As already mentioned, positive MACS enrichment is limited to select cells based on one surface marker (A) or a population of single-positive cells of different markers (A+B) but not a target population characterized by combinatorial expression of markers (A∩B). Though recent advances in MACS technology were made by application of different-sized magnetic beads that can be differentiated by the strength of the magnetic field and used for two-step positive enrichment [129], the described strategy is limited to very few iterations (two positive enrichment steps). To accomplish isolation of populations characterized by combinatorial expression of markers (A∩B), serial steps of positive enrichment would have to be aligned and only if magnetic labels can be removed from the cells, a second positive selection step for a different marker with the same magnetic particle will be possible.

3.3.3 Principle of the reversible *Strep*tamer Technology

Reversible TCR ligands were initially introduced to the field by Knabel et al. in 2002 as an advance of the aforementioned peptide-MHC (pMHC) multimer technology by Altman et al. [128]. Since multimerization of pMHC monomers is crucial to achieve stable binding to the TCR, it was hypothesized that pMHCs would spontaneously dissociate from the cell surface in their monomeric state. Consequently, the interaction of monomers with the respective backbone molecules (for multimerization) was designed in such a way that targeted disassembly of multimers into pMHC monomers and free backbone would become possible [130].

The concept of reversibility is based on the avidity gain resulting from the interaction with multipe pMHC molecule and the TCRs at the same time. The reversible pMHC monomers have rapid off-rates due to their relatively low binding affinity towards the TCR. However, to stably bind to the cell surface the monomers must be multimerized to establish a sufficient binding. The pMHC molecule is multimerized over an oligo-*Strep*tactin backbone and therefore capable of binding several TCRs at the same time resulting in a higher avidity and stronger binding. Multimerization is mediated by *strep*-tag/*strep*tactin interaction. *Strep*-tag is a nine amino acid long peptide initially made as a tool for affinity chromatography [131]. pMHC molecules are genetically fused with a *strep*-tag sequence bearing a high affinity towards *Strep*tavidin or *Strep*tactin, both of which can serve as the molecular backbones for multimerization. Streptactin is an engineered form of the streptavidin with a 10-fold enhanced binding affinity towards *Strep*-tag [132, 133]. This new family of pMHC multimers uses the *strep*-tag/*strep*tactin interaction and can be disrupted by addition of a strong competitor, which binds to the active binding sites of the *strep*tactin backbone with a 10^6-fold higher affinity as compared to *strep*-tag.

The vitamin D-biotin is such a competitor, which has an intrinsic 10^6-fold higher affinity towards *strep*tactin. In the presence of D-biotin, it binds to the *strep*tactin and, as a consequence, multimers are disrupted into monomers, because *strep*tag is displaced from *strep*tactin. Those monomers dissociate spontaneously from the cell leaving quasi untouched cells behind.

Recently, the reversible *Strep*tamer technology has been extended not just to a broad series of complex TCR ligands but to a continuously growing list of phenotypic markers. These S*trep*tamers targeting basically any surface antigen are termed Fab-*Strep*tamers. They harness the broadly available variety of surface antigens, which can be targeted by specific monoclonal antibodies. Fab-*Strep*tamers are built analogous to pMHC-Streptamers [130]. Their respective antigen-recognizing part is made of the variable Fab fragment of a monoclonal antibody and a s*trep*-tag peptide for the multimerization with a Streptactin backbone.

Similar to the pMHC monomers, reversibility requires an optimal affinity of Fab fragments for monomers in order for them to dissociate spontaneously from the antigen but still bind stably in their multimeric form as a result of several antigens being bound at the same time (increased avidity). Fab monomer affinity can be reduced, if necessary, by insertion of point mutations in the variable region of the antibody fragment [1].

Reversible selection reagents can overcome unwanted changes of the cell population caused by remaining surface markers like premature activation, cross-linking or blockade of receptors causing functional impairments, and the entrance of cells in the state of anergy and exhaustion or even premature cell death.

Issues of clinical relevance, which can be avoided by the use of reversible labels, are potential toxicity and immunogenicity of remaining sort-markers or potential allergic reactions. Lastly, the comparably difficult process to receive approval for non-removable sort-markers is of economic interest.

From a regulatory point-of-view, cell selections using reversible *Strep*tamers have been classified as 'minimally manipulative' to the cells. The status of cell products manufactured with *Strep*tamers without further cell culture and/or genetic modification is therefore the status of non-advanced therapeutic medicinal products (non-ATMPs). Reversible Fab-*Strep*tamers transfer the distinct advantage of negative enrichment –untouched target cells- to the more stringent positive enrichment, thus making the most of both general strategies [1]. This might have tremendous implementations on cell separation, both for research use and clinical T cell therapy.
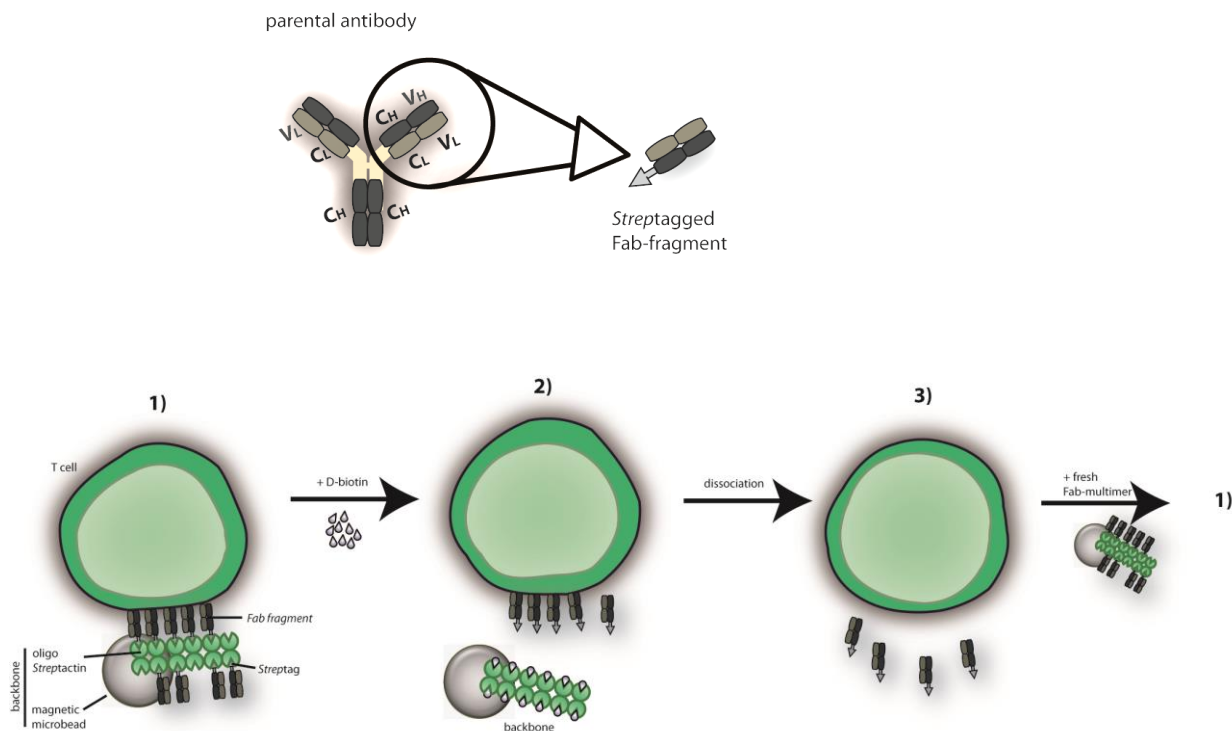
Fig. 1.4: Principle of reversible cell labeling with *Strep*tamer-coated magnetic microbeads.

Recombinant Fab fragments are derived from parental antibodies and expressed as fusionproteins with the nine amino acid long *strep*tag peptide. 1) A target cell is stably labeled with *Strep*tamer-coated magnetic microbeads. 2) Upon addition of the competitor D-biotin, the whole *Strep*tactin-coated microbead is released from the surface of the target cell. 3) Spontaneous dissociation ensues the disruption of the multimer. Cells can subsequently be washed and may be labeled again with a different Multimer or antibody.

3.3.4 Fab-*Strep*tamers and serial enrichment

*Strep*tactin-covered magnetic beads can be used for direct, positive magnetic enrichment. The *strep*tactin on the magnetic particles serves as a molecular backbone for Fab-multimers. Fab monomers are assembled to form a multimeric complex because they are fused to a *strep*-tag peptide which is moderately affine towards *strep*tactin. D-biotin is used to competitively bind and saturate the binding sites of the *strep*tactin backbone thus, leaving low-affinity Fab monomers on the cell surface, which dissociate spontaneously. Cells are no longer magnetically labeled and can be eluted in a magnetic field after one round of positive enrichment. As a result, quasi untouched cells of high purity are separated from the *Strep*tactin-covered magnetic beads. Residual soluble reagents (Fab monomers and D-biotin) can be removed by washing the cells by conventional centrifugation. Now, the quasi untouched cells can undergo another round of positive selection with a different Fab-multimer bead complex. In this way, this novel technology allows for the first time access to some therapeutically relevant T cell subpopulations such as T_{REGS} and T_{CM}, that require a constellation of markers for purification and were so far not accessible by minimally manipulating enrichment strategies.

Besides enabling serial positive enrichment in a closed system, the main advantage of this novel technology is its applicability to basically any surface antigen. So far, the rapid translation of

preclinical findings to a clinically applicable sort protocol has been difficult, for only a handful of T cell marker-specific monoclonal antibodies are approved for GMP-use by the regulatory authorities at present. With reversible Fab reagents being classified as minimally manipulating reagents, it is now possible to quickly develop suitable Fabs for virtually any newly found application.

3.3.5   Clinical isolation of T cell subpopulations

The first clinical-grade cell separation technology was the magnetic bead-based cliniMACS system [134]. It is based on the use of nanometer sized biotinylated super-paramagnetic particles with an average diameter of around 150 nm [135]. Other clinically available, general strategies for T cell isolation include functional isolation based on genetic screening [49, 136] and FACS-sorting [137]. One can argue that, among clinically available cell separation technologies, immunomagnetic separation is the best developed one at present. It is currently the only available method to generate large numbers of cells directly *ex vivo* without the need for *in vitro* expansion.

Direct clinical enrichment of defined cell populations based on surface markers has so far been limited to single parameters (marker). Human clinical trials using magnetic bead isolation of either CD4 or CD8 T cells prior to transfer of T cells have been conducted for both cancer and anti-viral therapies [69, 138]. Clinical cell isolation of CD34$^+$ cells and peptide-MHC multimer$^+$ cells have been conducted in clinical phase II and III studies [139-141].

A more precisely defined subset using more than one marker, however, so far required the combination of negative and positive selections in a serial fashion. For example, CD25 positive enrichment has been used in combination with CD8 and CD19 depletion for the isolation of TREGs to be administered to patients to prevent GvHD after stem cell transplantation [70]. A novel GMP-grade monoclonal antibody specific for human CD62L has recently been introduced; an advance, which made clinical-grade isolation of human memory T cell subsets possible. Clinical-grade isolation protocols using this CD62L-targeting antibody have recently been published by Wang et al.[142] and Terakura et al. [119]. The first clinical application of GMP-grade reversible HLA-streptamers originates from Schmitt et al. demonstrating evidence for clearance of CMV viremia upon transfer of CMV specific T cells in acute leukemia patients with recurrent CMV infection who have undergone allogeneic stem cell transplantation [92].

3.4 Current needs for clinical cell processing and adoptive transfer of T cells

Isolation of a defined cell product characterized by multiple cell surface markers still remains a major hurdle in cell processing from a regulatory point-of-view. Some practical challenges for the generation of well-defined T cell products as a therapeutic regimen still remain [143]. Isolation of T cell subsets must comply to GMP-standards [144]. It is mandatory in order to meet with regulations for clinical applications in most countries to conduct cell selections in a sterile and closed system. Negative and positive cell sorting using magnetic particles are directly applicable for clinical use because those are directly feasible in a closed system.

Isolation of central memory T cells, which are not further genetically modified or in vitro cultivated can retain the status of non-advance therapy medicinal products (non-ATMPs). According to the European commission, cells that are defined as non-ATMPs must not be substantially altered as a result of their processing. This includes *ex vivo* expansion or activation of cells. By producing non-ATMPs for personalized medicine it is possible to be flexible enough to rapidly translate novel findings of current research into clinically feasible applications.

Further requirements for isolation protocols are simplicity, reproducibility and minimal processing time to ensure economic feasibility for incorporation into human clinical trials.

Another general problem for T cell therapy is the poor access to clinical trials to a broad range of patients. Keeping the costs and level of complexity of the cell separation process as low as possible will be crucial in overcoming this limitation.

One key element of user-friendliness, simplicity and reproducibility is the automation of the cell purification process. Since there is currently no platform available, on which serial magnetic enrichment can be conducted, the automation of this process remains to be developed.

4 Aim of this thesis

Adoptive transfer of primary or genetically engineered T cells is currently emerging as a promising strategy to treat tumors or chronic infectious diseases, as shown in several clinical trials. Unimpaired functionality and longevity of transferred cells are crucial for therapeutic efficacy. The ideal subset for successful and sustained persistence of adoptively transferred T cells therapies is still controversial as different T cell subpopulations (e.g. central memory and effector memory) are not equally suitable for patient treatment. Recent efforts to elucidate the contribution of different subsets to the efficacy and safety of adoptive T cell therapy have led to the proposition that selection and physical isolation of the most suitable T cell subset for adoptive transfer might help enhance the clinical response on the one hand and eliminate unwanted side effects on the other hand. Therefore, a better understanding of how subset compositions interfere with diversity in clinical response rates and the occurrence of side effects could make this approach more predictable. Studies suggested that antigen-specific central memory T cells (T_{CM}) are most capable of giving rise to long-term persistent T cell responses, and thus seem to be most suitable for providing protective immunity in vivo upon adoptive transfer while minimizing the risk for T cell related toxicities.

Direct positive magnetic isolation of functional central memory T cells for clinical applications was so far hampered by the lack of multiparameter selection of the target CD8+CD62L+CD45RO+/CD45RA- memory T cells. The recently developed reversible Fab *Strep*tamer technology can bypass this general problem by enabling serial positive purification via multiple surface markers.

The aim of this thesis was to develop a novel serial three-step enrichment protocol for the clinical isolation of CD62L+CD45RA-CD45RO+ central memory CD4+ and CD8+ T cells using CD3, CD8, CD4, CD45RA, CD45RO and CD62L Fab-*Strep*tamers coupled to magnetic particles.

First, the respective Fab proteins were generated and their staining properties were compared to conventional monoclonal antibody staining. Then, after determining the main parameters that influence reversibility, a novel assay to evaluate regent reversibility was developed for quality assessment of Fab proteins. Next, magnetic selection protocols for the use with reversible *Strep*tamers were developed. To establish serial positive magnetic selection, magnetic particles of different sizes needed to be evaluated. Critical parameters that influence purity and cell recovery during the serial enrichment process were optimized to finally establish a three-step purification process with highest efficiency and the capacity to minimally influence the functionality of extracted cells. Finally, the technique was adapted to a GMP compliant procedure using equipment and consumables previously approved for the clinical use.

5 Results

5.1 Ex vivo *Strep*tamer staining for phenotypic markers on human PBMCs

Current strategies for clinical purification of T cells based on phenotypic antigens use paramagnetic beads enabling direct positive enrichment. Stable labeling of target cells is generally based on "irreversible" high affinity monoclonal antibody staining. Antibody conjugates are available in a covalently bound form featuring fluorophores, which enable detection by flow cytometry, or with paramagnetic particles, which enable separation in a magnetic field. However, remaining antibodies and particles on the cell surface of purified cells can interfere with their functional integrity. We hypothesized that (i) multiparameter cell sorting by serial positive enrichment could be achieved if the complete cell label could be removed after each separation step before entering the next purification cycle and (ii) that cells, which have undergone reversible serial positive enrichment, would be functionally unimpaired. Therefore, we generated reversible staining reagents for the purpose of cell surface labeling and specific cell separation of central memory T cells including αCD3, αCD4, αCD8, αCD62L, αCD45RO, and αCD45RA based on existing antibody fragments.

5.1.1 Clones and mutations of Fab fragments

It has been recently demonstrated that the *Strep*tamer technology, which was originally designed for reversible staining of T cell receptors using MHC-Multimers, can be transferred to create a broad spectrum of reversible antibody-like staining probes. Therefore, low-affinity antibody-derived Fab-fragments were generated, which stain like parental antibodies when multimerized via *Strep*-tag and *Strep*-Tactin, but can subsequently be removed entirely from the target cell population by targeted monomerization. Multimerization of Fab-fragments becomes possible via genetic fusion of the heavy chain of the Fab fragments to a OneSTrEP-tag sequence (*Strep*-tag), and subsequent co-expression together with the light chain in the periplasm of *E. coli*. The relatively high binding affinity of *Strep*-tag to *Strep*-Tactin ensures binding to multiple sites of tetrameric *Strep*-Tactin molecules, which is used as a backbone for multimerization. In some cases, the generation of Fab-fragments from dimeric parental antibodies is already enough to obtain a fully reversible reagent. However, in most cases the Fab-fragments are still of too high binding affinity to support reversibility of staining within a reasonable time frame. In that case, we have succeeded in the past for several examples of Fab-fragments to reduce the binding affinity without losing specificity by single amino acid exchange in

regions aside from the complementarity determining region (CDR). For the present thesis work, Stage cell therapeutics provided me with various mutated Fab fragments and plasmids relevant for T_{CM} purification. **Table 5.1** gives a detailed overview of all Fab proteins that have been used. For some proteins, a large number of different mutations or expression batches of the same plasmid have been made. Every batch required careful individual testing after the protein had been purified. As a first step in this evaluation, purified Fab-fragments were multimerized with a fluorophore-conjugated *Strep*-Tactin for analysis of antigen-specific surface stainings by flow cytometry.

Specificity	Mutation	Plasmid	sequence	conc. [ug/mL]	staining	Reversibility
CD3						
CD4	H918		ok		yes	yes
CD8	C85Sheavy				yes	yes
CD62L	wt				yes	yes
CD62L	86				yes	yes
CD62L	87				no	-
CD62L	88				no	-
CD62L	89				no	-
CD62L	cys					
CD45RO	wt	p1641	ok	163	yes	yes
CD45RO	L11Sheavy	p1642	ok	121	yes	yes
CD45RO	wt	p1643	ok	188	yes	yes
CD45RO	L11Sheavy	p1644	ok	88	no	-
CD45RO	L11Aheavy	p1643	ok	70	no	-
CD45RO	104Aheavy	p1643	ok	90	no	-
CD45RO	Y37Alight	p1643	ok	30	no	-
CD45RO	Y41Alight	p1643	ok	60	no	-

Table 0.1: Overview of different Fab-fragments for the formation of *Strep*tamer-based reagents

All recombinant Fab fragments that were used in this thesis work are listed in this table. The heavy chain of Fab fragments from parental antibodies is genetically fused to the OneSTrEP-tag sequence (*Strep*-tag) and expressed together with the light chain in the periplasm of *E. coli*. Mutations are indicated by the amino acid residue that has been exchanged by mutagenesis PCR. Some purified Fab proteins have been provided by Stage cell therapeutics, Göttingen, as indicated. For all others, I received the expression vector and derived recombinant proteins by myself. For detailed information on `staining´ and `reversibility´ see following sections.

5.1.2   Evaluation of Fab Streptamer stainings

To demonstrate that Fab-*Strep*tamer staining is identical to conventional antibody staining, both techniques have been used on multiple donor-derived PBMCs from healthy volunteers. Fab fragments were multimerized with PE- or APC-conjugated *Strep*-Tactin for analysis by flow cytometry. We used fresh PBMCs from healthy blood donors and employed control stainings with commercially available antibodies to test the ability of Fab-*Strep*tamers to stably and specifically stain cells in the same way that antibodies do.

CD3-specific recombinant Fab proteins were derived from the OKT3 antibody clone. CD3- specific Fab-*Strep*tamers using PE-conjugated *Strep*-Tactin were incubated with PBMCs at a ratio of 0.75 µg *Strep*-Tactin per 10^6 cells. **Fig. 5.1a** shows specific CD3-staining for one representative donor and a control without the specific Fab-fragment to exclude unspecific fluorescence by the *Strep*-Tactin backbone. Variations in CD3-frequencies are based on inter-individual differences between donors. We have performed CD3-specific Fab *Strep*tamer stainings in 5 individual experiments using PBMCs from a different donor each time. Control stainings with a commercially available mAb-conjugate for flow cytometry served as positive controls for CD3 frequencies in a respective donor. We could show in independent experiments that CD3 frequencies determined by *Strep*tamer staining and frequencies from antibody staining are equal (**Fig. 5.1b**). CD3 Fab-*Strep*tamers can specifically stain CD3$^+$ cells in the same amount of time (20 minutes) under the same experimental conditions as commercial monoclonal antibodies.
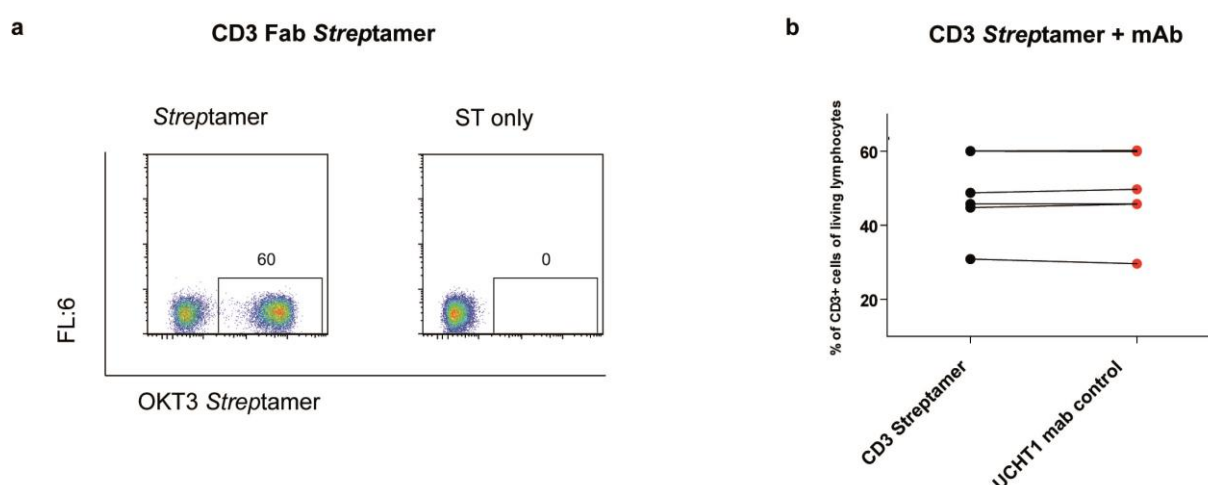
Fig. 0.1: CD3-specific Fab-*Strep*tamer staining of human PBMCs

Multimers of CD3-specific Fab fragments were generated at a ratio of 0.2 µg Fab and 0.75 µg (PE-labeled) Streptactin (ST) per 10^6 cells. All steps were conducted at 4°C **a**. CD3 *Strep*tamers of the OKT3 parental antibody clone specifically stain a subset of human living lymphocytes (pre-gated). `ST only´ indicates the control staining using PE-labeled *Strep*-Tactin without recombinant Fab protein. Numbers in dot plots indicate gate frequency. **b**. CD3 *Strep*tamer stainings (black dots) and respective control stainings using the commercially available UCHT1 clone (red dots) performed on blood PBMCs from 5 different healthy donors.

The same strategy was applied to test the performance of CD4-specific Fab-*Strep*tamers. Using different fluorescent dye-conjugates of antibody and *Strep*tamer for flow cytometry enabled us to perform simultaneous staining with CD4 Fab-*Strep*tamers and a CD4-specific mAb. Thereby, we confirm that CD4 Fab-*Strep*tamers specifically stain the same subset of cells as commercial anti-CD4 antibodies. Controls include samples stained with just dye-conjugated backbone without Fab protein and monoclonal antibody staining alone. A small fraction of cells were only positive in one of the two staining strategies. This might be due to some cells with very low CD4 surface expression, which could be stained differently with multivalent Fab-*Strep*tamers and bivalent parental antibodies bringing out minimal differences in binding avidity of the two clones. Indeed, CD4 *Strep*tamers were derived from a different parental antibody clone (OKT4) than control antibodies (13B8.2). However, conventional CD4$^+$ T cells are characterized by a high relative expression of CD4. This population is not affected by these small staining differences and appears double stained in both strategies (**Fig. 5.2a**). To account for naturally occurring scattering in the CD4$^+$ frequencies between donors, we performed multiple individual stainings with CD4 antibodies and *Strep*tamers. (**Fig. 5.2b**). The frequency of CD4$^+$ PBMCs among living lymphocytes is identical for both, *Strep*tamer and antibody stainings in n=5 donors respectively.
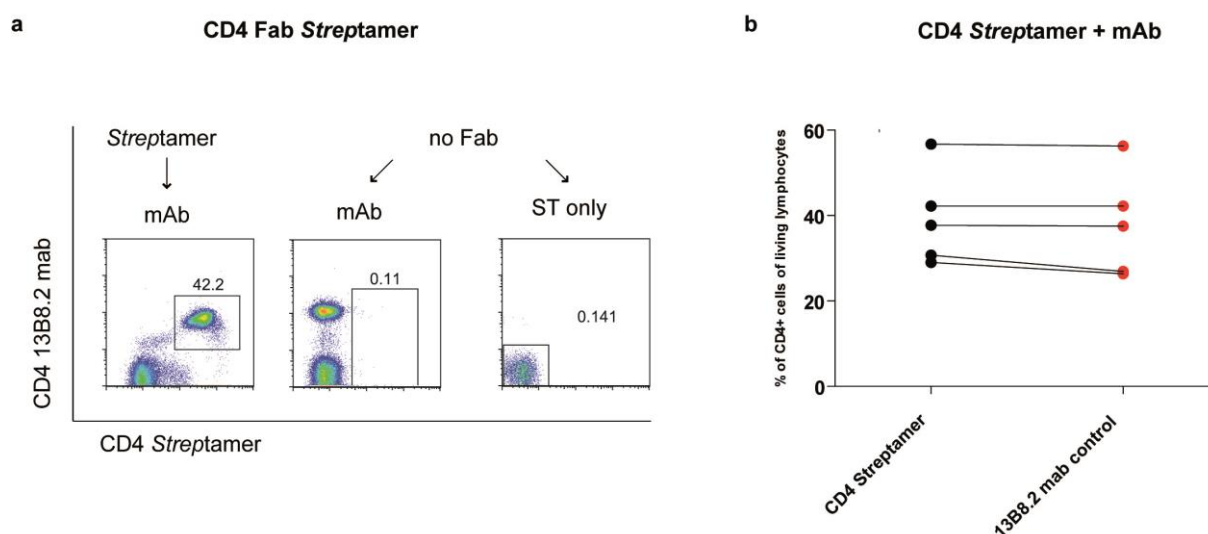

Fig. 0.2: CD4-specific Fab *Strep*tamer stainings of fresh PBMCs

*Strep*tamers of CD4-specific Fab fragments were generated as described for CD3 *Strep*tamers **a**. CD4 *Strep*tamers specifically stain the CD4$^+$ subset of human living lymphocytes (pre-gated) as verified by the double staining using the commercially available CD4 mAb clone 13B8.2 and the OKT4-derived Fab *Strep*tamers. Numbers in dot plots indicate gate frequency. **b**. CD4 *Strep*tamer (black dots) and mAb stainings (red dots) performed on 5 different healthy donors.

CD3 and CD4 Fab-*Strep*tamers were generated using an equivalent of 0.75 µg *Strep*-Tactin of dye-conjugated *Strep*-Tactin backbone. For previously evaluated Fabs this amount has been found to be optimal for the staining of up to 5x10^6 cells without causing a considerable unspecific background. However, the amount of recombinant Fab protein had to be determined for each protein meaning each specificity or mutation and every single expression batch. Therefore, titrations of Fab protein amounts

for multimerization were performed as a standard before new batches of protein expressions were used for further experiments. This type of *Strep*tamer staining and titration testing has become part of the quality control for every new recombinant Fab protein batch in the meantime.

For CD8 Fab evaluation we first titrated the amount of Fab reagent per 10^6 fresh PBMCs over a fixed amount of dye-conjugated backbone (0.75 µg *Strep*-Tactin), thereby changing the *Strep*-Tactin-to-Fab ratio in each titration step. Further, we tested different *Strep*tamer-to-cell ratios for a given *Strep*-Tactin-to-Fab ratio to answer the question how both ratios as variable parameters contribute to *Strep*tamer staining intensities. We show a series of CD8 *Strep*tamer stainings with varying *Strep*-Tactin-to-Fab ratios in **Fig. 5.3.** Staining intensities drop significantly when less Fab protein is used during *Strep*tamer formation. Ideally, the *Strep*tamer staining should depict a similar population of cells to be CD8$^+$ positive as compared to staining with a conventional antibody. In order to reach this, we had to choose a slightly different *Strep*-Tactin-to-Fab ratio of 0.75 µg: 0.1 µg for CD8 Fab *Strep*tamers. Two *Strep*-Tactin-to-Fab ratios were chosen (one too low and one optimal) to test the second parameter *Strep*tamer-to-cell ratio. Increasing amounts of *Strep*tamer reagent were added on a per cell basis. Our data show that increasing the *Strep*tamer-to-cell ratio cannot compensate for a poorly chosen *Strep*-Tactin-to-Fab ratio. Variations following changes in *Strep*tamer-to-cell ratios are less abundant than changes in the *Strep*-Tactin-to-Fab ratios. We conclude from these data that the latter parameter is crucial for the constitution of Fab *Strep*tamers and that a certain minimum of binding sites on the *Strep*-Tactin backbone must be engaged during multimerization in order to establish an adequate staining intensity.
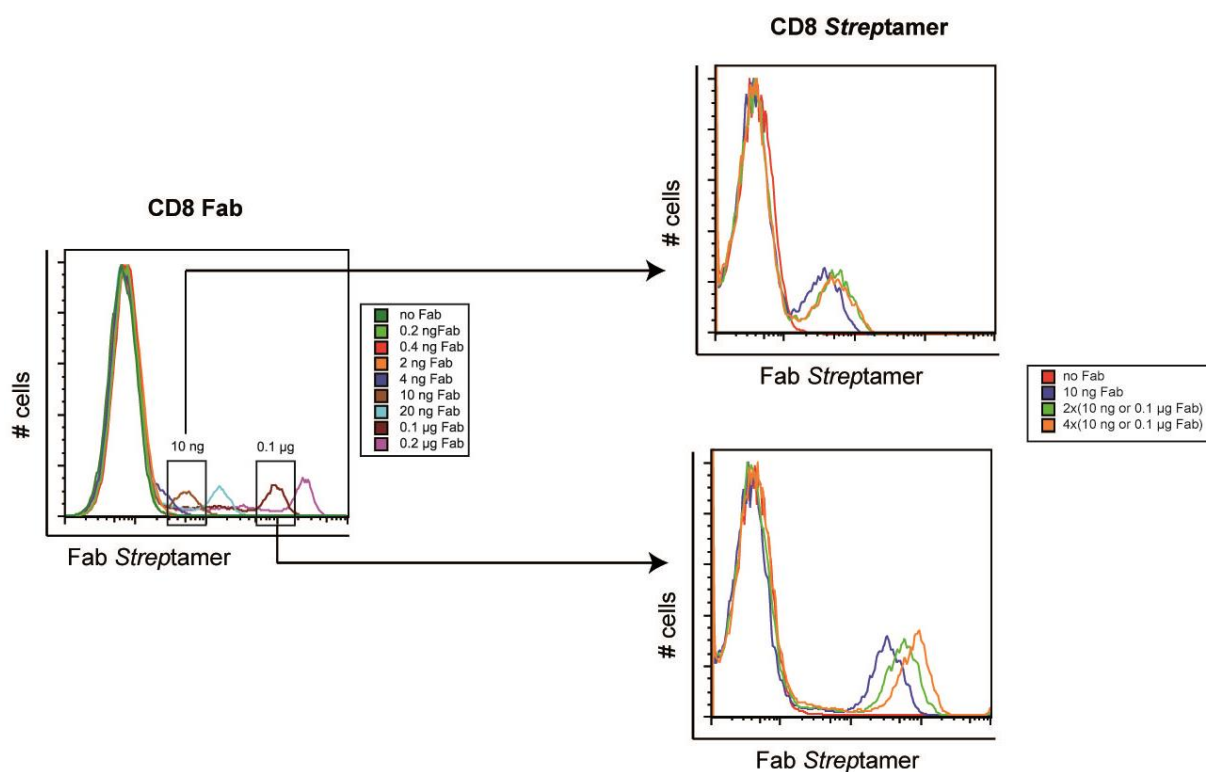
Fig. 0.3: Titration of CD8 *Strep*tamer multimerization

0.75 µg (PE-conjugated) *Strep*-Tactin was multimerized with increasing amounts of recombinant CD8-specific Fab protein and stainings were performed on 10^6 fresh PBMCs per sample. The multimerized staining reagents were further titrated over 3 different *Strep*-Tactin: Fab ratios (shown for 10 ng and 0.1 µg Fab). All stainings were performed under the previously stated conditions.

Again, we used simultaneous stainings for evaluation of the specificity of CD8 *Strep*tamer stainings. Co-stainings with two different CD8-specific monoclonal antibodies are shown in **Fig. 5.4a**. As expected, the mAb staining with the same clone from which the CD8 Fab is derived (OKT8) resulted in a dimmer CD8 staining and lower frequency of CD8$^+$ cells when applied simultaneously with the corresponding *Strep*tamer. In contrast, a brighter staining intensity in simultaneous use of both reagents resulted from mAb staining with a different clone. We therefore continued to use the B.11 clone for all following stainings. The resulting CD8 frequencies of *Strep*tamer stained PBMCs and antibody stained PBMCs are alike in n=9 donors (**Fig. 5.4b**). We conclude that CD8 *Strep*tamer staining and mAb staining yield uniform frequencies. This uniformity holds true for all pairs for different donor material.
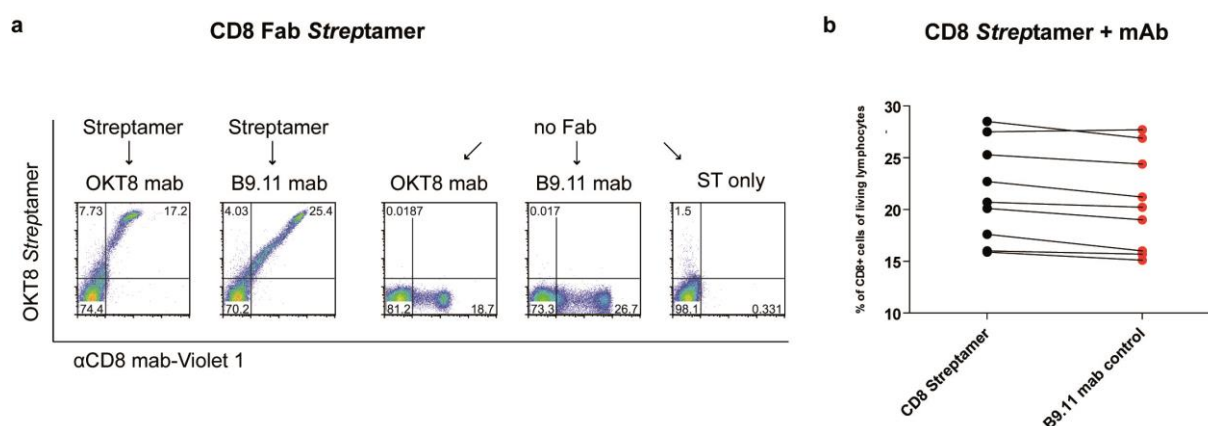
Fig. 0.4: Simultaneous CD8 Fab-*Strep*tamer and mab staining and CD8 frequencies in healthy individuals

CD8-specific Fab *Strep*tamers were made at a ratio of 0.1 µg Fab and 0.75 µg (PE-labeled) *Strep*-Tactin per 10^6 cells. **a.** CD8 *Strep*tamers of the OKT8 parental antibody clone specifically stain CD8$^+$ living lymphocytes (pre-gated). Specificity is verified by double stainings with *Strep*tamers and commercially available mAb clones (OKT8 and B9.11). `ST only´ indicates the control staining using PE-labeled *Strep*-Tactin without recombinant Fab protein. **b.** CD3 *Strep*tamer stainings (black dots) and stainings with the commercial anti-CD8 B9.11 mAb (red dots) performed on blood PBMCs from 9 different healthy donors respectively.

For evaluation of a CD62L Fab, as shown for CD8 Fabs, we also performed titrations of the *Strep*-Tactin-to-Fab ratio. **Fig. 5.5** displays a representative titration experiment with the unmutated CD62L Fab protein over a fixed amount of 0.75 µg PE-conjugated *Strep*-Tactin. An antibody control staining using the same fluorophore (PE) is included (brown graph). Based on the staining intensities of *Strep*tamer stainings we decided to use a *Strep*-Tactin-to-Fab ratio of 0.75 µg: 0.2 µg per 10^6 cells (orange graph). *Strep*tamers made with this ratio yielded the brightest staining equal to the control mAb staining in staining intensity.

Apart from the unmutated CD62L Fab, a total of 5 different mutated CD62L Fab proteins were tested at different *Strep*-Tactin-to-Fab ratios with Fab contents ranging from 10 ng to 20 µg (100-fold increase as compared to standard). The mutated proteins were made as part of a panel of CD62L Fabs with different affinities for evaluation. Since neither the standard ratio nor an increase in Fab content during multimerization could establish proper *Strep*tamer stainings for the 5 mutated CD62L Fabs, representative *Strep*tamer stainings of all Fab proteins at the standard *Strep*-Tactin-to-Fab ratio of 0.75 µg: 0.2 µg per 1x10^6 cells are shown in **Fig. 5.6a**. The poor stainings with mutated CD62L Fab proteins are not a consequence of a particularly low CD62L expression in one individual donor but showed the same unsatisfactory staining on donor-PBMCs from other individuals. Only the CD62L wildtype (wt) Fab compares to the antibody control in staining performance as verified by stainings with 6 different donor-derived PBMCs (**Fig. 5.6b**). Confirmation of specificity of the CD62L *Strep*tamer staining was obtained by simultaneous stainings with CD62L *Strep*tamers and commercially available antibodies (**Fig. 5.6c**). In conclusion, the CD62L Fab wt Fab stains CD62L$^+$ lymphocytes like the commercially available mAb clone LT-TD 180.
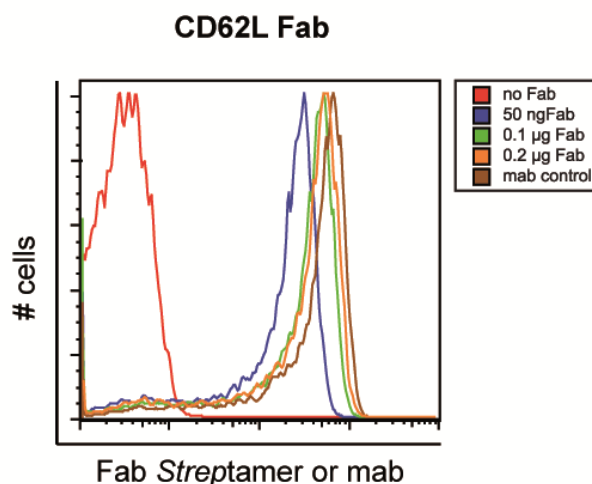
Fig. 0.5: Titration of CD62L *Strep*tamer multimerization

Stainings were performed on 10^6 fresh PBMCs using CD62L-specific *Strep*tamers or phycoerythrin-(PE)-conjugated anti-CD62L monoclonal antibody. For multimerization 0.75 µg (PE-conjugated) *Strep*-Tactin was multimerized with increasing amounts of recombinant CD62L-specific Fab protein and stainings were performed under the previously stated experimental conditions.
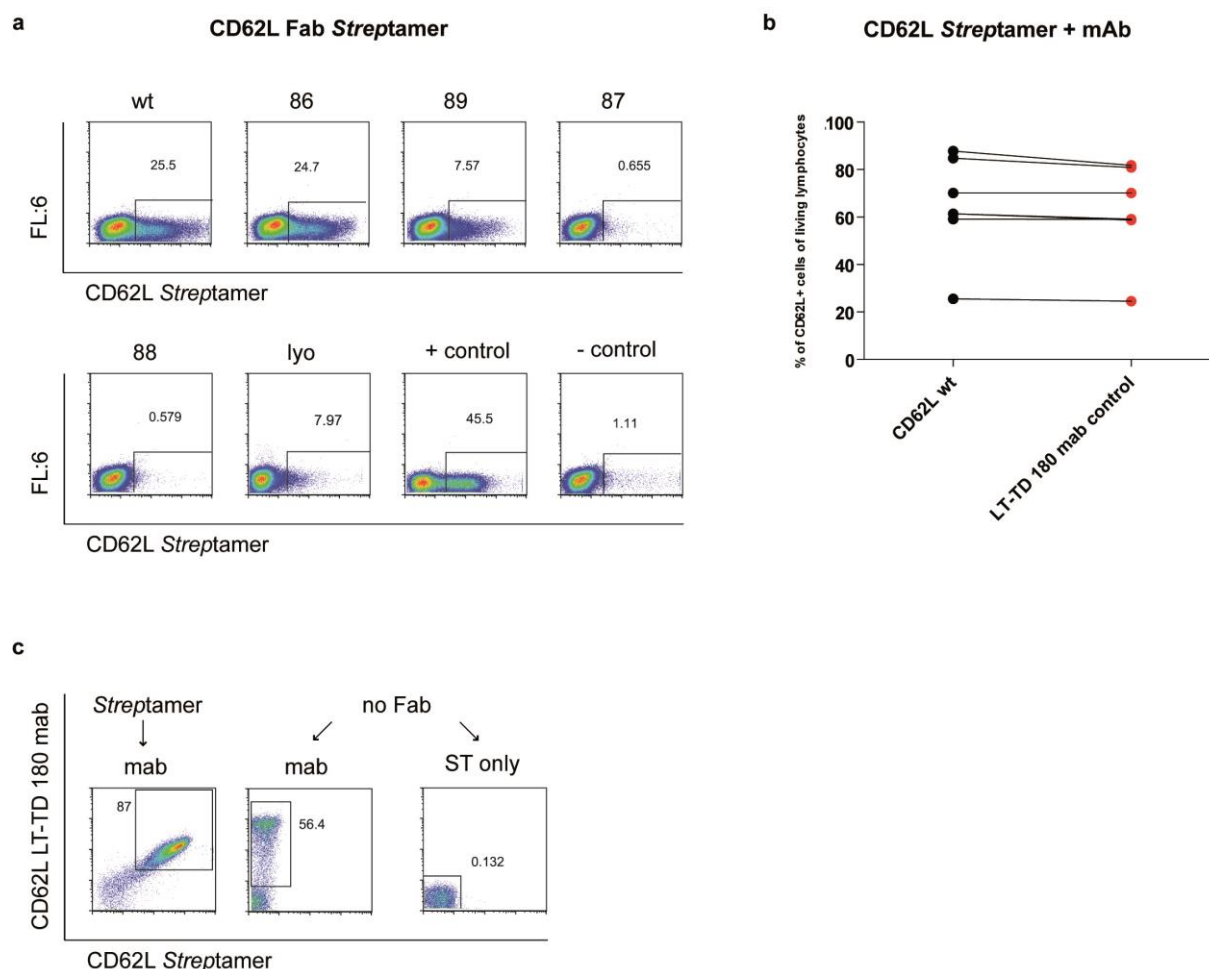
Fig. 0.6: CD62L-specific *Strep*tamer stainings using a panel of mutated and unmutated Fabs

Fab-*Strep*tamers were made as described for CD3 and other Fab-*Strep*tamers. **a**. Different mutated and an unmutated CD62L *Strep*tamer of the parental antibody clone DREG56 were used to stain a subset of living lymphocytes (pre-gated). **b**. CD62L *Strep*tamer stainings and mAb stainings using the commercially available anti-CD62L clone LT-TD 180 were performed on different healthy donor PBMCs (n=6). **c**. CD62L *Strep*tamer specificity is verified by double staining with *Strep*tamers and the commercially available mAb clone LT-TD 180.

For human CD45RO, only one antibody clone (UCHL1) has so far been successfully generated and commonly used. Plasmids for expression of recombinant CD45RO fusion proteins with the OneSTrEP-tag sequence in *E. coli* were kindly provided by Dr. Stefan Dreher. Functionally assembled Fab fragments were purified following protein expression by affinity chromatography using a *Strep*-Tactin protein purification column. First, we tried to address the question, which CD45RO Fab-*Strep*tamers stain like parental antibodies. In **Fig. 5.7a** we show the staining performance of a panel of unmutated and mutated Fab fragments multimerized in the presence of PE-labeled *Strep*-Tactin. Notably, the specimens p1641 wt and p1643 wt as well as their mutated forms p1642 L11Sheavy and p1644 L11Sheavy show very good surface staining of human PBMCs. Further mutations were made based on the specimen p1643 wt apart from L11Sheavy. Those mutations p1643 L11Aheavy, p1643

104Aheavy, p1643 Y37Alight, p1643 Y41Alight, p1642 55Aheavy and p1644 55Aheavy do not show sufficient surface staining. 0.2 µg Fab-fragment was used for multimerization with 0.75 µg *Strep*Tactin. This ensures an approximately equimolar ratio between Fab fragments and free *Strep*tag binding sites on the backbone. All Fab fragments were then multimerized with a different Fab: *Strep*-Tactin ratio increasing the amount of Fab fragments to ensure that variations in protein concentration are compensated for. Titrations using up to 100-fold higher Fab concentrations could not compensate for the lack in staining intensities for some mutated CD45RO Fabs. To confirm these data at least 2 replicates of *Strep*tamer stainings were made using each mutant on different donor-PBMCs each time. For the 4 Fabs with good staining, PBMCs from 3 donors were analyzed using either *Strep*tamers or the commercially available UCHL1 clone for flow cytometry (**Fig. 5.7b**). With the exception of one mutated CD45RO, which showed a drop in staining intensity on one donor compared to the mAb control, the other 3 CD45RO Fabs stained equal CD45RO-positive frequencies. The same 4 CD45RO Fabs were then simultaneously stained with the commercial mAb to verify specificity of the staining. Both Fab Streptamers and mAbs are based on the same antibody clone UCHL1, and as expected, both strategies yielded very good surface staining of an identical subset of cells (**Fig. 5.7c**).

One CD45RO Fab-fragment (p1643 wt) with superior yield in protein expression was selected to test the performance of a Fab protein aliquot, which had been frozen (-80°C) and thawn 10 times side by side with an aliquot which was stored at –80°C and was never opened before. We could not detect any significant differences in *Strep*tamer stainings (**Fig 5.7d**), indicating a remarkable stability towards freezing-thawing cycles of these Fab fragments.

In summary, we could show that *Strep*tamer staining is fast and robust and can substitute conventional antibody staining after careful evaluation of parameters including *Strep*-Tactin-to-cell ratio during multimerization and *Strep*tamer-to-cell ratio during staining. Other parameters, which can affect *Strep*tamer surface staining were found to be temperature, staining time, cell concentration and volume. This is not surprising, as the very same parameters are also known to affect staining with commercially available antibodies. However, just like with commercial antibodies variations in these parameters showed only mild effects on the staining intensity Fab *Strep*tamer stainings.
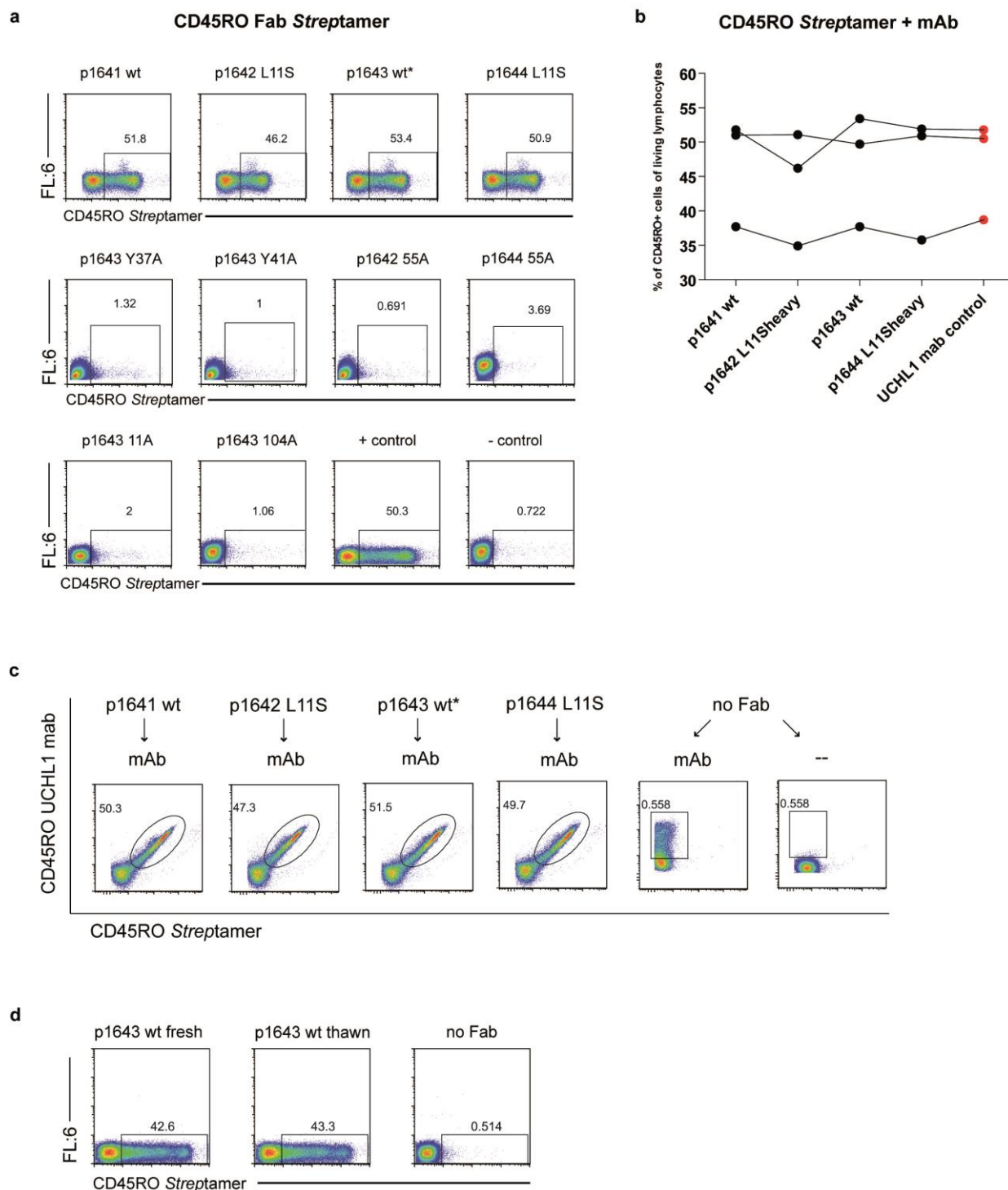
a CD45RO Fab *Strep*tamer

p1641 wt — 51.8
p1642 L11S — 46.2
p1643 wt* — 53.4
p1644 L11S — 50.9

p1643 Y37A — 1.32
p1643 Y41A — 1
p1642 55A — 0.691
p1644 55A — 3.69

p1643 11A — 2
p1643 104A — 1.06
+ control — 50.3
- control — 0.722

FL:6 / CD45RO *Strep*tamer

b CD45RO *Strep*tamer + mAb

% of CD45RO+ cells of living lymphocytes

p1641 wt, p1642 L11Sheavy, p1643 wt, p1644 L11Sheavy, UCHL1 mab control

c

CD45RO UCHL1 mab / CD45RO *Strep*tamer

p1641 wt → mAb — 50.3
p1642 L11S → mAb — 47.3
p1643 wt* → mAb — 51.5
p1644 L11S → mAb — 49.7
no Fab → mAb — 0.558
no Fab → -- — 0.558

d

p1643 wt fresh — 42.6
p1643 wt thawn — 43.3
no Fab — 0.514

FL:6 / CD45RO *Strep*tamer

Fig. 0.7: Multimer staining of CD45RO+ cells using a panel of mutated and unmutated CD45RO Streptamers

Multimers of CD45RO specific Fab fragments were newly generated prior to each experiment using 0.2 µg Fab and 0.75 µg phycoerythin (PE)-labeled *Strep*Tactin/ 10^6 cells. **a.** CD45RO specific Fab *Strep*tamers of the same parental antibody clone stain the CD45RO^{+} subset of human PBMCs in their unmutated form or when the pointmutation L11S is introduced in the heavy chain of the variable region in the Fab fragment. **b.** 4 CD45RO Fab *Strep*tamers were tested on 3 donors to compensate for variations in the frequency of CD45RO expression. Each dot represents a different healthy donor. **c.** The specificity of the 4 functional Fab *Strep*tamers was verified by simultaneous staining with the commercially available

parental antibody clone UCHL-1. **d**. Comparison between fresh aliquot of CD45RO Fab and 10 times freeze-thawn protein. *selected for following expressions.

5.2 Reversibility of Fab *Strep*tamer stainings

The *Strep*tamer technology should enable serial positive enrichment, thus enrichment of cell subsets defined by simultaneous expression of more than one phenotypic antigen like it is the case for central memory T cells. The most crucial step for sequential positive enrichment is the full reversibility of the *Strep*tamer reagent following each selection step. So far, we have verified the specificity of all single components necessary for TCM selection by *Strep*tamer stainings and flow cytometry. Next, we needed to develop a flow cytometry-based protocol to test the efficiency of reversibility of surface bound Fab/*Strep*-Tactin backbone components from the cells.

5.2.1 Critical parameters for reversibility of Fab fragments

The protocol for testing full reversibility of *Strep*tamer stainings is based on stainings of fresh PBMCs with Fab *Strep*tamers as described in the previous chapter. Multimerization of Fab proteins with fluorescent dye-conjugated *Strep*-Tactin allows direct visualization of Streptamer-stained cells via flow cytometry. When D-biotin is added, the signal is lost because the dye-conjugated *Strep*-Tactin is disrupted from the multimer complex and therefore also from binding to the cell surface. Depending on the binding affinity of Fab monomers, subsequently also the Fab molecules will dissociate. This step was so far not directly verifiable with current methods. Both kinetics (backbone disruption and Fab dissociation) are important for evaluation of Fab performance and are depicted in **Fig. 5.8a**. We used a fully reversible CD62L *Strep*tamer staining to illustrate the general strategy of reversibility testing. A schematic view of all necessary steps on a single-cell level (above) and obtained flow cytometry data from the removal process (below) are shown. Fab-*Strep*tamer stained samples are indicated by grey graphs overlaid with controls for Fab-unspecific background/autofluorescence (empty graphs). After the backbone is removed from the previously stained cells it is crucial to test for remaining Fab monomers on the cell surface. We developed a simple test by re-staining washed cells (to remove d-biotin and soluble Fab fragments in the cell supernatant) with a fresh fluorophore-coupled but unmultimerized *Strep*-Tactin backbone. The absence of any fluorescence signal after re-staining with unbound *Strep*-Tactin indicates full Fab dissociation. In order to control for effective removal of D-biotin, we included an additional control staining adding pre-multimerized Fab *Strep*tamers; minute amounts of D-biotin are enough to disassemble at least a fraction of the *Strep*tamers, which can be detected by a reduced staining intensity. This strategy turned out to be a highly sensitive test for detection of any remaining surface-bound Fab monomers. Similar to the experiments described above to optimize conditions for *Strep*tamer staining, we needed to identify the

most relevant parameters for efficient reversibility. **Fig. 5.8b** gives an overview on the most important parameters which were tested. As a first step, we attempted to determine the optimal concentration, total quantity and duration for D-biotin incubation. After that, we focused on controlling the washing of the cells to provide enough time and optimal conditions for Fab dissociation. Parameters that have been tested were specifically total wash volume, temperature, time and the number of wash repetitions. By repetitive washing, the reagent concentration in the supernatant is strongly reduced. This procedure seems to improve Fab dissociation in some cases by changing the equilibrium of the binding kinetics. Furthermore, we determined the detection limit of *Strep*-Tactin re-staining, which plays an important role in controlling the extent of Fab dissociation.
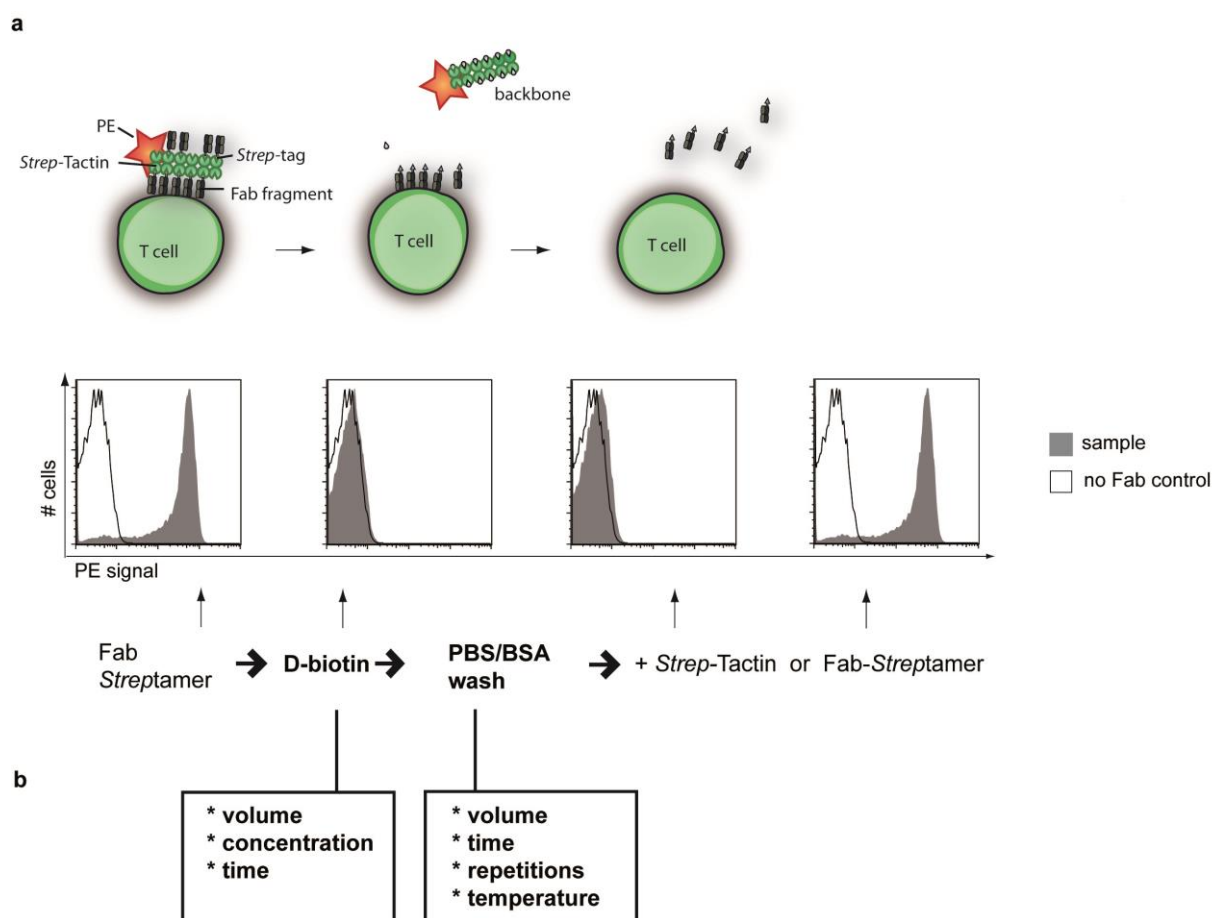

Fig. 0.8: Developing an assay to measure Fab *Strep*tamer reversibility

A schematic view on the single-cell level and a fully reversible CD62L Fab-*Strep*tamer staining (histograms) is shown to reveal all necessary steps in the process of reagent removal including *Strep*-Tactin re-staining to control Fab, *Strep*-Tactin, and D-biotin removal (**a**). For a detailed protocol on testing *Strep*tamer reversibility see section below. Critical parameters for reversibility are highlighted underneath the relevant steps of the process (**b**).

Next, we sought to identify the sensitivity and detection limit of *Strep*-Tactin re-staining as described above. By titrating in decreasing amounts of monomeric Fab-StreptagIII, we found that Fab concentrations 100-fold lower than to the initial staining conditions could still be detected. For 10^6

PBMCs, this threshold is equivalent to 2 ng of unbound Fab (**Fig. 5.9**). For most Fabs, 20 ng is the minimum amount required to establish any visible staining on 10^6 cells. For a few Fab-*Strep*tamers also smaller amounts of 10 ng Fab and slightly below can still promote some staining (see **Fig. 5.3** for reference), a concentration that still exceeds the detection limit of the re-staining assay by a factor of 5.
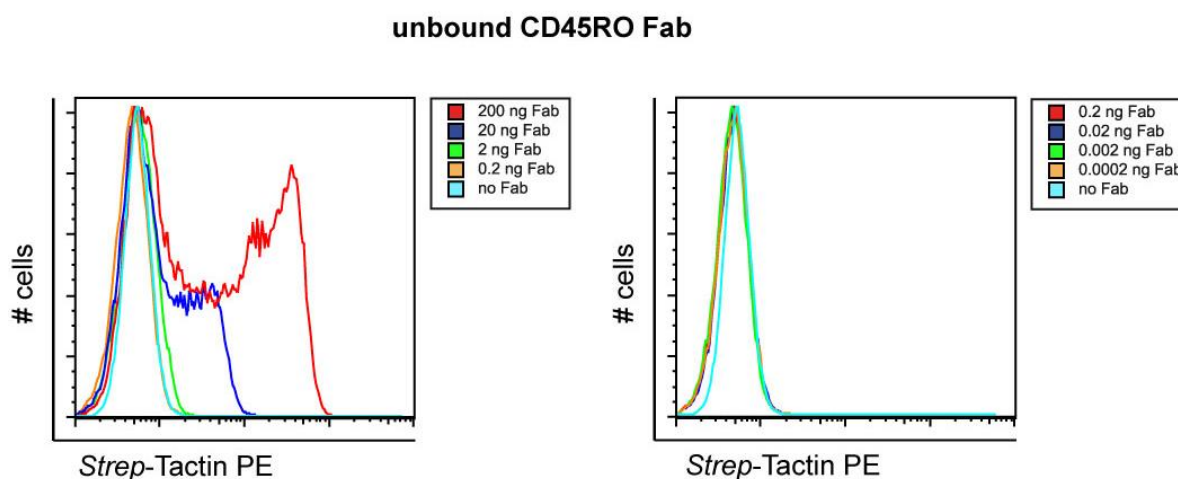
unbound CD45RO Fab

Fig. 0.9: Detection limit of *Strep*-Tactin staining for unbound Fab proteins

10^6 fresh PBMCs were incubated with the indicated amounts of CD45RO Fab protein for 20 minutes before addition of a 0.75 µg *Strep*-Tactin equivalent of PE-conjugated unmultimerized *Strep*-Tactin. After 20 minutes, all samples were analyzed by flow cytometry.

5.2.2   Development of an assay for testing reversibility of Fab fragments

Taking into account the previously stated parameters, we started out by testing different concentrations of D-biotin ranging between 1 µM and 10 mM to remove *Strep*tamer staining from freshly stained PBMCs to determine the necessary amount of D-biotin for targeted *Strep*tamer disruption. It is advantageous at this point to determine the lowest necessary D-biotin concentration, since it can become laborious to remove D-biotin afterwards. D-biotin has a 10^6-fold higher affinity towards *Strep*-Tactin compared to the Fab fusion protein. For this reason, a 20-minute-incubation period is believed to exceed the necessary time to replace all binding sites by far. In **Fig. 5.10a** a representative titration of the D-biotin concentration is shown. Concentrations of 100 µM or more remove a previously established *Strep*tamer staining in all experiments. There is a clear titration effect showing that even very low D-biotin concentrations can affect the staining intensity without completely removing the staining. Although the kinetics of Fab displacement from the backbone by D-biotin are not expected to depend on Fab specificity, differences in surface antigen-expression can lead to differences in the amounts of accumulated Fab-*Strep*tamer before D-biotin is applied, which might affect the measurement. Therefore, we performed titrations of the D-biotin concentration in independent experiments on different donor PBMCs using CD45RO, CD4 and CD8 Fab specificities

(**Fig. 5.10b**). Independently of Fab specificities, we were able to determine a threshold concentration of 100 µM D-biotin for the successful removal of *Strep*tamer stainings. In following experiments, 100 µM or 1 mM D-biotin was used for targeted monomerization. The overall amount of D-biotin is mutually dependent on the volume of D-biotin solutions besides the respective concentration. Notably, for $5x10^6$ cells a volume of 200 µL was sufficient to remove the *Strep*tamer signal for all tested Fab *Strep*tamers. Further experiments conclusively confirmed that larger cell numbers required respective multiples of 200 µL of a D-biotin solution per $5x10^6$ cells.
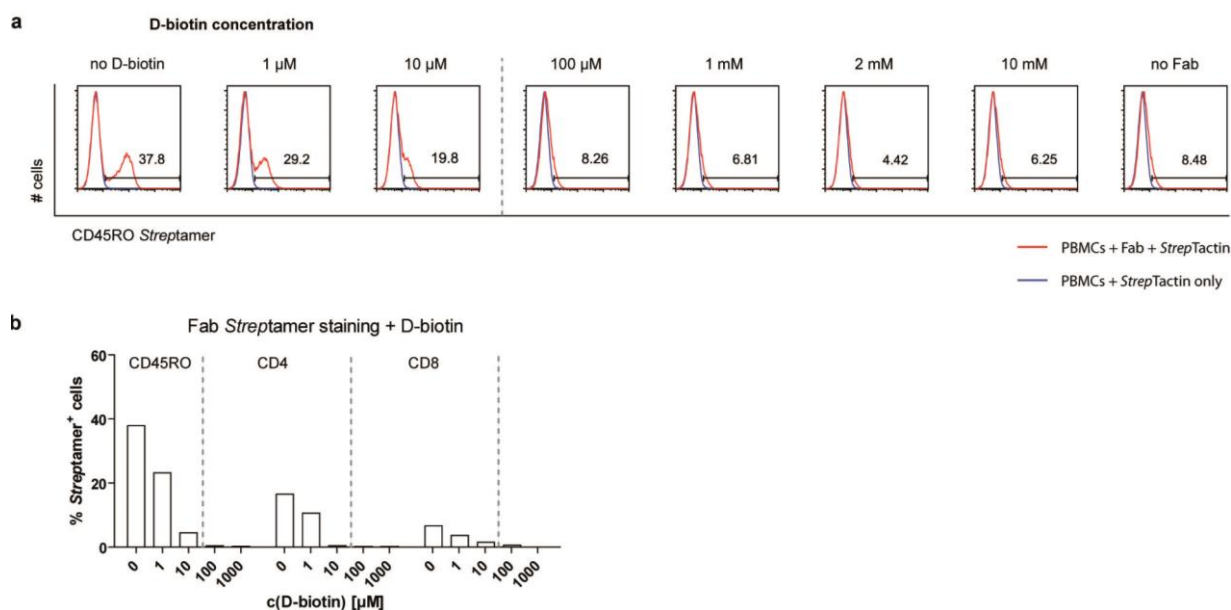

Fig. 0.10: D-biotin concentrations of 100µM clearly disrupt *Strep*tamer staining independent of target antigens

$5x10^6$ fresh PBMCs were stained with *Strep*tamers as described in section **5.1**. Different D-biotin concentrations were applied for 20 minutes to disrupt *Strep*tamer stainings. **a**. Cells were stained with a CD45RO-specific Fab *Strep*tamer, washed, and incubated in cold (4°C) PBS/0.5%BSA containing D-biotin at the indicated concentrations. **b**. Cells were stained with CD45RO, CD4, or CD8 *Strep*tamers. Independent of the specificity, 100 µM and in some experiments even 10 µM D-biotin was sufficient to disrupt the staining.

For the subsequent step – the dissociation of monomeric Fab fragments – however, higher volumes than 200 µL might have a positive influence on Fab dissociation, which already occurs during D-biotin incubation as well. To address this, we have titrated the wash volume during D-biotin treatment in increasing amounts. Only after D-biotin was removed, slight differences became abundant: samples washed with higher volumes, revealed lower staining intensities upon re-staining with dye-conjugated *Strep*-Tactin (data not shown).

Since also the complete removal of D-biotin is a very crucial subsequent step after *Strep*tamer disruption, which presumably also depends - similarly to Fab removal - on the wash volume, we reasoned that it would be most beneficial to create optimal conditions for removal of Fab and D-biotin in a single step while using as little D-biotin as necessary in the previous step.

Next, we aimed at analyzing the kinetics of Fab monomer dissociation during the first step-incubation with D-biotin. We re-stained CD45RO *Strep*tamer-stained cell aliquots after varying incubation periods with 1 mM D-biotin and performed subsequent washes for D-biotin and Fab removal from the supernatant to prevent re-formation of *Strep*tamers with unbound *Strep*-Tactin. We could demonstrate that incubation of at least 20 minutes is sufficient to prevent re-staining with residual Fab monomers and fresh *Strep*-Tactin after washing (**Fig. 5.11**). However, when incubation times are kept shorter (e.g. 10 minutes), small amounts of residual Fab monomers were still detected. Overall, our data indicate that it is not necessary for *Strep*tamer disruption to provide long incubation periods (> 20 min) with D-biotin.
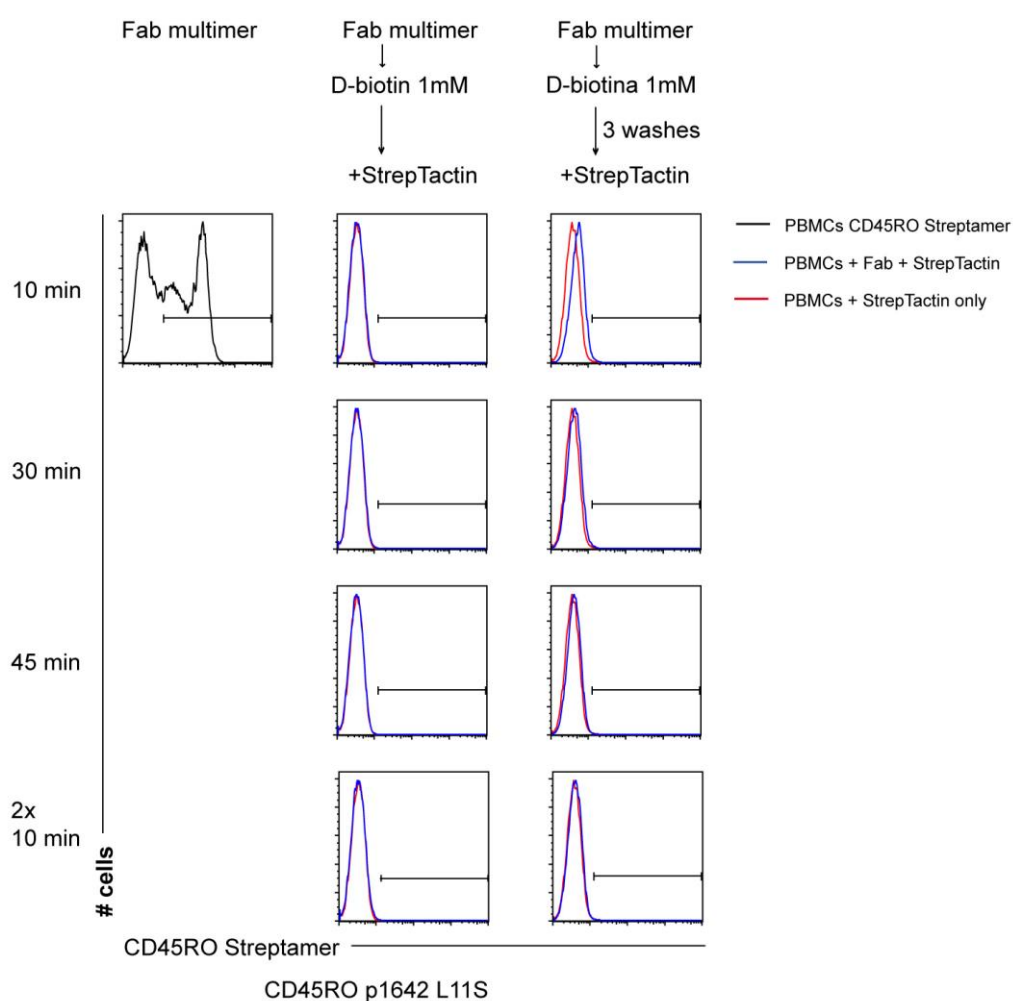
Fig. 0.11: Disruption kinetics of *Strep*-Tactin-based Fab-*Strep*tamers with D-biotin

$2x10^7$ fresh PBMCs were stained with a CD45RO-specific Streptamer and were split into 4 identical aliquots of 5x10^6 cells. Each aliquot was exposed to a 1 mM D-biotin solution (PBS/0.5%BSA/1 mM D-biotin) for 10, 30, 45 or 2x10 minutes. Cells were re-stained with fresh PE-conjugated *Strep*-Tactin in the presensce and absence of D-biotin (samples marked with 3 washes were considered biotin-free). All steps were conducted on wet ice (4°C). Red graphs represent control samples which were treated with PBS in place of Fab proteins.

Lastly, we aimed at determining the necessary wash volume and number of repetitive washes for the complete removal of Fab protein and D-biotin. The most time-sensitive parameter is most likely the spontaneous dissociation of Fab monomers from their target antigen. Since D-biotin does not further influence this step and an increasing number of wash steps might create a favoring equilibrium for dissociation, we thought to analyze *Strep*tamer re-staining depending on the number of wash steps (n) rather than the total wash volume.

$$c_n = \frac{c_0}{\left(\frac{V_2}{V_1}\right)^n}$$

(1) number of steps n, volume of protein solution V_1, volume of wash buffer V_2, initial concentration of Fab protein c_0, final concentration of Fab protein after n washes.

Formula 1 shows the effect of repetitive wash steps on the Fab protein concentration as a function of the number of washes. The same applies for the removal of the D-biotin or any soluble substance.

To determine the minimal number of washes necessary to remove D-biotin, we performed *Strep*-Tactin re-staining on *Strep*tamer stained cells, which had undergone a different number of wash steps upon addition of D-biotin. As shown in Fig. **5.12,** at least two biotin-free washes are needed to detect a *Strep*tamer signal in flow cytometry, indicating that at this point no more D-biotin interferes with the *Strep*tamer staining. We have previously seen how even very low concentrations of D-biotin lower the staining intensities of established *Strep*tamer stainings. In contrast to Fab dissociation, time kinetics only play a neglectably small role in D-biotin removal. The dissociation kinetics of surface-bound Fab monomers is most likely the most critical factor for complete removal. Since dissociation kinetics are specific to each individual Fab fragments, these have to be evaluated separately for each Fab Streptamer. We have demonstrated before (**Fig. 5.11**) that 20 minutes were sufficient for anti-CD8-Fab monomers to spontaneously dissociate from the cell surface. In this case this is the same time frame we also proposed as optimal for D-biotin incubation in combination with subsequent washing (see above), and these different steps (multimer disruption with D-biotin, Fab dissociation and removal of D-biotin/Fab by washing) could be elegantly combined by the following protocol: one wash with D-biotin followed by two additional washes with d-biotin-free buffer with a 10 minute incubation step in each wash step. Thus, the requirements for D-biotin removal by at least two centrifugation steps as well as the requirement for at least 20 minutes dissociation time are met. Consequently, we set up experiments testing this protocol. Multiple aliquots of the same *Strep*tamer-stained cells were incubated with D-biotin for 10 minutes and underwent one, two, or three additional washes à 10 minutes each. There is a clear difference between samples that underwent three 10-minute washes in total and those that underwent only one or two wash steps (**Fig. 5.12**; note that the Fab *Strep*tamer preparation used in this experiment maintained a fraction of a non-reversible component

for visualization of slight differences). In the following, all newly generated Fab Streptamers were tested for reversibility with this 'D-biotin incubation combined with washing' procedure and in combination with the flow cytometry-based assay. Only reagents that demonstrated full reversibility under these conditions were further used for *Strep*tamer-based cell selection.
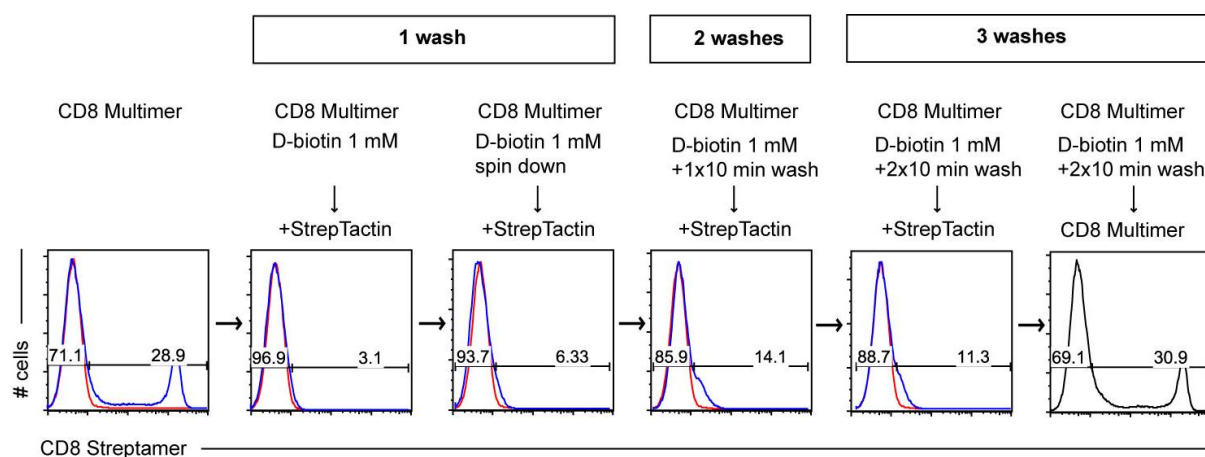

Fig. 0.12: Kinetics of Fab dissociation depending on the number and duration of additional wash steps

Fresh PBMCs were *Strep*tamer-stained and allocated to multiple aliquots. All aliquots were incubated with D-biotin for 10 minutes on wet ice and subsequently underwent one, two, or three additional washes à 10 minutes each in the cold (4°C). Samples were re-stained with unbound, PE-conjugated *Strep*-Tactin including control re-staining with Fab-*Strep*tamers.

5.2.3   Evaluation of anti-human Fab fragments for reversibility

From the above summarized results we concluded that (i) a 10-minute incubation with D-biotin is largely sufficient to fully disrupt Strep-Tactin-based Fab-*Strep*tamers, (ii) that two additional washes with a 10-minute incubation time during each wash are sufficient for the removal of residual Fab monomers, (iii) complete removal of D-biotin requires at least two washing/centrifugation steps, when 1 mM D-biotin is used. The flow-based reversibility assay can be subsequently applied for further quality control of remaining Fab-fragments. We next compared different unmutated and mutated Fab proteins for reversibility under these proposed conditions. Freshly isolated PBMCs were stained with PE-labeled Fab-*Strep*tamers. The cells were analyzed either before (**Fig. 5.13**, first column from the left) or after (second column) treatment with D-biotin. After two additional subsequent washing steps, potential remaining Fab-monomers were detected using unbound PE-labeled Strep-Tactin (third column from the left). A secondary Fab-*Strep*tamer staining served as a control for the successful removal of D-biotin (Fig. 5.13, right column). We demonstrated complete dissociation of the wild type CD62L Fab-fragment by revealing that no substantial residual Fab protein was detected by *Strep*-Tactin re-staining after 3 washes. Hence, *Strep*tamer stainings with the unmutated CD62L Fab fragment are fully reversible.
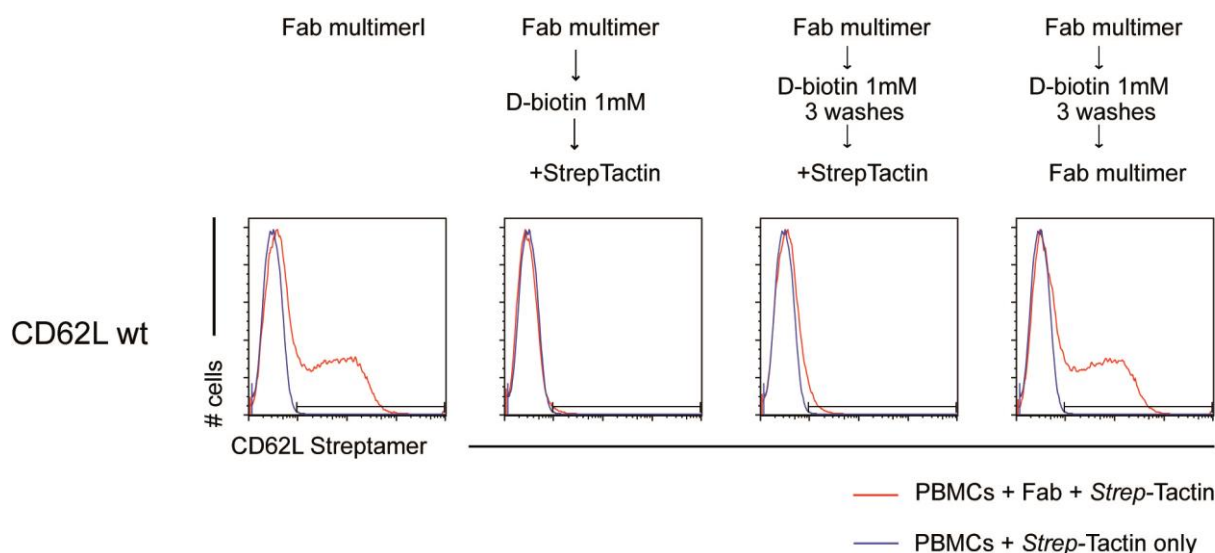
Fig. 0.13: Reversibility of CD62L Fab-*Strep*tamer: complete CD62L Fab monomer dissociation

10^7 PBMCs were stained with a CD62L-specific Fab-*Strep*tamer and subsequently exposed to D-biotin for 10 minutes on wet ice. Cells were then washed 2 times for 10 minutes each time at 4°C and subsequently re-stained with unbound, PE-conjugated *Strep*-Tactin or fresh CD62L Fab-*Strep*tamer as indicated.

Next, we tested CD8 Fab *Strep*tamer reversibility similarly. Although different donors showed varying results, we were always able to detect small amounts of residual Fab protein by *Strep*-Tactin re-staining indicating incomplete Fab dissociation. We hypothesized that these recombinant Fab preparations might contain a small fraction of non-reversible contaminants (e.g. by small aggregation). If this is the case, then it should be possible to accumulate this component on the cell surface by adding non-multimerized Fab-preparations. Therefore, we tested direct staining of cells with Fab *Strep*tamers with (Multimer) and without (Fab +ST) prior pre-incubation and direct staining of cells with non-multimerized Fab protein and addition of PE-conjugated *Strep*-Tactin after 20 minutes (Fab Mono). The same respective protein amounts were used on identical aliquots of the same PBMCs. The pre-incubation time of Fab protein and *Strep*-Tactin does not affect initial *Strep*tamer staining for CD8 (**Fig. 5.14a** left column). However, *Strep*-Tactin re-stainings differ distinctly between varying staining strategies. The Fab monomer staining with *Strep*-Tactin addition after 20 minutes of incubation of Fab monomers indeed accumulated the 'irreversible' component in the Fab preparation, whereas with conventional *Strep*tamer staining only small amounts of 'irreversible' component could be detected (**Fig. 5.14a** third column from the left). If the 'Fab monomer staining' approach allows to specifically test for potential 'irreversible' components, the 'irreversible' staining phenomenon should increase with increasing monomer concentrations. And indeed, increasing amounts of Fab protein show a substantial increase of *Strep*-Tactin re-staining (**Fig. 5.14b**). Others in the laboratory subsequently improved the Fab purification to fully remove the 'irreversible' components. In this context, the monomer staining procedure has become the standard test to demonstrate the quality/purity of fully reversible Fab preparations.
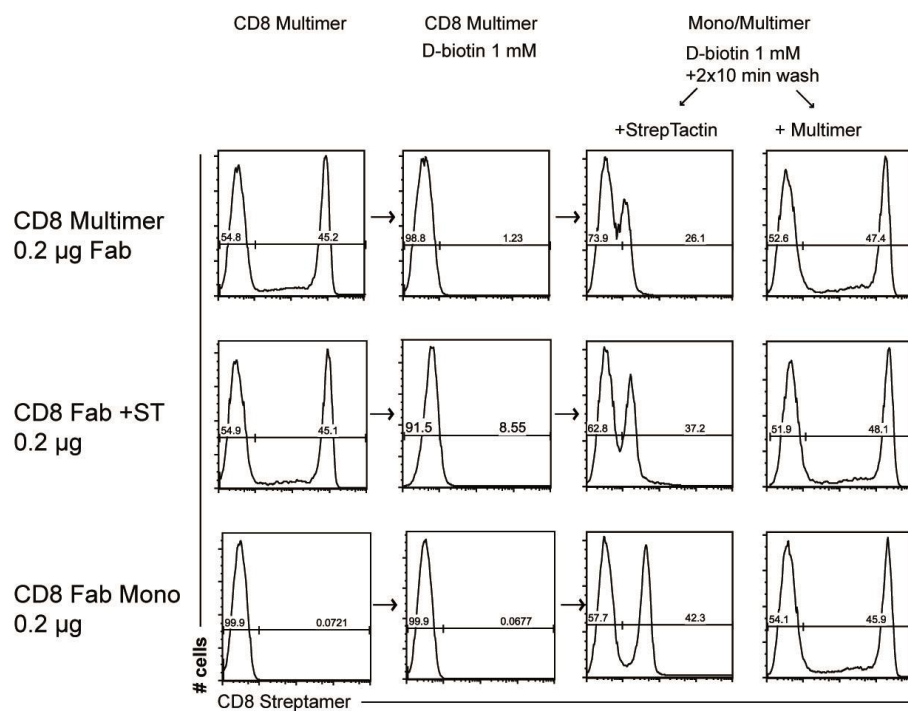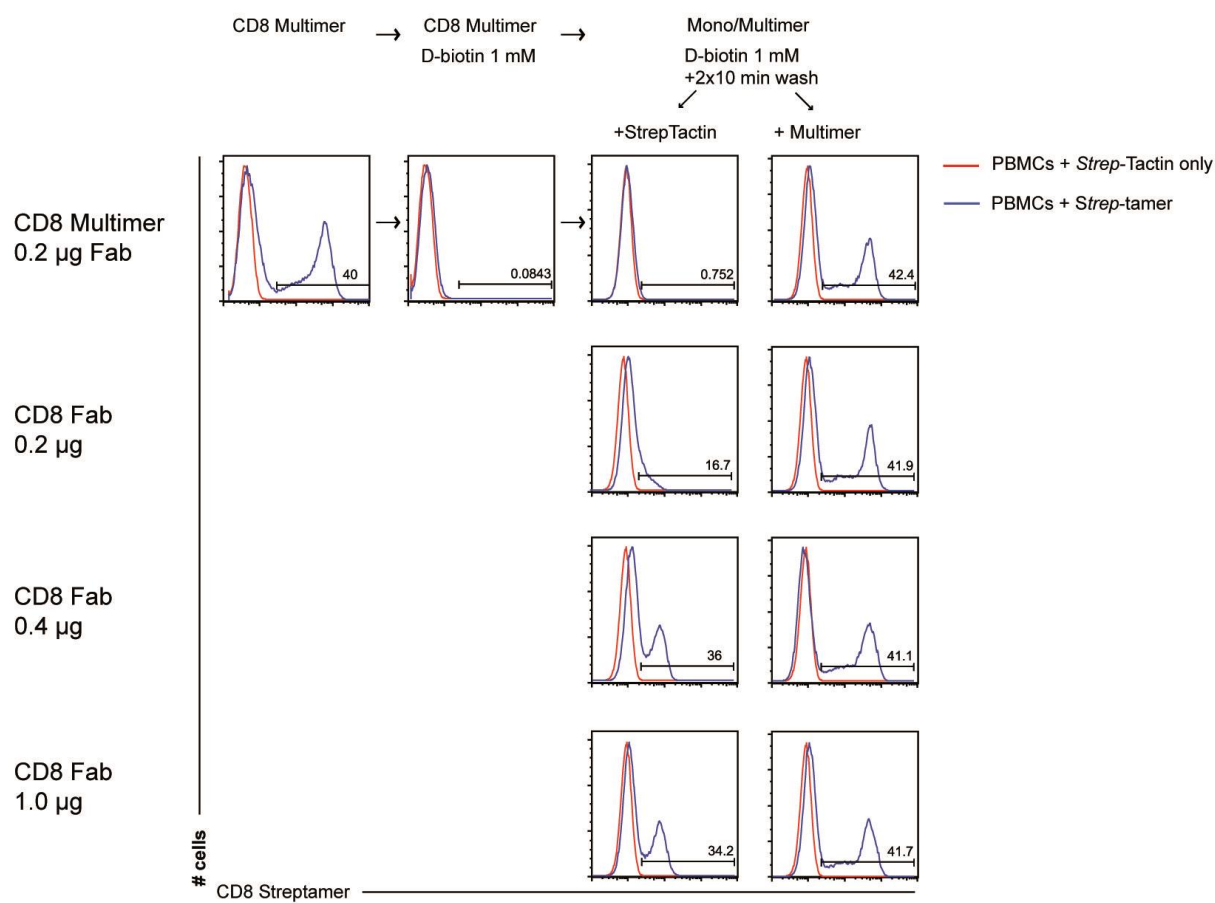
Fig. 0.14: Different multimerization strategies result in differences in *Strep*-Tactin re-staining

10^7 fresh PBMCs were stained with a CD8 Fab-*Strep*tamer, or incubated with unbound Fab monomers for 0 or 20 minutes before *Strep*-Tactin-PE was added. In the latter strategy, cells were analyzed by flow cytometry before *Strep*-Tactin addition as a control for unbound Fab background. Cells of all groups were subsequently exposed to 1mM D-biotin for 10 minutes on wet ice (4°C). Cells were then washed 2 times for 10 minutes at 4°C each time and re-stained with unbound, PE-conjugated *Strep*-Tactin or fresh CD8 Fab-*Strep*tamer.

The monomer staining assay initiated the idea to test whether Fab-*Strep*tamer staining could be generally improved if just the components (Fab monomer and *Strep*-Tactin-backbone) are added to the target cells separately (instead of adding preformed *Strep*tamers). This way the multimerization process should preferentially take place on the surface of cells expressing the Fab-specific antigen ('on-cell multimerization'). We tested this hypothesis and could indeed detect slightly higher staining intensities by 'on-cell multimerization' (**Fig. 5.15**). 10^6 fresh PBMCs were stained with monomers (with or without 20 minute incubation before *Strep*-Tactin addition) or pre-formed *Strep*tamers. We detected differences in staining intensities when the multimerization strategy is changed, independent of the respective *Strep*-Tactin-to-Fab ratio. Varying *Strep*-Tactin: Fab ratios resulted in dimmer or brighter staining depending on the Fab amount used, but for each ratio the pattern Fab + *Strep*-Tactin, 20 min > Fab + *Strep*-Tactin > *Strep*tamer regarding staining intensity is maintained.

For other Fabs than CD8 as well, side-by-side comparisons of the 'on-cell multimerization' strategy with the conventional strategy using pre-formed *Strep*tamers revealed differences in staining intensities of varying extent depending on the Fab specificity and even on the individual protein batch. For reversibility testing, is has become standard in the meantime to always apply the 'on-cell multimerization' strategy, since we found that the 'on-cell multimerization' pulled out more abundant *Strep*-Tactin re-staining in the case of inhomogenous Fab preparations.
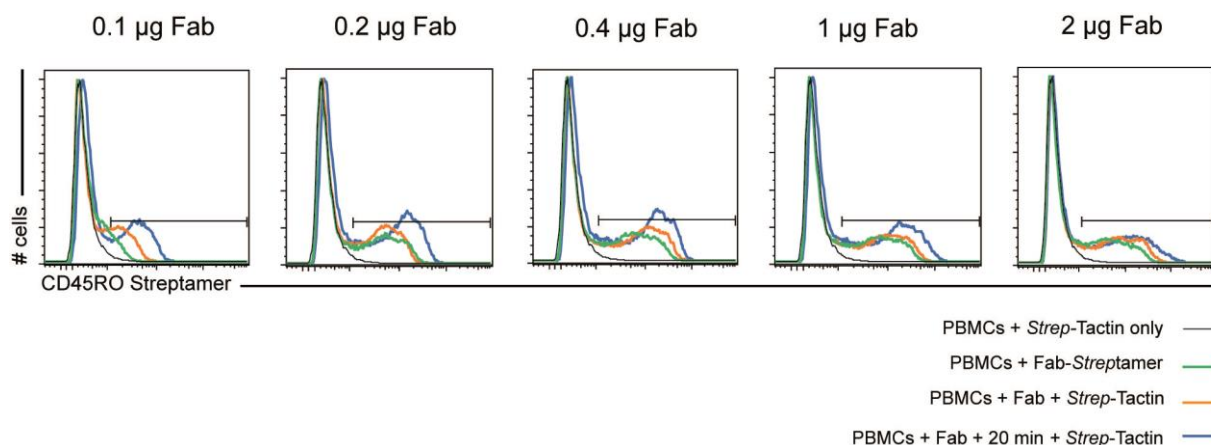
Fig. 0.15: Multimerization strategies affect staining intensities independently of the Fab concentration

10^6 fresh PBMCs were stained with a pre-incubated CD45RO Fab-*Strep*tamer (green histograms), or incubated with unbound Fab monomers for 0 (orange histogram) or 20 minutes (blue histogram) before *Strep*-Tactin-PE was added. From left to right: increasing amounts of Fab monomers were incubated with 10^6 cells or used for *Strep*tamer formation. *Strep*-Tactin was always used at 0.75 µg equivalent. All stainings were performed on wet ice (4°C).

We used this observation to test whether increasing the temperature during the dissociation step could help to eliminate also this component. For that reason, we tested two different temperatures selected by their relevance for clinical use. We first tested the CD8 Fab preparation containing the – at 4°C – 'irreversible' component using the standard reversibility assay at 4°C and room temperature (22°C) and found a dramatic difference between cold and warm conditions. Under warm conditions, the Fab dissociation was complete and no substantial re-staining could be detected (**Fig. 5.16**). Two donors with very different CD8 population sizes were compared and, as expected, the staining on the larger population was found to perform weaker in reversibility, as seen by means of a slightly increased staining intensity of *Strep*-Tactin re-staining. Under warm conditions, again, the reversibility could be rescued completely.
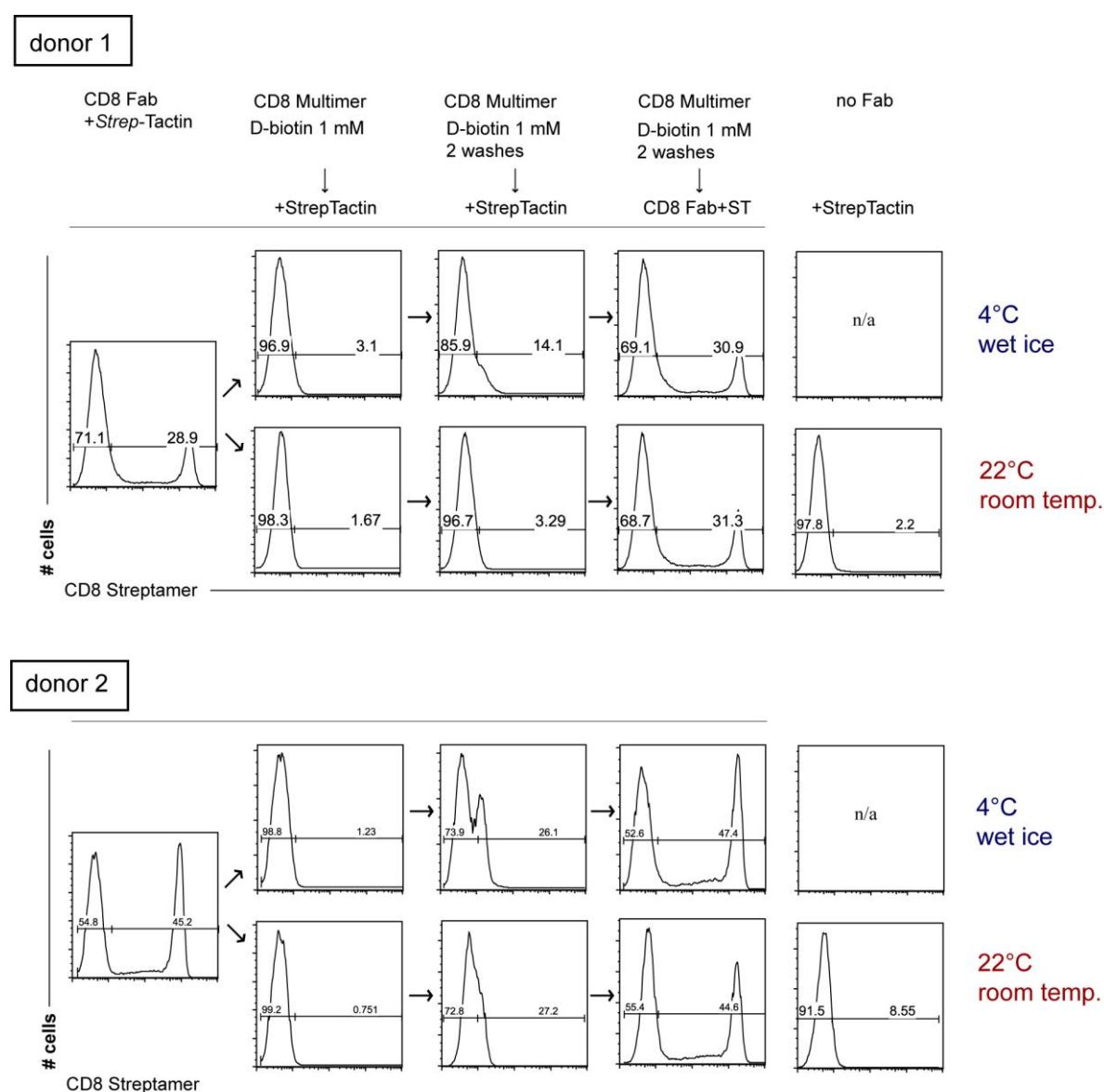
Fig. 0.16: FACS analysis of CD8 Fab-monomer reversibility at different temperatures

10^7 fresh PBMCs from two different donors were stained with Fab proteins and *Strep*-Tactin as previously described and the staining was subsequently reversed using 1 mM D-biotin in a three-step wash protocol as described. D-biotin and wash buffers were kept at either 4°C(wet ice) or 22°C (room temperature) during the process.

We next evaluated all 4 recombinant CD45RO Fab proteins that previously showed good surface staining using the reversibility test setup. Our panel of CD45RO Fabs consists of two pairs of a wildtype form and a mutated form, respectively. They differ in the light chain: one was generated by gene amplification of the UCHL1 hybridoma (p1641-42), the other was synthesized from the published sequence (p1643-44). Sequence analysis revealed variations in 7 amino acid residues thereof 6 within the constant region and 1 within the framework of the variable region. Interestingly, we could show that both wildtype Fabs performed unequally indicating that slight variations in the protein structure can have an impact on reversibility. The p1641 wt Fab exhibited a higher staining intensity upon *Strep*-Tactin re-staining than the p1643 wt (synthetic light chain) indicating incomplete Fab removal. The same holds true for the mutated forms. Introduction of the L11Sheavy mutation into both plasmids resulted in superior reversibility in the p1644 Fab (synthetic light chain) retaining the same pattern as the wildtype pair. In **Fig. 5.17a**, reversibility of both Fab pairs are shown in direct comparison using the same donor blood leukocytes. All four proteins were also tested on at least one other independent blood donor to account for inter-experimental differences (**Fig. 5.17b**). Although some variability can be observed between donors, most likely due to differences in individual CD45RO expression, the p1643 wt Fab and both mutated Fabs revealed better relative reversibility. Unfortunately, protein expression yielded very little protein from the mutated plasmids. Therefore, we decided to proceed with the p1634 wt Fab for selection experiments.
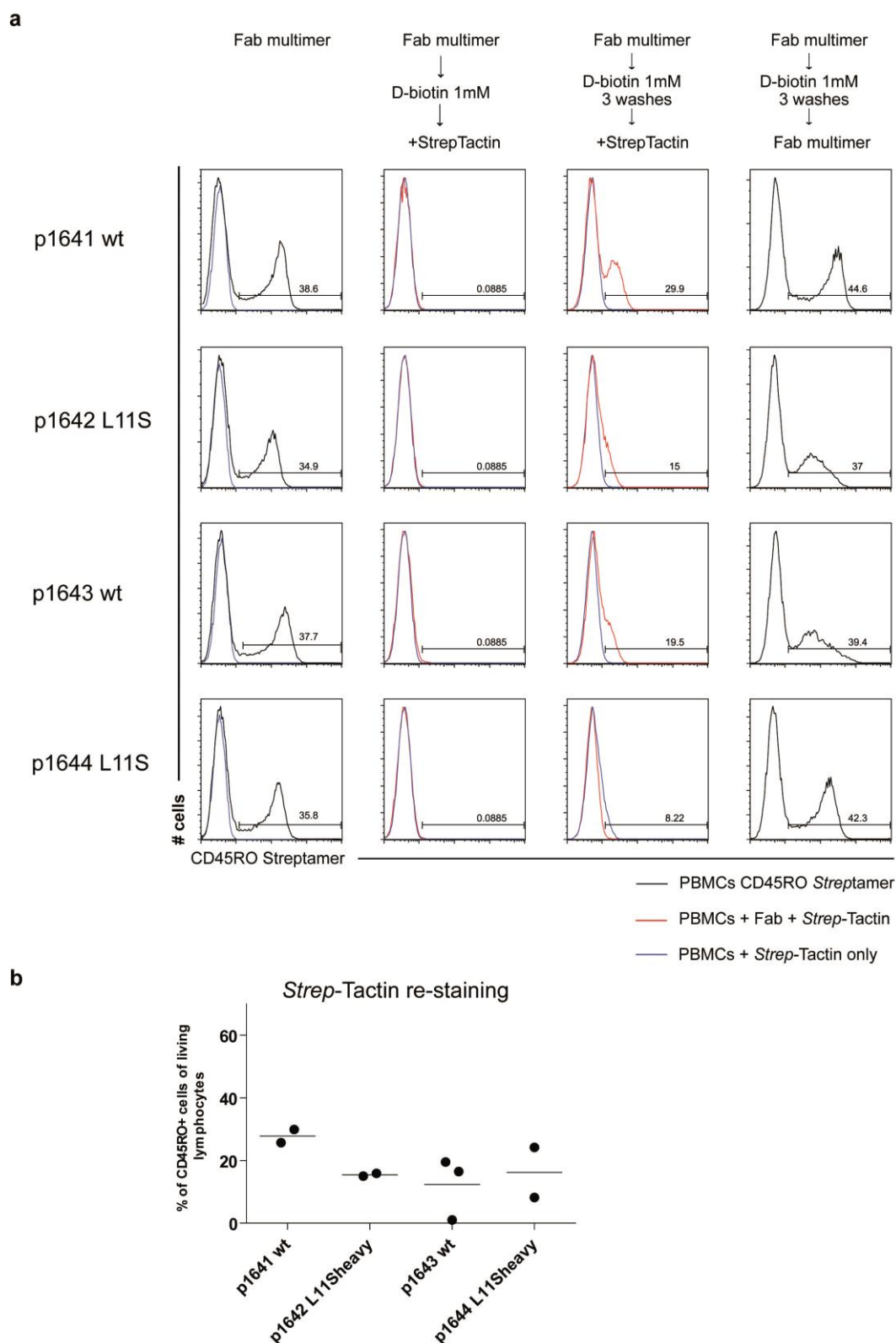
Fig. 0.17: Reversibility of CD45RO Fab *Strep*tamer stainings

10^7 fresh PBMCs were stained with 4 different Fab proteins and *Strep*-Tactin as previously described and the staining was subsequently reversed at 4°C using 1 mM D-biotin in a three-step wash protocol. **a**. Representative experiment compares all 4 Fabs in *Strep*tamer staining and reversibility. Live cells are shown. The numbers in dot plots indicate the percentage of cells within gates. **b**. Two or more repetitions of the described assessment of staining and reversibility. Dots represent the number of independent experimnets using different donor PBMCs (n=3 for p1643 wt, n=2 for all others).

We have previously shown that a temperature shift from 4°C (wet ice) to 22°C (room temperature) resulted in the complete removal of Fab fragments. We hypothesized that a smaller increase in temperature might have a similar beneficial impact on the reversibility while cells can still be maintained cooled. Interestingly, an intermediate temperature of 12°C (waterbath) was insufficient for complete reversibility in the most sensitive reversibility assay applying the 'monomer strategy'. Shifting the temperatue to 22°C resulted in the complete removal of CD45RO p1643 wt. We observed substantial *Strep*-Tactin re-staining after the 3-wash removal regimen upon addition of 1 mM D-biotin at 12°C, while performing all removal steps at 22°C led to complete Fab dissociation.

Interestingly, remaining reagent did not negatively interfere with control *Strep*tamer stainings (**Fig. 5.18**). This experiment indicates that increasing the washing temperature during Fab dissociation to room temperature should largely broaden the spectrum for Fab proteins that can be used for reversible staining and sequential positive selections. Furthermore, at higher temperatures also the sometimes contaminating 'at 4°C irreversible' components can be fully removed. 'On-cell multimerization' yielded higher staining intensities for some Fab *Strep*tamers, but is prone to accumulate more of the contaminant to the cell surface. Obviously this problem can just be overcome by shifting the washing temperature up.

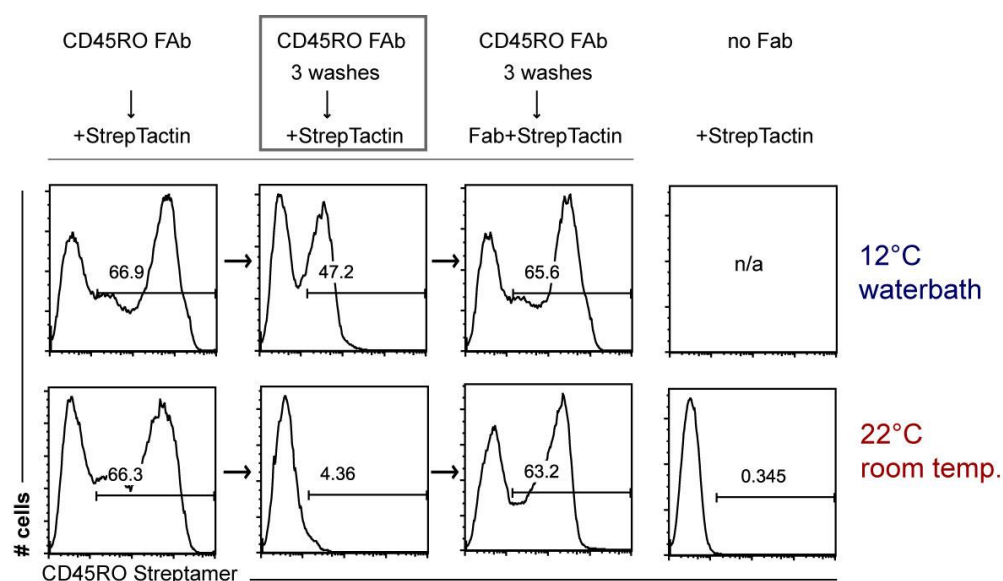**Fig. 0.18: Temperature dependency of CD45RO Fab dissociation kinetics**

10^7 fresh PBMCs were stained with monomeric CD45RO Fabs for 20 min before PE-labeled *Strep*-Tactin was added to the mix. The staining was subsequently reversed at 4°C using 1 mM D-biotin in a three-step wash protocol at 12°C (waterbath) or 22°C (RT). Living lymphocytes are shown. The numbers in histograms indicate the percentage of cells within gates.

5.3 Streptamer-based selection of *ex vivo* human PBMCs using nano-sized paramagnetic microbeads
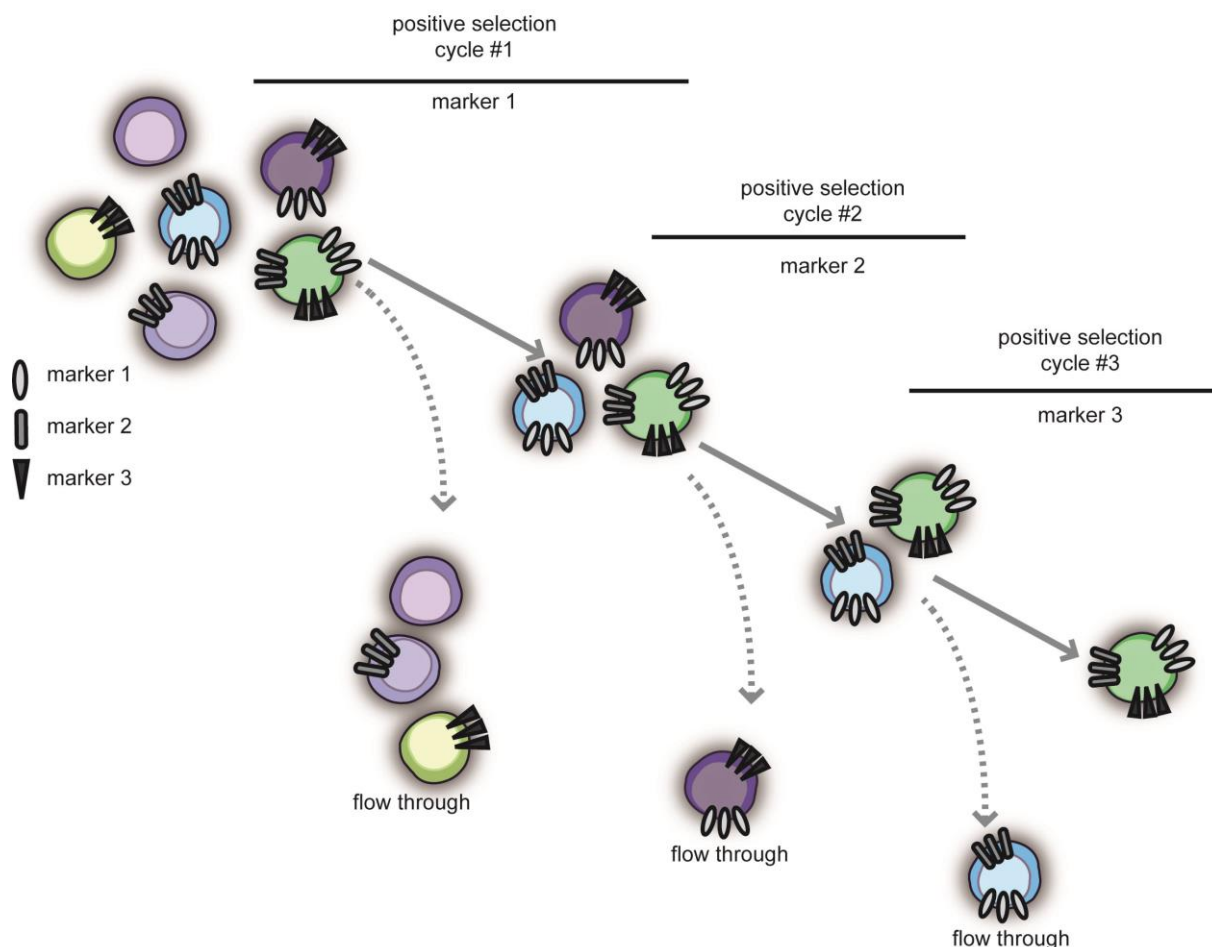
Fig. 0.19: Schematic overview on a sequential positive selection over three different cell surface antigens

The target population in this sequential positive enrichment procedure is defined by the simultaneous expression of all three markers. Each step represents one positive enrichment step leaving only positive cells for marker 1 in the first positive fraction after the first step. The second selection starts with only cells that are positive for marker 1 and results in a positive fraction of double positive cells (marker 1+2). In the final selection only triple positive cells are selected. This scheme reflects a strategy that can be used to enrich central memory T cells.

For the purpose of cell selection, Fab-*Strep*tamers can be generated with *Strep*-Tactin-coated magnetic beads. Depending on the specific size and surface of the beads, careful titrations of the *Strep*-Tactin-to-Fab ratio had to be performed to identify optimal conditions for cell enrichment. The polysaccharide-coated beads are 50 nm -150 nm in diameter and are covalently bound to *Strep*-Tactin on the surface. They are designed for the use with selection columns or the current state-of-the-art CliniMACS® clinical selection system. We have generated Fab *Strep*tamers specific for human CD4, CD8, CD62L, CD45RO, and CD45RA based on *Strep*-Tactin coated nano-sized magnetic beads

(provided by STAGE cell therapeutics, Göttingen) to answer the question, if our Fab-based reagents can replace conventional 'irreversible' antibody-based selection reagents. For multimerization of Fab proteins with *Strep*-Tactin coated magnetic beads we mixed 2 μg of Fab protein with a 7.5 μg *Strep*-Tactin equivalent of magnetic bead suspension at least 45 minutes prior to use. The above-stated quantities refer to the use on 10^7 PBMCs respectively unless indicated otherwise. We then measured cell viability by PI staining of lymphocytes and purity of the positive fraction after magnetic selection by re-staining with fluorophore-conjugated antibodies. For the recovery, positive target cells were counted before and after selection. The ratio of the number of positive target cells after selection to the target cell number before selection equals the recovery.

$$recovery = \frac{Cell\ number\ in\ positive\ fraction}{cell\ number\ before\ selection} * \frac{purity}{relative\ target\ cell\ frequency} * 100$$

We have performed positive selections of target cell populations with relative target cell frequencies between 20% (CD8) and almost 80% (CD62L) among living lymphocytes. All selections using CD4, CD8, CD62L, and CD45RO Fab-*Strep*tamers yielded very good viabilities, purities and recovery rates. For CD4 selection for example, the recovered positive fraction contained 99.8% CD4$^+$ living lymphocytes. Similar results were obtained for positive selections of CD8$^+$, CD62L$^+$, and CD45RO$^+$ selections. **Fig. 5.20a** illustrates all obtained results from one representative experiment for each marker. All initial relative frequencies and final purities of the positive cell fraction are shown. For CD45RA selections – an alternative to positive selection for CD45RO –, we chose to perform a negative selection. Therefore, the flow through during magnetic selection was collected. In this case the CD45RA depleted fraction is shown instead of the positive fraction from CD45RA enrichment. In **Fig. 5.20b** a summary of selection data generated using nano-sized magnetic beads is shown for each Fab including cell viability after selection, final purity (pre-gated on living lymphocytes) and recovery rates. The calculated recovery rates show a stronger variation between donors as opposed to the consistently uniform purities. Neither resulting viability and purity nor cell recovery correlate with the initial frequency of target cells. We have confirmed our observations by producing at least 2 (2-10) replicates.
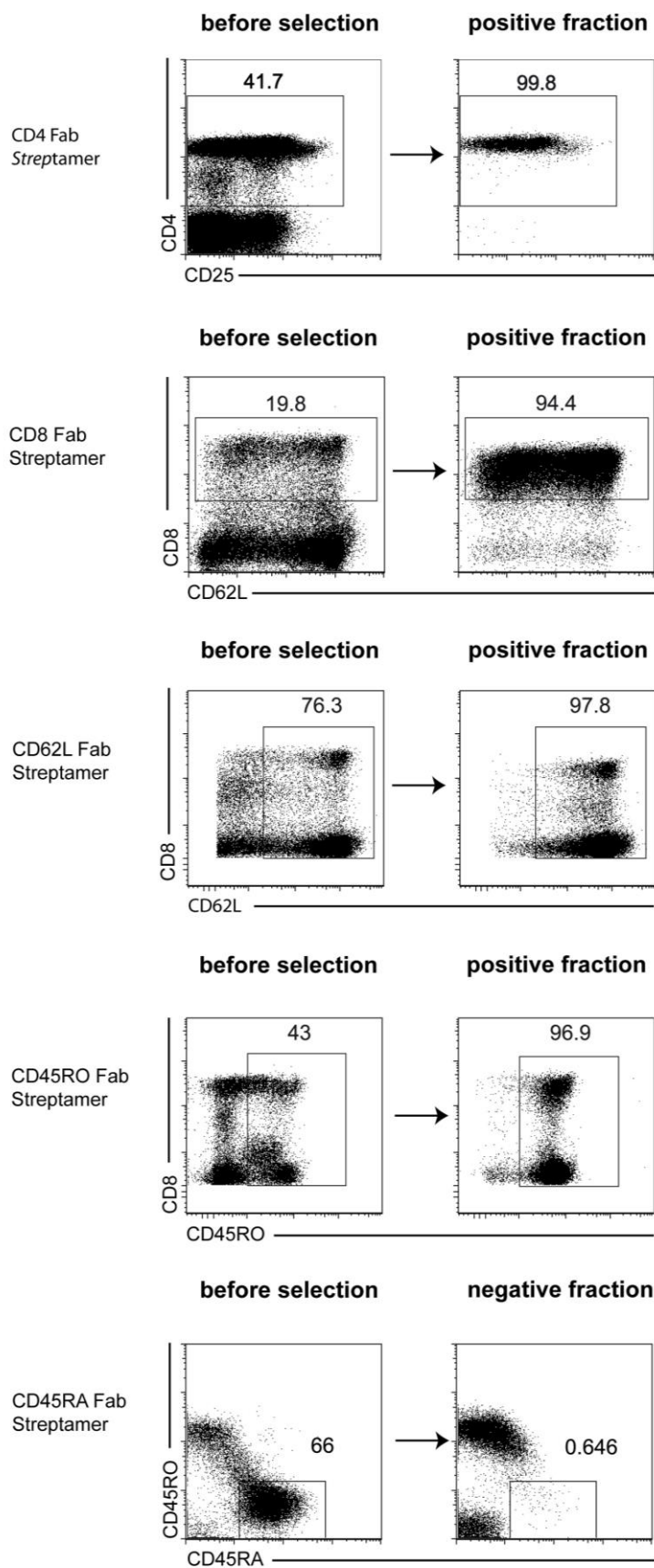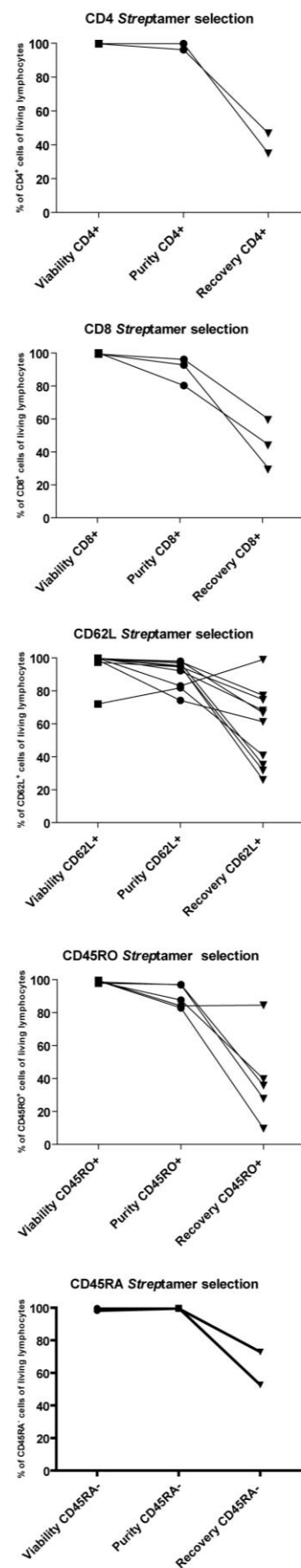
Fig. 0.20: A compilation of Fab-*Strep*tamer-based positive selections with nano-sized magnetic particles

a. 2x10^7 or 5x10^7 fresh PBMCs were prepared for column-based direct positive magnetic enrichment with Fab-*Strep*tamers of 5 different specificities. Each dot plot represents a fraction of cells taken either before or after the selection procedure upon re-staining with fluorescent antibodies for flow cytometry. The gates indicate the percentage of cells that are positive for each marker that was used for the respective selection. CD45RA selection aimed at the CD45RA-negative fraction. **b**. Purities, viability and recovery are plotted for selections with all 5 Fab-*Strep*tamers. All experiments were performed with at least 2 different donors (n=2 for CD4, n=3for CD8; n=10 for CD62L, n=5 for CD45RO; and n=2 for CD45RA).

When multiple positive selection steps are performed, all reagents must be removed from the positive cell fraction before it can undergo a second selection step. For nano-sized magnetic bead-based Fab-*Strep*tamers the removal of the *Strep*-Tactin backbone, which is covalently bound to the surface of the magnetic beads, as well as Fab monomers and excess D-biotin can be achieved by centrifugation and sequential wash steps. Small aliquots of the positive fraction can be re-stained with unbound *Strep*-Tactin as a control for Fab removal during the process as shown in the *Strep*tamer staining section. Similarly, a second selection step can only successfully lead to selection of cells in the positive fraction when D-biotin is efficiently removed, since otherwise the contact between cells and magnetic particles would be disrupted by excess D-biotin. We have now tested the sequential positive enrichment of CD45RO$^+$/CD8$^+$/CD62L$^+$ cells based on our positive results for the reversibility of Fab-based *Strep*tamer stainings. All three selection steps were performed with a D-biotin treatment using PBS/BSA/1 mM D-biotin and three wash steps of 10 minutes each in between selections. The first two sequential positive selection steps (CD45RO 1st, CD8 2nd) yielded a 90.5% pure CD45RO positive subpopulation for the first selection but only 25.5% purity of the second positive fraction following the second selection. Although the relative CD8 frequency has increased over the second selection (from 16.6% to 25.5%), no clear segregation of positive and negative cells was possible during the second selection We included reagent removal controls after each selection step by taking aliquots of the positive fractions. The first selection yielded a pure subpopulation, which tested negative for residual Fab monomers. Nonetheless, the second selection did not perform as desired. The same observation holds true for the third selection for CD62L$^+$ cells. No further purification occurred after the first positive selection step although the cells tested negative for residual Fab on the cell surface after both steps. Instead, the CD45RO$^+$ cell population was dragged through all selection steps and was not lost during multiple cycles of positive enrichment (**Fig. 5.21a**). The results suggest that the magnetic labels could not be completely removed from the CD45RO$^+$ population and might have been incorporated in folds of the cell membrane or into the intracellular space because of their small size. Very similar results were obtained from two or three step selections using different Fabs specific for other target antigens as shown in **Fig. 5.21b**. Independent nanobead-based positive selection experiments over one or two parameters confirm our previous findings. Final purities of the first or second target-positive fractions are shown resulting from different combinations of antigens that were targeted. Purities obtained during the second positive selection were substantially lower in all experiments and ranged in an unacceptable area mostly below 60%.

Based on these observations, we sought to investigate potential parameters that might help obtain good purities in nanobead-based sequential positive enrichments more thoroughly. We have therefore performed sequential CD8 (1st) and CD45RO or CD62L (2nd) selections using the nanobead technology. First, we tested positive fractions again for residual Fab monomers after a single subsequently reversed positive selection step. Instead of FACS staining with unbound *Strep*-Tactin, we now used unbound *Strep*-Tactin coated magnetic nano-sized beads. Similar to the re-staining with PE- or APC-conjugated *Strep*-Tactin, the incubation with *Strep*-Tactin coated magnetic beads after D-biotin and washing should result in magnetic cell labeling if cells had still Fab monomers on their surface. We performed positive selections with CD8, CD62L and CD45RO Fabs that have previously been tested negative in PE-conjugated *Strep*-Tactin re-stainings and one CD45RO wt Fab that has previously shown some *Strep*-Tactin-PE re-staining as a control that is known to be not completely reversible. The three positive populations selected with reversible Fabs were incubated with *Strep*-Tactin coated magnetic beads for 20 minutes and underwent a second selection step in which bead-labeled cells are separated from unlabeled cells. Surprisingly, 22% of the positive fraction was held back in a magnetic field in the second selection (*Strep*-Tactin control) step. From the CD45RO positive fraction selected with a partly irreversible Fab, 38% of the positive fraction was found in the second positive fraction. A proportion of cells might fail to lose their Fab markers upon D-biotin incubation, but this effect is not likely to be entirely based on 'irreversible' Fab monomers (seen even for fully reversible Fabs) since no substantial re-staining with fluorescent *Strep*-Tactin occurred in a similar setting and a difference in retention between a completely reversible Fab (in Strep-Tactin-PE re-staining) and a partly irreversible Fab was assessed (25% vs. 38%). When we repeated the experiment with different completely reversible Fabs and found 22%-28% retention in n=3 experiments (data not shown). This could be in line we our hypothesis that Fab-bead complexes are not removed from the surface in the first place because they are trapped in the cell membrane or might even get incorporated into the cell plasma.

For previous re-stainings with PE-labeled *Strep*-Tactin, we have set up controls without a specific Fab protein to determine unspecific *Strep*-Tactin binding. It is crucial for *Step*-Tactin coated nanobeads to conduct these controls as well. A selection from PBMCs with un-multimerized *Strep*-Tactin-beads without any Fab proteins at all resulted in a similar proportion of cells (4%; n=2) to wind up in the positive fraction of a magnetic selection step. This result rules out that attachment to the cell surface during the incubation period of *Strep*-Tactin coated beads alone is accountable for the failure of sequential positive enrichments. Nevertheless, a contribution of unspecific *Strep*-Tactin binding to the observed effect cannot be ruled out here. For that reason, we have tried to identify a sensitive target within the PBMC compartment for unspecific *Strep*-Tactin binding by Fab-free cell separations with *Strep*-Tactin coated nanobeads only. We could not find a difference between flow-through and positive fractions when both were subject to a positive enrichment step following incubation with *Strep*-Tactin coated nanobeads only nor was any of the fractions more or less prone to magnetic

labeling in the second selection cycle compared to the combined fractions or compared to fresh unselected cells. Taken together, we were able to determine unspecific labeling on a fraction of cells but failed to identify a *Strep*-Tactin-sensitive target that can be pre-cleared from the mixture of cells.

We proceeded on the assumption that unspecific binding of *Strep*-Tactin coated nanobeads occurs and expected it to be succumbed to the *Strep*-Tactin-to-cell ratio. Therefore, we titrated the amount of *Strep*-Tactin coated beads per cell. We found increasing occurrence of unspecific clustering of cells and beads indicated by unspecific retention in a magnetic field depending on the relative amount of *Strep*-Tactin coated nanobeads applied. These 'magnetically labeled' cells were pooled and incubated with increasing amounts of *Strep*-Tactin coated nanobeads for a second time. Surprisingly, even when the *Strep*-Tactin concentration in the second step was diluted 10fold, the number of cells in the positive fraction was still in the same range as when the *Strep*-Tactin was not diluted at all. We could not determine any titration effect. We conclude that magnetic particles are accumulated on the cell membrane or get trapped on the creased surface of the cells or even get internalized. This effect is in part Fab-independent and in part facilitated by multimerized conglomerates of beads with specific Fab proteins which help accumulate beads on the surface. In all experiments, cells that were retained before got carried through following selection steps because second positive fractions lack good purities but do not show substantial losses in cell numbers.

D-biotin could be ruled out as a factor, because the outcome of experiments was unchanged whether cells were pre-treated with D-biotin before the first selection step or in between steps compared to a D-biotin-free control group.

Taken together, unspecific binding with *Strep*-Tactin coated magnetic nanobeads regards about 4% of fresh human PBMCs. Assuming a maximal purity of 96% that can be achieved with this system in a single selection step, a three-step-selection would decrease the maximal possible purity to 88% assuming a steady proportion of unspecific labeling, which is already unsatisfactory for high-purity sorts of a specific subset of cells with a superior safety profile. Beyond that, our experiments have shown that in a second selection the Fab-independent unspecific labeling went up to 26% of cells of the first positive fraction, indicating that the cells which are initially selected are stably labeled with magnetic beads and are carried through the remaining selection steps. Depending on the initial cell number, then a substantial number of contaminating cells are positively selected throughout the entire process. Especially when large amounts of cells are selected in a clinical setting, the contamination rate would comprise several tens of millions of unspecific cells in a selection out of 10^9 PBMCs. We conclude that multiparameter selections on the nano-sized magnetic bead-based cell selection system are currently not feasible.

a

before selection

1st
CD45RO Fab
*Strep*tamer

2nd
CD8 Fab
*Strep*tamer

3rd
CD62L Fab
*Strep*tamer

positive fraction

b

2-step positive selections
with nano-sized beads

◆ Purity 1st pos selection
■ Purity 2nd pos selection
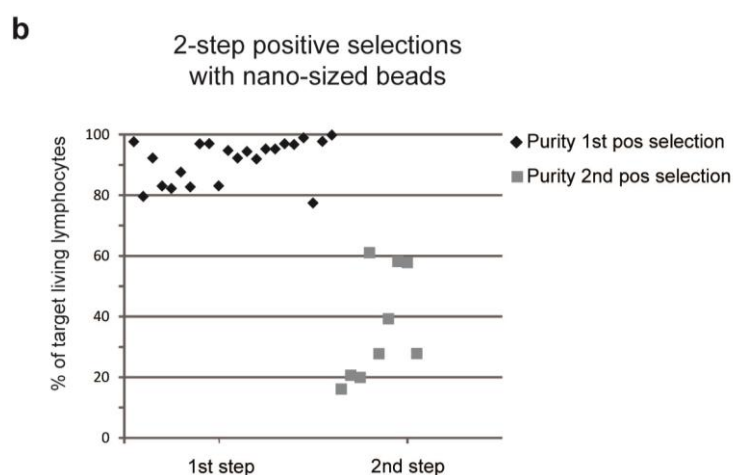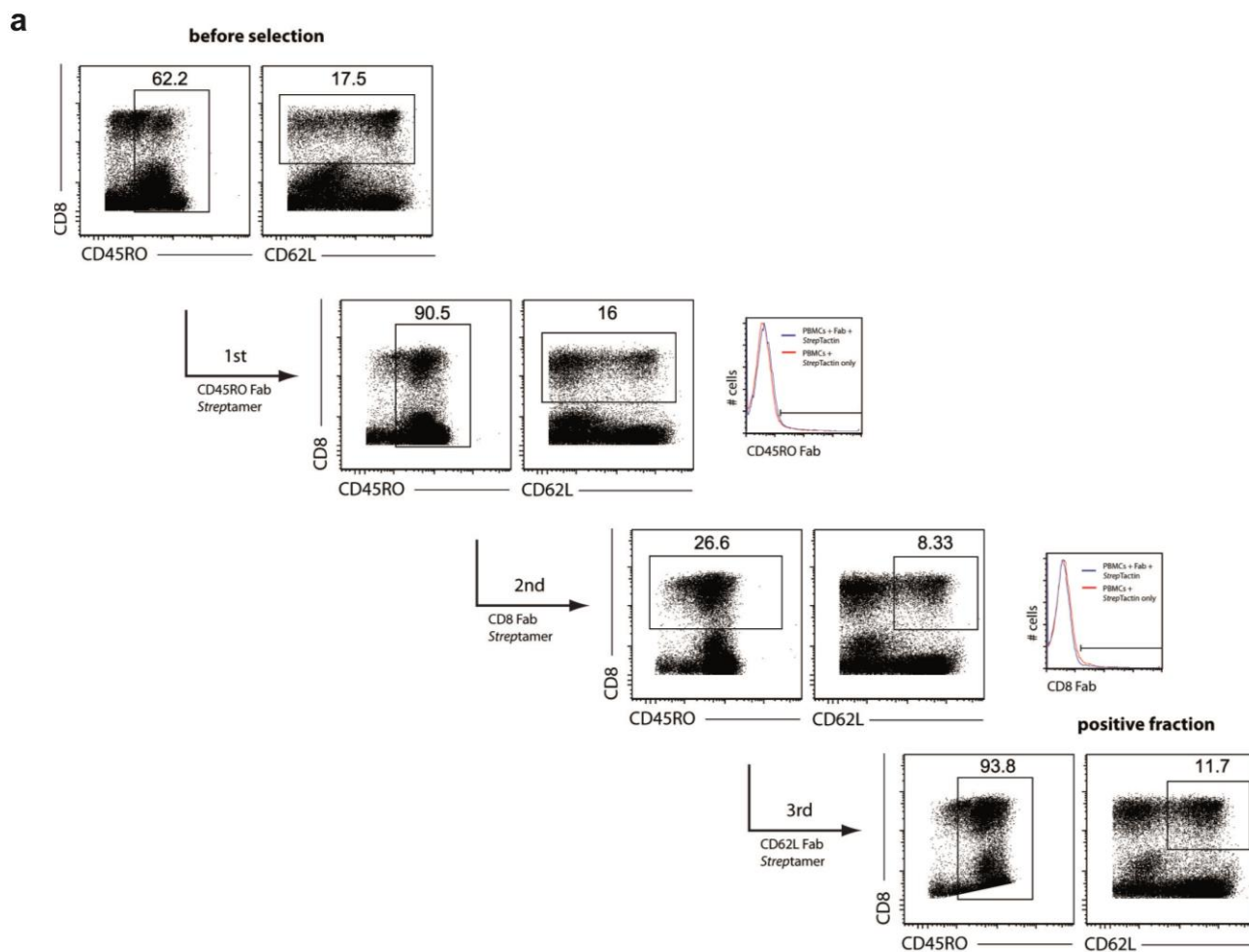
Fig. 0.21: Serial Fab-*Strep*tamer-based positive selection with nano-sized magnetic particles over three parameters

10^8 fresh PBMCs were prepared for column-based direct positive magnetic enrichment as previously described. **a**. Each dot plot represents a fraction of cells taken either before or after the selection procedure upon re-staining with fluorescent antibodies for flow cytometry. The gates indicate the percentage of cells that are positive for each marker which was used for

the respective selection. Histograms depict *Strep*-Tactin re-staining of an aliquot from the positive fraction 1 or 2 and control PBMCs which have never been exposed to Fab proteins. **b**. Final purities as percentage of living lymphocytes in the positive fraction 1 or in the positive fraction 2 (after 2 cycles of positive enrichment with reagent removal in between).

5.4 Development of a pre-clinical multi-parameter purification protocol using larger magnetic microbeads

An alternative approach to the nano-sized magnetic particles is the use of larger magnetic microbeads of at least 1µm in diameter, which can be applied with column-free cell separation systems using a hand held permanent magnet. The *Strep*-Tactin coated larger magnetic microbeads that were used in this thesis work have been developed by Stage cell therapeutics. Such particles might be advantageous because they are less prone to internalization or trapping effects and they could substantially speed up the selection and removal process due to the increased magnetic forces conferred to a cell. Furthermore, larger beads are easier to detect and easier to remove completely from the cells. Also from a regulatory point-of-view, the removal of larger beads might be advantageous because they are easier to track and the complete removal can be better controlled. Because of their size, microscope-aided tracking and under optimal conditions even microscopy-aided counting is possible. First, we used the size-advantage of larger magnetic particles to track co-localization of target cells and Fab-conjugated magnetic microbeads throughout a positive magnetic purification step followed by D-biotin treatment. **Fig. 5.22** illustrates microscopic images of all steps of a CD62L-specific selection from fresh PBMCs. Co-incubation with a CD62L-specific magnetic bead *Strep*tamer results in formation of clusters between a fraction of the cell mixture and the magnetic particles (red circles, CD62L$^+$ subset; **Fig. 5.22a**). Upon magnetic separation only cells clustered with microbeads are found in the positive fraction, whereas cells that have not clustered with magnetic beads are removed entirely by washing (**Fig. 5.22b**). After a 10-minute D-biotin incubation, cells and beads are both found in the positive fraction, but are now separated and no longer co-localized in clusters, indicating that cells are fully released from the magnetic beads (**Fig. 5.22c**).
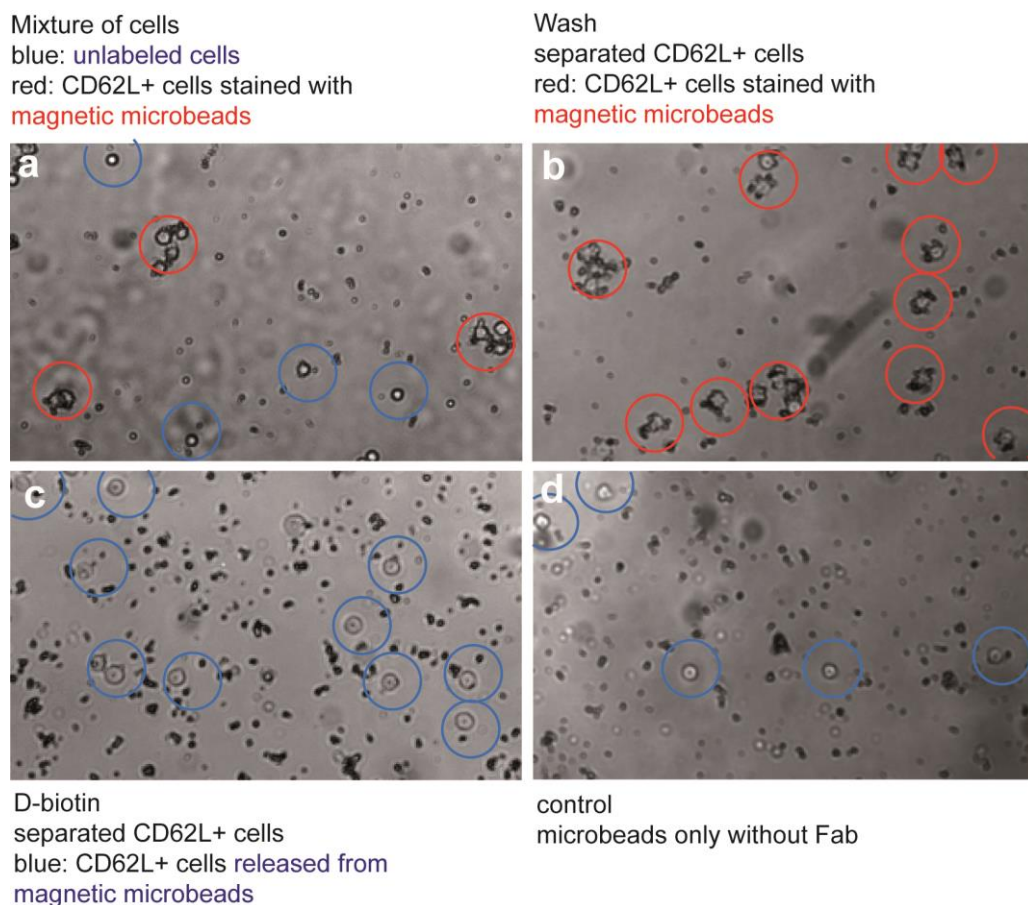
Mixture of cells
blue: unlabeled cells
red: CD62L+ cells stained with
magnetic microbeads

Wash
separated CD62L+ cells
red: CD62L+ cells stained with
magnetic microbeads

D-biotin
separated CD62L+ cells
blue: CD62L+ cells released from
magnetic microbeads

control
microbeads only without Fab

Fig. 0.22: Microscopic tracking of positive magnetic selection and removal of magnetic microbeads

CD62L-specific microbeads were used as a selection reagent to separate CD62L+ cells from a PBMC mixture. **a**. The mixture of cells was incubated with CD62L specific magnetic microbeads which co-localize and cluster with the CD62L+ subpopulation of the cells. **b**. Unlabeled cells were washed away in a magnetic field. **c**. 5 mL of a 1 mM D-biotin solution was added to the positive fraction to release all clusters. **d**. The mixture of cells was co-incubated with only magnetic microbeads without a Fab-mediated specificity as a control for unspecific co-localization.

5.4.1 Optimal parameters for magnetic microbead selections

We now sought to identify the optimal parameters for selections using larger magnetic microbeads (termed microbeads in the following). We have used a *Strep*-Tactin equivalent of 7.5 µg of *Strep*-Tactin-coated magnetic microbeads together with 2 µg of CD8 Fab for multimerization of a CD8-specific selection reagent for the purification from a starting number of 10^7 cells unless indicated otherwise. A selection with CD8-specific Fab *Strep*tamers was performed during which cell fractions before and after the separation procedure were re-stained with a commercial CD8 antibody or with a PE conjugated CD8 Fab *Strep*tamer along with a CD3 antibody. CD8 expression was higher on CD3$^+$/CD8$^+$ double positive cells (T cells) and resulted in the complete depletion of those cells in the negative fraction (**Fig. 5.23**). The *Strep*tamer re-staining (**Fig. 5.23**; upper panel) was useful for us to judge the depletion rate from the negative fraction and the purity of the positive fraction in the most direct possible way. Since both re-stainings depict redundant information, the CD8-specific antibody

clone B9.11 (**Fig.5.23**, lower panel) was used for all relevant re-stainings in the following. The CD8 positive cell population comprises of a high expressing T cell fraction (CD3+) and a lower CD8 expressing CD3 negative fraction. The high expressing subset is clearly favored during the selection process resulting in a higher proportion of CD8+ T cells in the positive fraction. The differences in the flow-through (negative) fractions are even more obvious. The depletion from the negative fraction is an indirect measure of the cell recovery rate, when all cells are collected for flow cytometry analysis. The lower the count and specific frequency in the negative fraction, the higher are the recovery rates. For CD8+ T cells both purity and depletion are in the maximal possible range of close to 100%.
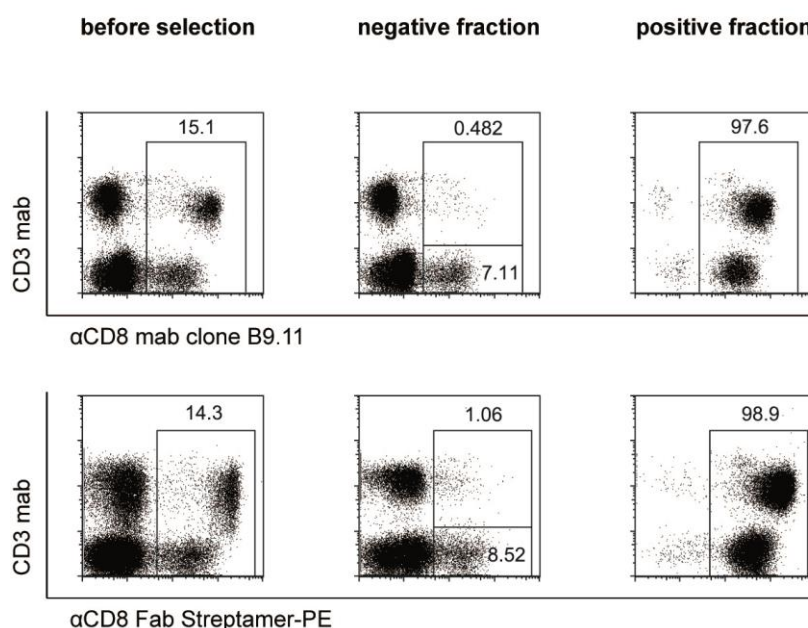

Fig. 0.23: CD8-specific *Strep*tamer selection using larger magnetic microbeads

5×10^7 fresh PBMCs were magnetically labeled with CD8 *Strep*tamers for magnetic separation using a column-free system with a simple hand-held magnet. All fractions were counted and aliquots were re-stained with either PE-conjugated CD8 *Strep*tamer (upper panel) or the commercially available PE-conjugated antibody clone B9.11 (lower panel). Live lymphocytes are shown. The numbers in dot plots indicate the percentage of cells within gates.

As mentioned earlier, the use of different *Strep*-Tactin backbones makes titrations of the *Strep*-Tactin-to-Fab ratio inevitable. We have used the CD8-specific Fab to test selection at different *Strep*-Tactin-to-Fab ratios. In the range of $1.25 - 5.0$ µg CD8 Fab per 2.5×10^7 cells the respective recovery rates but not the purities showed a significant difference (**Fig. 5.24a**). To confirm this, blood from 1, 2, or 4 different donors was included in independent experiments (**Fig. 5.24b**). The next titration was conducted in order to test the influence of the incubation time on purities and recovery rates of CD8 cell selections using larger magnetic microbeads. This test has a dual purpose: on the one hand, we expect to retain more CD8+ cells when the incubation time is increased, on the other hand, we wanted to test for unspecific binding, which might occur when the incubation period is too long. Fortunately,

no unwanted cells were found in the positive fraction after 20 minutes, 40 minutes or 60 minutes of incubation (**Fig. 5.24c**). The recovery rates, however, did increase in correlation with the incubation time in a range from 20-60 minutes (**Fig. 5.24d**). This effect can be exploited for setting up selection protocols when only very little donor cells are accessible in order to increase the recovery rates if necessary. For all other sorts, however, the incubation time for each positive selection step should not exceed 30 minutes because the process of multiple selections would otherwise get too time consuming.
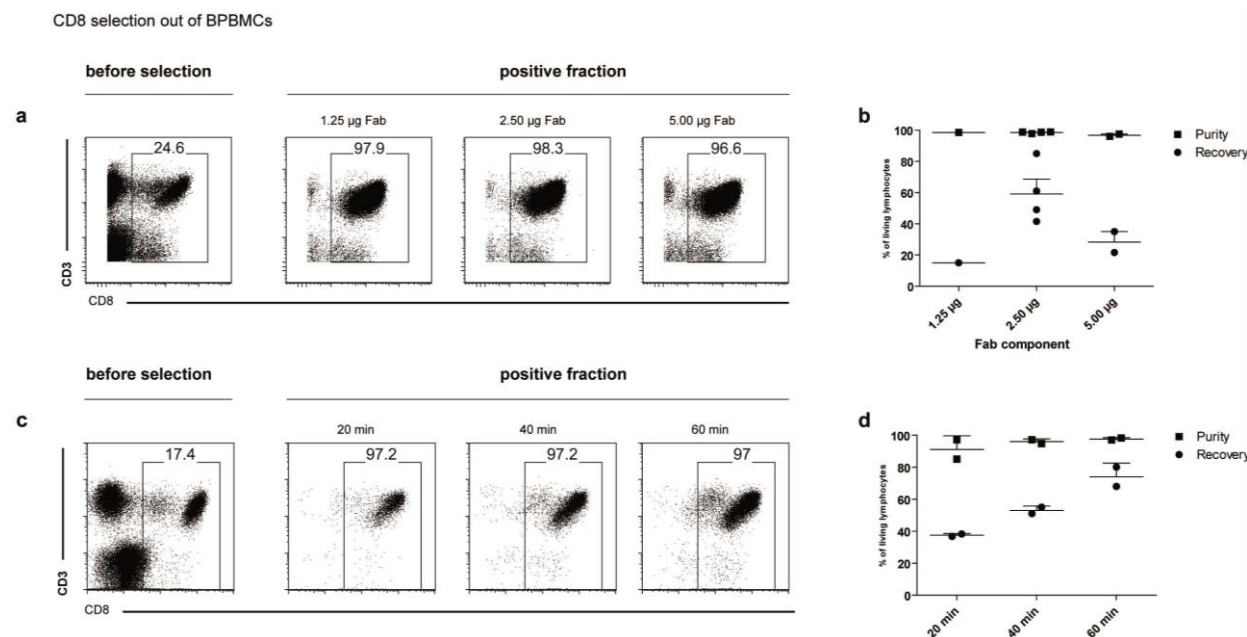

Fig. 0.24: Recovery rates but not purities of CD8 *Strep*tamer selections correlate with protein amount and incubation time

2.5×10^7 fresh PBMCs were separated using different CD8 specific *Strep*tamers with varying *Strep*-Tactin-to-Fab ratios. All fractions were counted to determine cell numbers and aliquots were re-stained with CD8 antibodies to determine purities. **a**. For the selection of 2.5×10^7 PBMCs, 1.25, 2.5 or 5.0 μg Fab protein was multimerized with a *Strep*-Tactin equivalent of 22.5 μg of magnetic microbeads. **b**. Summary of multiple experiments performed with different donor blood. Purities and recovery rates are shown depending on the Strep-Tactin-to-Fab ratio. **c**. Selection of CD8$^+$ PBMCs using multimers of 5.0 μg Fab. Incubation time was 20 minutes, 40 minutes, or 60 minutes before separation in a magnetic field. **d**. PBMCs from two different donors are shown.

5.4.2 Sequential positive magnetic enrichment over two parameters

For magnetic bead-based Fab-*Strep*tamers, the removal of the *Strep*-Tactin backbone, which is covalently bound to the magnetic beads, can easily and rapidly be done by magnetic separation with a permanent magnet after D-biotin is added for *Strep*tamer disruption. To demonstrate that larger magnetic bead-based *Strep*tamers are fully reversible and sequential positive enrichment is possible, we performed first positive selections using CD8 *Strep*tamers followed by a second positive selection for CD62L positive cells. Very good purities for the intermediate positive fraction (97.7% of live

lymphocytes) and the final (second) positive fraction (97% of live lymphocytes) were obtained (**Fig. 5.25**). Among 22 independent replicates of sequential CD8/CD62L positive selections from different donor-PBMCs we observed only very little variation between overall purities but a larger spread between individual recovery rates (shown in right graph). When we repeated these experiments multiple times we thereby also interchanged orders of CD8 and CD62L selection steps. There was no evidence that a specific order of reagents/separation steps resulted in better overall purities. Therefore, we believe that it is advantageous to start serial positive selections with the specificity that is represented by the lowest number of positive cells within the original cell specimen, since this strategy should allow performing selections with lowest amounts of reagents and buffers.
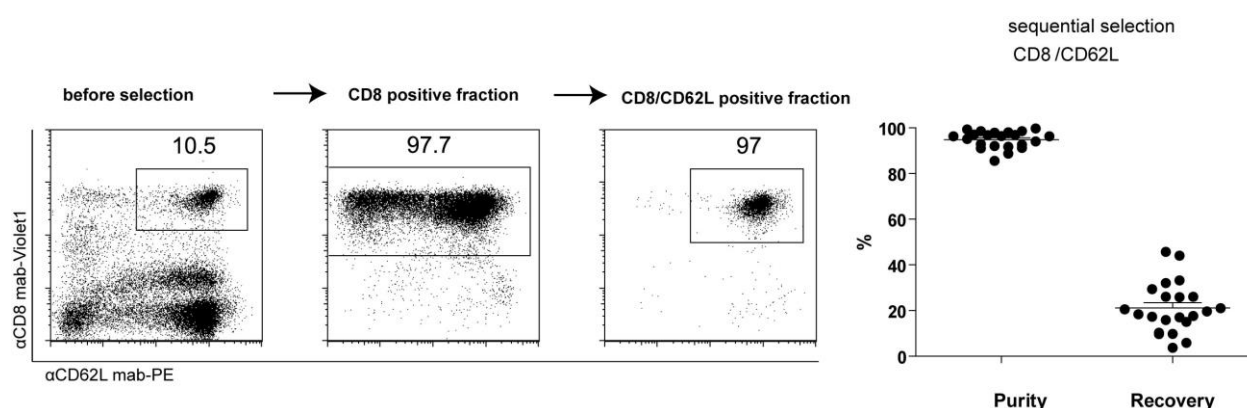

Fig. 0.25: Sequential positive enrichment of a CD8$^+$/CD62L$^+$ cell subset from fresh human PBMCs

A two-parameter positive magnetic enrichment was performed on 10^8 fresh human PBMCs. Aliquots from before the selection and each positive fraction are shown. The numbers in dot plots indicate the percentage of cells within gates. Purities and recovery rates were taken from 22 independent experiments from 2×10^7-10^8 initial PBMCs.

We assumed that by further evaluation of different selection parameters and conditions the overall recovery rates could be improved. Those experiments included a fine titration of the CD62L reagent. CD8$^+$ cells were incubated with a CD62L-specific microbead reagent with varying *Strep*-Tactin-to-Fab ratios like previously described above for CD8. Similarly, higher Fab concentrations did not yield higher cell recovery rates. We detected an optimum in cell recovery at a *Strep*-Tactin-to-Fab ratio of 1 µg per 10^7 pre-selected CD8$^+$ cells. We have verified the cell recovery on the level of absolute cell numbers as well (**Fig. 5.26**). Furthermore, we titrated wash steps and wash volume without recognizing a correlation with the cell recovery rates. A larger wash volume generally resulted in higher purities but slightly lower cell recoveries.
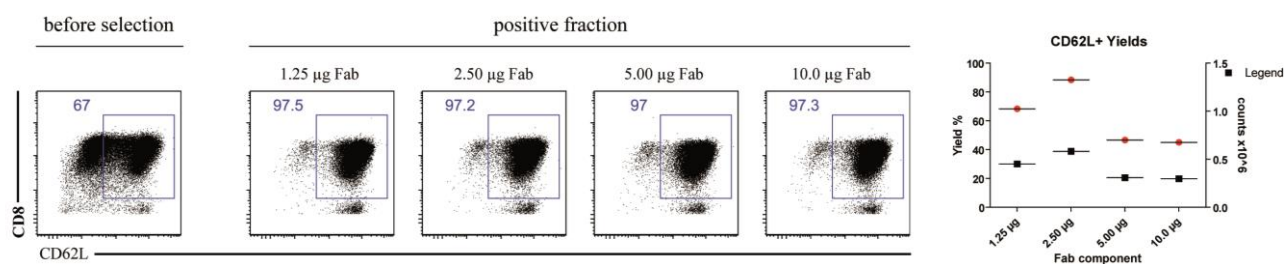
CD62L selection out of CD8+ cells

Fig. 0.26: Different Strep-Tactin: Fab ratios influence the recovery rates but not purities of CD62L *Strep*tamer selections

2.5×10^7 pre-selected CD8$^+$ PBMCs were separated using different CD62L specific *Strep*tamers with varying *Strep*-Tactin-to-Fab ratios. All fractions were counted to determine cell numbers and aliquots were re-stained with CD8 and CD62L antibodies to determine purities. Precisely, 1.25, 2.5, 5.0 or 10.0 µg Fab protein was multimerized with a *Strep*-Tactin equivalent of 2.5 µg of magnetic microbeads. Absolute cell numbers were determined (red graph and right axis) and cell recovery rates were calculated based on the initial cell number (black graph and left axis).

5.4.3 Sequential positive magnetic enrichment of central memory T cells

Ultimate goal of this thesis work was the development of a protocol enabling efficient enrichment of central memory T cells (T$_{CM}$), either CD8$^+$ or CD4$^+$. In order to do so, we started by sequential targeting of the markers CD8, CD62L and CD45RO, which should allow enrichment of CD8$^+$central memory T cells (T$_{CM}$) in a three-parameter sequential purification setup. A representative complete selection cycle is depicted in **Fig. 5.27**. CD8$^+$ T cells were almost completely depleted from the negative fraction and recovered at 98.3% purity in the first step. 94.7% of all recovered CD8+ cells were CD8$^+$/CD62L$^+$ double positive before CD62L selection in this donor and were enriched to 99.3% purity in the CD62L selection step with some target cell loss during the second wash. The final step yielded a 89% overall purity and reached a cell recovery of 18% (referring to the absolute T$_{CM}$ number before selection). These data show for the first time that positive enrichment of a complex cell population is possible with multiple reversible selection reagents. Since reversible MHC *Strep*tamers are already in clinical use and GMP-conform selection protocols have been approved by regulatory authorities for this purpose, it seems feasible to transfer the serial positive enrichment procedure with Fab-*Strep*tamers similarly to clinical applications. So far, clinical CD8$^+$ T$_{CM}$ enrichment has only been described by use a series of depleting antibodies such as CD4, CD14 and CD45RA in a single negative selection step followed by a positive selection step for CD62L$^+$ cells. To our knowledge, this strategy never reached purities of CD8$^+$ T$_{CM}$s any close to what we describe here for the Fab-*Strep*tamer selections.
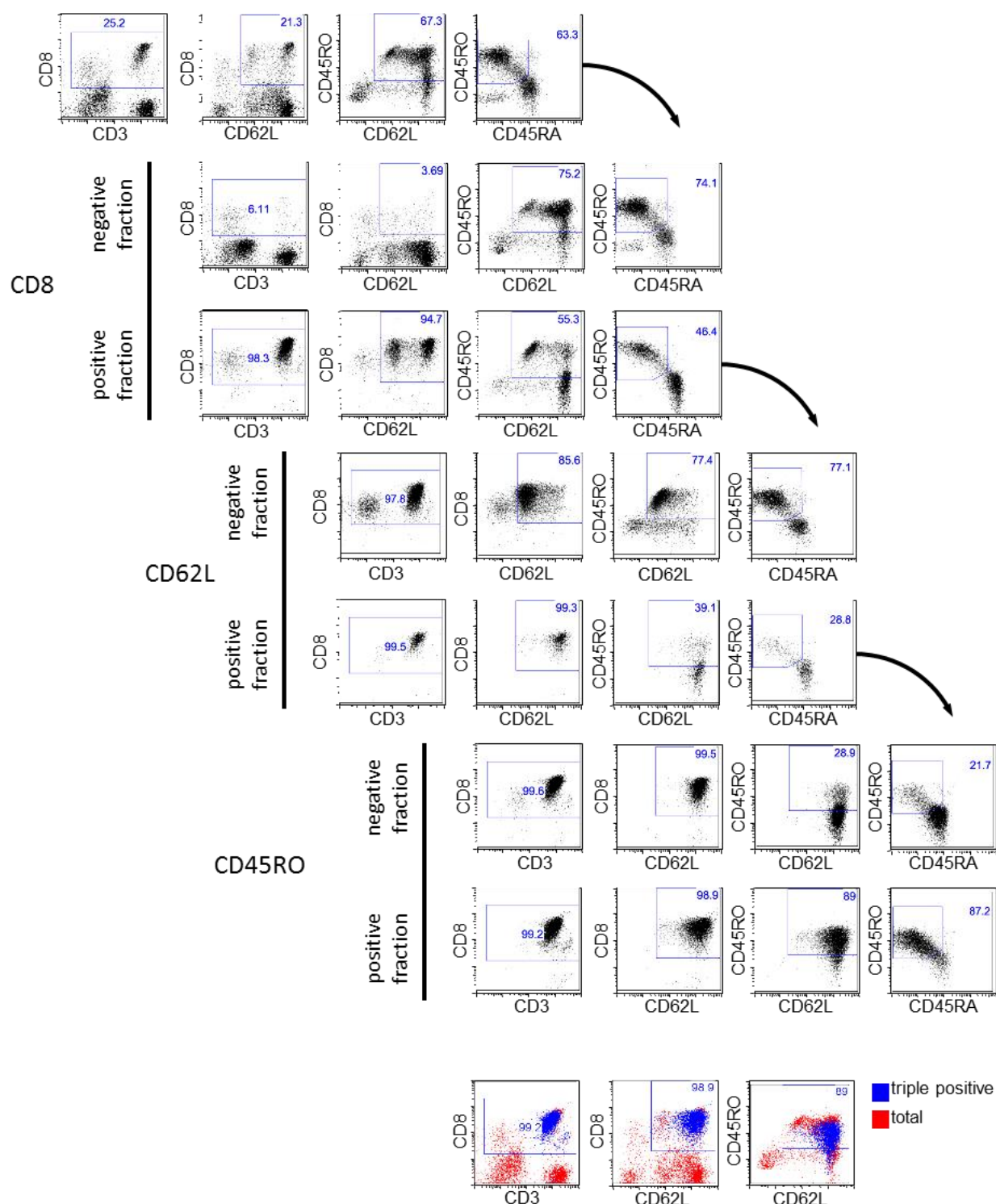
Fig. 0.27: Sequential positive enrichment of human central memory T cells

5×10^8 fresh human PBMCs were incubated with anti-CD8 Fab-*Strep*tamers conjugated with Strep-Tactin-functionalized magnetic microbeads. The CD8 positive fraction was collected and treated with 1 mM D-biotin and washed twice to remove remaining reagents. In a subsequent second selection step, CD62L positive T cells were enriched from the $CD8^+$ fraction as described for the first step. Finally, $CD45RO^+$ cells were enriched using a CD45RO specific Fab-*Strep*tamer conjugated to Strep-Tactin-coated beads. Living lymphocytes obtained before and after each selection step are shown.

5.4.4 CD45RA depletion

As an alternative to the positive CD45RO selection step in the T_{CM} enrichment protocol, it is also possible to enrich for the desired population by depletion of CD45RA$^+$ cells. Expression of CD45RA should in principle exclude expression of CD45RO. We have tested direct CD45RA Fab-*Strep*tamer depletion based on magnetic microbeads from fresh human PBMCs. For re-staining we chose monoclonal antibodies for both CD45RA and CD45RO to demonstrate that CD45RA depletion can in principle substitute the CD45RO positive selection step. As shown in **Fig. 5.28,** CD45RA selection targeted exclusively CD45RA$^+$ cells enabling the successful recovery of CD45RO$^+$ cells. Double negative cells are neither CD8$^+$ nor CD3$^+$ cells and therefore never appear after CD8 selection (**Fig. 5.29**). Importantly, the recovery rates are in a similar range as recovery rates obtained from CD45RO selections (mean = 45.7%, n=5). We estimated that recovery rates from CD45RA depletion might even surmount those of CD45RO positive selections. For this reason, we were interested in a direct comparison between a CD45RO positive selection versus a CD45RA depletion following positive enrichment of CD8$^+$/CD62L$^+$ cells to create the desired setting for T_{CM} enrichments. Surprisingly, CD45RA depletion not only resulted in superior cell recovery rates but yielded a greater overall purity compared to CD45RO positive selection (**Fig. 5.29**). Here we have tested CD45RA depletion as part of a sequential enrichment protocol together with a CD8/CD62L-positive enrichment. When donor PBMCs from the same blood were split in two aliquots and depletion was either performed before or after CD8/CD62L positive selection following the same protocol with the same reagents, CD45RA depletion after CD8/CD62L positive selection resulted in a slightly better purity and recovery rate. We have confirmed this result in three independent experiments (data not shown). The new protocol design for a three-step purification of T_{CM} using CD8/CD62L/CD45RA is based on these results.
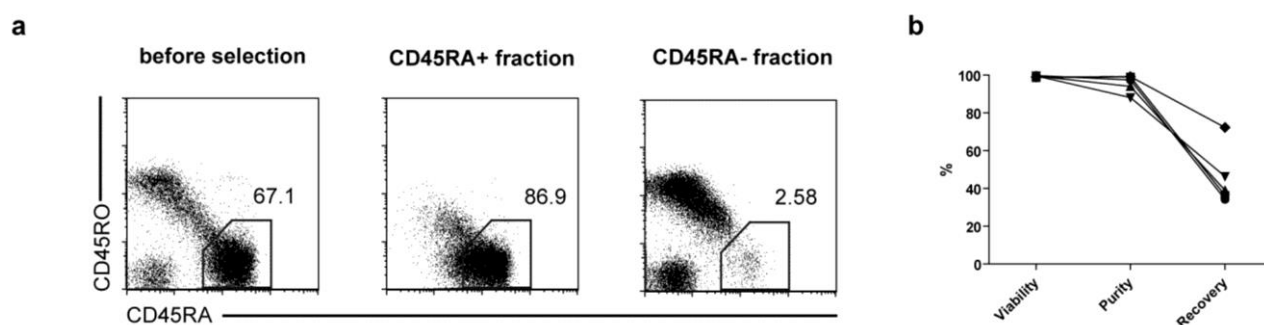
Fig. 0.28: A CD45RA *Strep*tamer-based reagent for positive enrichment and depletion of human CD45RA$^+$ cells.

CD45RA depletion was performed using specific Fab-*Strep*tamers conjugated to *Strep*-Tactin-coated magnetic microbeads. Living lymphocytes are shown for each step of the procedure including the unwanted positive fraction of CD45RA$^+$ cells. One representative experiment from 5 independent blood donors is shown in **a**. **b**. n=5, gated on living lymphocytes. Viability, purity and recovery rates are shown.
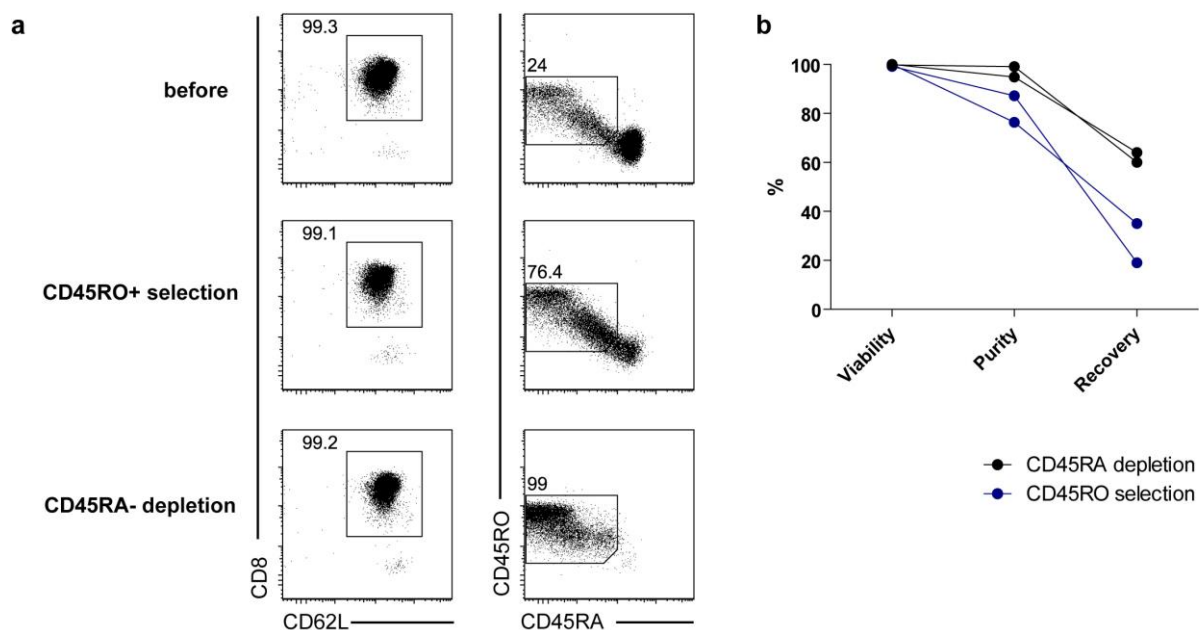
Fig. 0.29: Sequential selection of memory T cells using CD45RO for positive selection or CD45RA for depletion

Pre-selected $CD8^+/CD62L^+$ cells were subjected to a CD45RO positive selection step or a CD45RA depletion step using specific Fab-*Strep*tamers conjugated to Strep-Tactin-coated magnetic microbeads. **a**. Living lymphocytes of one representative experiment are shown. Numbers in dot plots indicate the relative frequency of events inside the gates. **b**. Two independent experiments are shown. Sequential selections including a negative depletion step (black graphs) or a positive selection step (blue graphs).

We have applied the new TCM purification protocol as shown in **Fig. 5.30**. One representative complete three-step selection cycle out of 6 independent experiments (all performed exactly under the same experimental conditions) for enrichment of $CD8^+$ central memory T cells is shown. Very high purities were reached in the two positive enrichment steps and for CD45RA depletion in the example. The final cell product purity was 96% $CD8^+$ $CD45RO^+/CD45RA^-$ $CD62L^+$ $T_{CM.}$ We have obtained similar high purities of T_{CM} in all 6 independent experiments with PBMCs derived from different donors averaging in an overall purity of 97.8% ± 1.58 of cells in the final T_{CM} fraction. There was no correlation between initial T_{CM} frequencies and overall purity of final T_{CM} fractions. Surprisingly, the recovery rates averaged at 29.5% ± 14.1 with higher variability between different donors. We further aimed at dissecting the contribution of each selection step to the overall cell recovery and purity. Therefore, data from two- and three-step experiments performed under the exact same conditions on different donors were analyzed. Interestingly, the variability between donors was highest for CD8 and lowest for CD62L although CD62L yielded lower recovery rates in general (**Fig. 5.31**). We conclude that each selection step contributes to a different extent to the overall target cell recovery in T_{CM} selections. We demonstrated here that reversible Fab-*Strep*tamers can be effectively used in a serial selection procedure for robust enrichment of $T_{CM}s$ to very high purities using only 3 reagents.
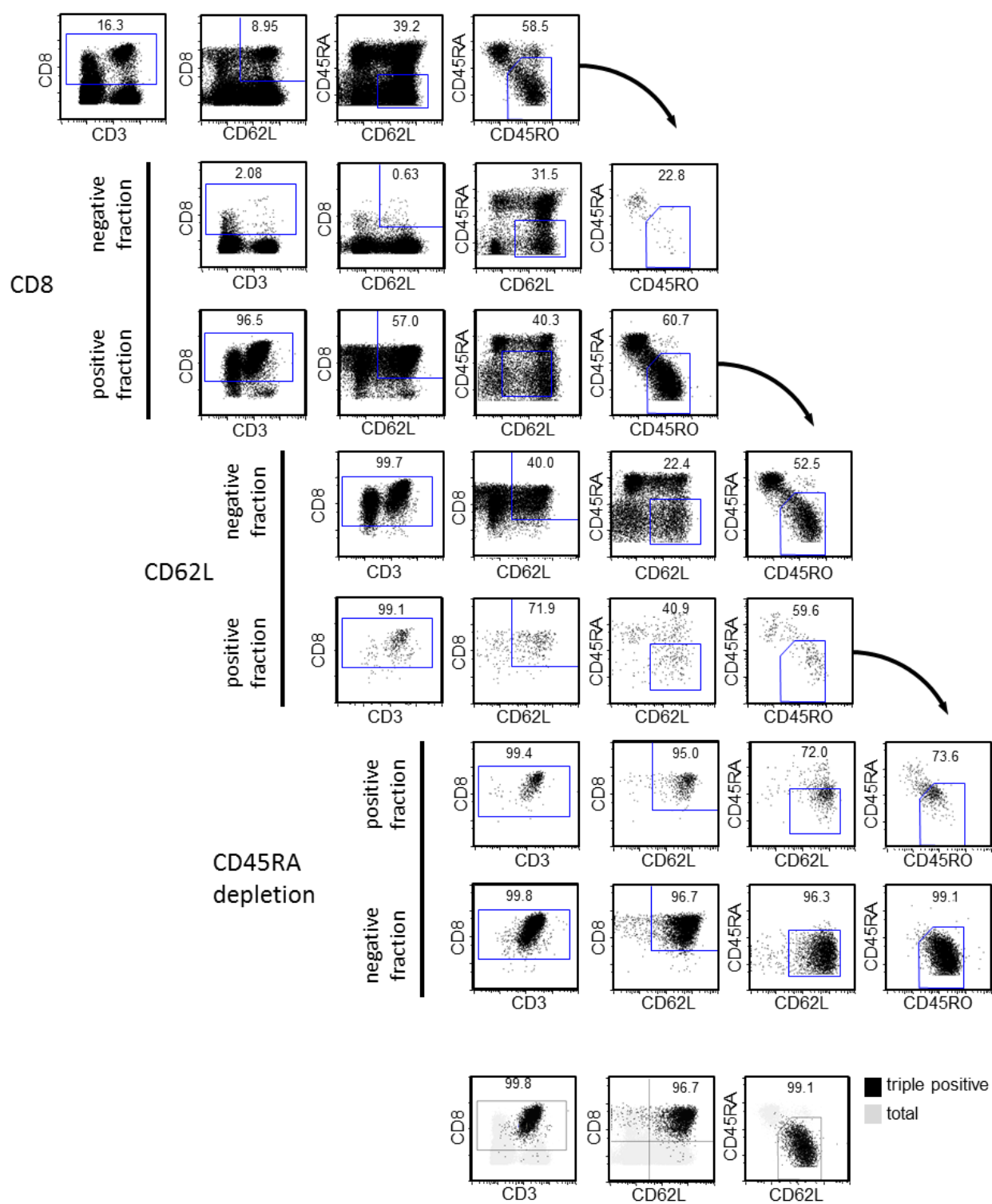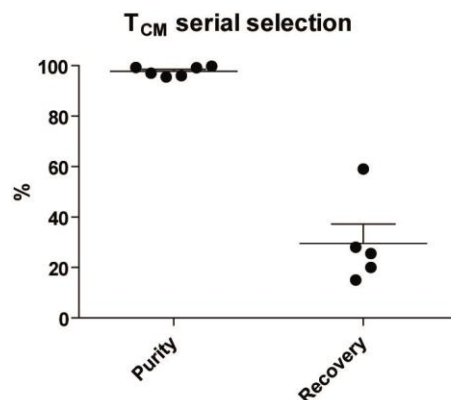
Fig. 0.30: Sequential positive enrichment of human central memory T cells using CD8, CD62L, and CD45RA Fab-*Strep*tamers

3×10^7 - 10^8 fresh human PBMCs were incubated with anti-CD8 Fab-*Strep*tamers conjugated with Strep-Tactin-functionalized magnetic microbeads. The CD8 positive fraction was collected and treated with 1 mM D-biotin and washed twice to remove remaining reagents. In a subsequent second selection step, CD62L positive T cells were enriched from the CD8$^+$ fraction as described for the first step. Finally, CD45RA$^+$ cells were depleted using a CD45RA specific Fab-*Strep*tamer conjugated to *Strep*-Tactin-coated beads. Living lymphocytes obtained before and after each selection step are shown for one representative experiment of 6 independent experiments from different donor material.
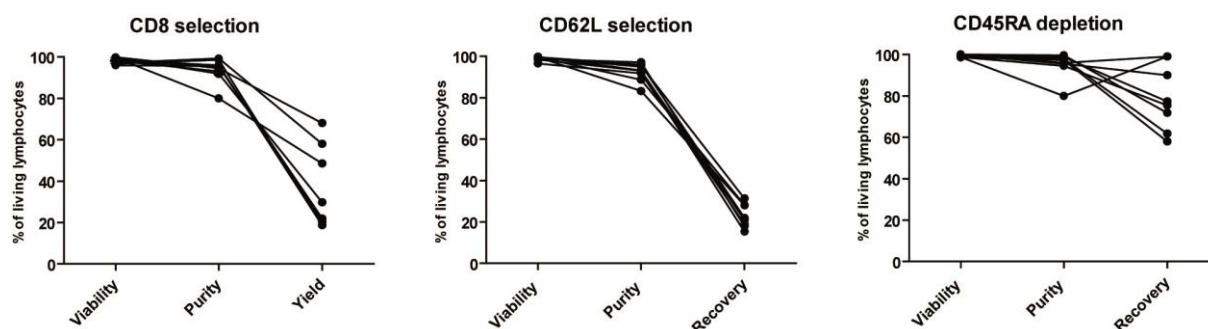
Fig. 0.31: Separately diagrammed selection steps of T$_{CM}$ purification

3×10^7 - 10^8 fresh human PBMCs were incubated with anti-CD8 or anti-CD62L Fab-*Strep*tamers conjugated with Strep-Tactin-functionalized magnetic microbeads. The positive fraction was collected and treated with 1 mM D-biotin and washed twice to remove remaining reagents. In a subsequent second selection step, CD62L positive T cells or CD45RA negative cells were enriched from the positive fraction as described for the first step. For some experiments, CD45RA$^+$ cells were depleted using a CD45RA specific Fab-*Strep*tamer conjugated to *Strep*-Tactin-coated beads. Living lymphocytes after each selection step were counted and analyzed by flow cytometry. Viability, Purity and recovery are shown.

5.4.5   Sequential selection of CD8 and CD4 central memory T cells

Some approaches in adoptive T cell therapy favor the simultaneous administration of CD8 and CD4 cells and suggest a combinatorial adoptive transfer of CD8 and CD4 central memory T cells. It might be advantageous to be able to control the ratio between CD4 and CD8 T$_{CM}$ in the cell product. Different strategies could allow the purification of central memory T cells expressing CD8 or CD4 with more or less control on the CD4: CD8 ratio. One is the sequential enrichment of both CD8 and CD4 central memory T cells separately. This strategy would require an additional selection step in the

process or a substantial loss in cell numbers when PBMCs are split prior to selection. Alternatively, cells could be selected as described in the previous section by replacement of the CD8 Fab with a CD3-specific Fab, which selects both T cells, CD4 and CD8. Alternatively, CD4- and CD8-specific Fab Streptamers could be mixed and simultaneously used within a positive selection step. We have tested these strategies in the following sections. First, we hypothesized that simultaneous selections of CD4 and CD8 T_{CM}s enable the highest degree of control on the CD4: CD8 ratio of the final product. We therefore replaced CD8 Fabs in *Strep*tamer preparation with a mixture of CD4 and CD8 Fabs. Using this mixed reagent for positive selection out of fresh PBMCs, we observed substantial differences in recovery rates for CD4 and CD8 T cells. When the individual Fab proteins were mixed at a ratio of 1:1, CD4 T cells were selected at a higher ratio compared to CD8 T cells. Thus, a shift in CD8: CD4 ratio is generated in favor of the CD4 subpopulation. In **Fig. 5.32a** we show an example where the CD4 proportion of all T cells shifted from initially 75% CD4 T cells to over 90% CD4 T cells after selection with a mixture of CD4- and CD8-specific *Strep*tamers at the same ratio. We hypothesized that we could adjust the CD4:CD8 Fab ratio in the mixture so that the CD4: CD8 T cell ratio after selection matches a desired ratio (e.g. 1:1). Therefore, we tested decreasing CD4: CD8 Fab ratios from 1:1 to 1:16 and observed a linear correlation between doubling the CD8 Fab fraction in the mix and doubling the frequency of CD8 T cells in the positive fraction (**Fig. 5.32b**). However, as demonstrated by the results from two independent donors, in order to achieve a particular CD4:CD8 T cells ratio, one must know the initial frequency to adjust the CD4/CD8 Fab Streptamer mixture correctly. Donor #1 (**Fig. 5.32b** left panel) had an initial ratio of CD8: CD4-positive T cells of 0.25; in this case a CD4: CD8 Fab *Strep*tamer ratio of 1:8 was necessary to obtain similar numbers of CD8 and CD4 T cells (1:1 ratio). Donor #2 (**Fig. 5.32b** right panel) had an initial ratio of CD8: CD4-positive T cells of 0.5; in this case a CD4: CD8 Fab Streptamer ratio of 1:4 was needed to obtain similar numbers of CD8 and CD4 T cells. The same correlations hold true when calculating absolute cell numbers as shown in **Fig. 5.32c**. These data indicate that it might be possible to predictably enrich for defined CD8 to CD4 ratios if the initial CD8 and CD4 T cell frequencies are known prior to selection.
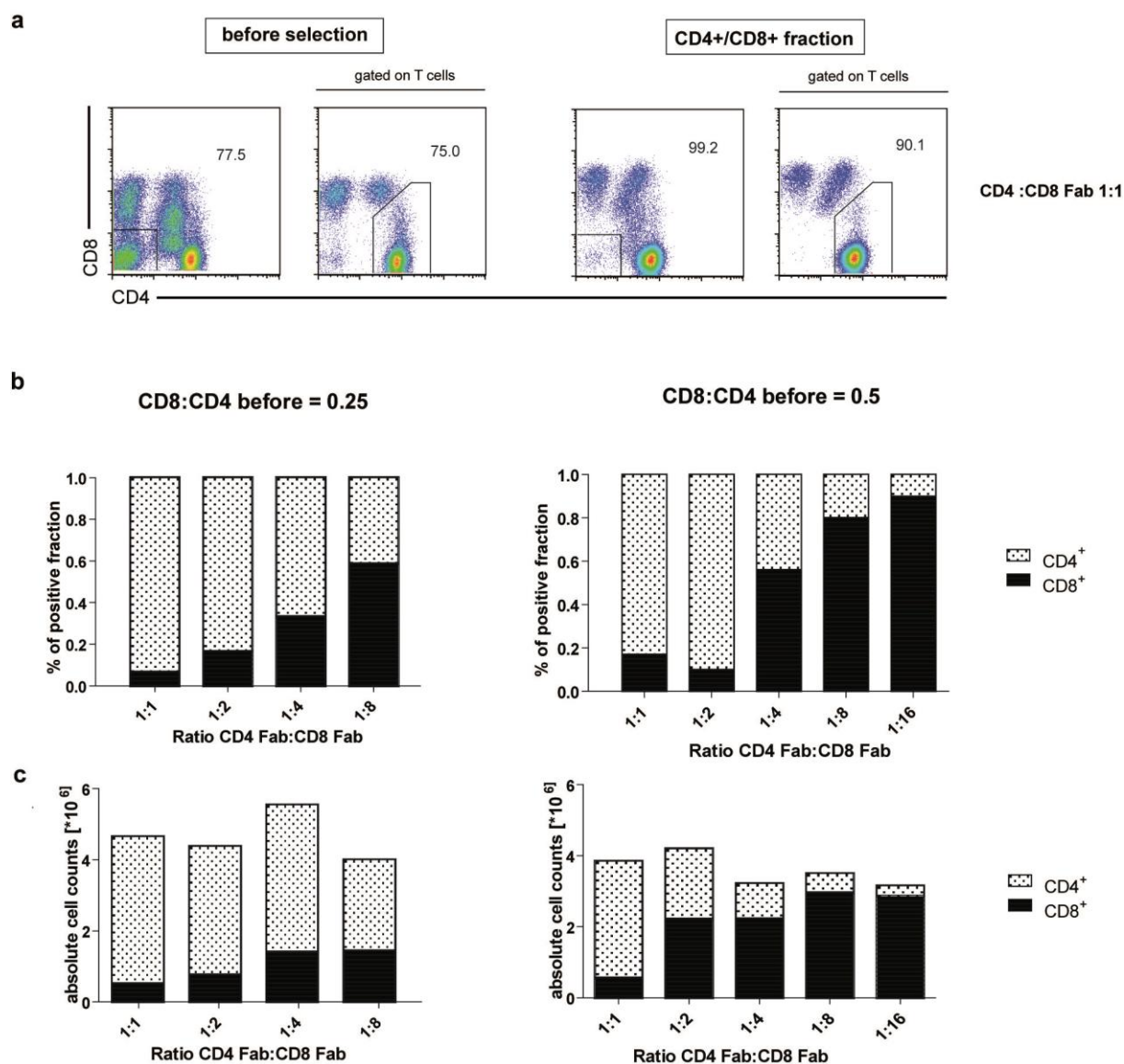
Fig. 0.32: The outcome ratio between CD4 and CD8 T cells in selection with mixed reagents can be set to a desired value

*Strep*tamers with previously mixed CD4- and CD8-specific Fab fragments were made at a ratio of 2 μg Fab and 7.5 μg (bead-conjugated) *Strep*-Tactin per 10^7 cells. **a**. We have used 1 μg CD4 Fab and 1 μg CD8 Fab for multimerization of 7.5 μg (bead-conjugated) *Strep*-Tactin for the selection out of 10^7 fresh PBMCs. **b**. Aliquots of 10^7 PBMCs from two independent donors were selected with different mixes. CD4: CD8 Fab ratios for each selection are indicated. **c**. Absolute cell numbers were determined by counting positive fractions and multiplication with frequencies in CD4 or CD8 gates.

5.5 A *Strep*tamer technology-based protocol for the selection of human T_{CM} in compliance with GMP-manufacturing of cell products

The next thesis goal was to develop a selection protocol that enables GMP-conform T_{CM} selections in a closed system. Our laboratory recently succeeded in generating a CD3-specific Fab fragment for the selection of central memory T cells that was successfully implemented in the serial enrichment procedure. CD3/CD62L/CD45RA based T_{CM} selections combine both advantages, the fast and easy three-step enrichment with the possibility to isolate CD4 and CD8 T_{CM} at the same time without the need for prior analysis of donor frequencies. The T_{CM} selections described in the following were performed in a closed sterile system of custom-made sets of tubing and bags provided by Stage Cell Therapeutics. All bags and connection tubes are designed for single-use and hold all necessary junctions for filling, washing, and D-biotin treatment for one selection step. Welding of tubes was performed with a Terumo Medical TSCD® II welding unit (to create a new connection) or a conventional tube welding device (to close a tube) enabling transfer of collection bags to new tubing systems for subsequent selection steps. The magnet used was the DynaMag™ CTS™ Magnet by Life Technologies and holds one selection magnet (magnet 1) and a second, smaller magnet for secure removal of any residual magnetic particles (magnet 2). Both magnets and custom made tubing sets are shown in **Fig. 5.33**. Up to 10^{10} cells are co-incubated with CD3-specific magnetic microbeads in the selection bag which is subsequently sealed in place between the connection tubes to buffer and D-biotin reservoir above and the collection bags below the selection bag. The selection bag is filled up with buffer from the reservoir by opening the blue valve for 10-20 seconds. After 1 minute on the magnet the horizontal white valve is opened to conduct buffer including unlabeled cells into the collection bag for the negative fraction (**Fig. 5.33a**). This wash procedure is repeated twice after the white valve is closed. Two valves can never be opened simultaneously at all times. CD3- cells are now pooled in the negative fraction and the target cells in the selection bag are treated with D-biotin by opening the red valve for 2-5 seconds (**Fig. 5.33b**). Note that the green color indicates all areas that are in contact with D-biotin. Analog to the wash process, the vertical white valve is opened to release cells in D-biotin into the collection bag for the positive fraction. This step is repeated another time. In contrast to the wash steps, the target cells are now flushed into a collection bag while only unbound magnetic particles alone are retained in the magnetic fields of the two magnets. Red arrows indicate the whereabouts of target cells during positive selection during washes and removal (**Fig. 5.33a+b**). The following CD3 positive selections were performed followed by D-biotin treatment for reagent removal as described. After three centrifugation steps including a 10-minute incubation each time (see section 5.2) A subsequent CD62L positive selection step comprising all the exact same steps as described for CD3 selection was performed using a fresh set of tubes and bags. After removal of the CD62L reagent, a CD45RA- Fab *Strep*tamer-based depletion was performed similarly without the D-

biotin steps because in this case the unlabeled fraction equals the target fraction. It is directly collected in the bag for the positive fraction (vertical white valve) to ensure that the second magnet works as a backup to catch any residual magnetic labels or unwanted labeled cells.
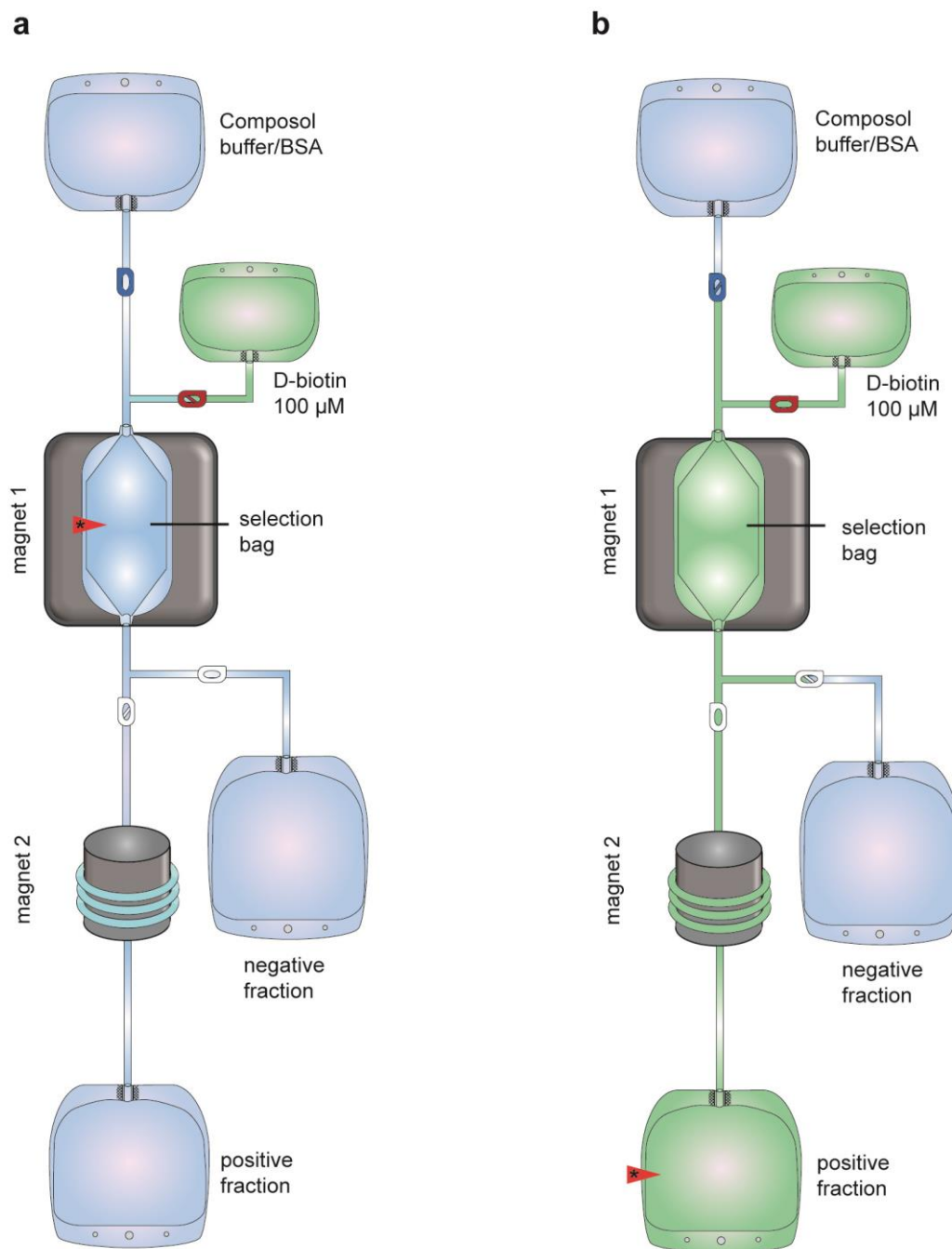
Fig. 0.33: Selection procedure in a custom design bag- and tubing set for the clinical DynaMag^{TM} CTS^{TM}

Single use clinical plastic bag and tubing system in the set up for use with the DynaMag^{TM} CTS^{TM}. Magnets 1 and 2 are part of the DynaMag^{TM} CTS^{TM}. The system remains closed throughout the whole process. Connections can be altered by a clinical welding device. Selections and welding can be performed in any environment and remain sterile. Selection bags are connected to the buffer reservoir and the D-biotin reservoir above and to the collection bags for negative and positive system below. **a**. Magnetically labeled cells are in te selection bag. Unlabeled cells are washed with buffer and are collected in the negative fraction bag. For washing, the blue clip is opened for 10 seconds to fill the selection bag with buffer. Subsequently, the horizontal white clip is opened to release buffer and unlabeled cells into the negative fraction bag. The wash process is repeated twice. **b**. Magnetically labeled target cells in the selection bag are flushed with D-Biotin from the reservoir when the

red clip is opened. Incubation time is 10 min to release cells from magnetic beads. Cell are subsequently released into the collection bag for the positive fraction passing the second magnet for secure removal of any residual magnetic particles. This step is repeated one more time. Blue indicates D-biotin-free buffer, green indicates buffer containing D-biotin. *location of target cells at given timepoints.

A representative TCM purification out of 5×10^8 PBMCs is shown in **Fig. 5.34a**. We show our complete gating strategy applied on lymphocyte singlets and all relevant gates to determine viability and purities of each step which is represented by a row (read from top to bottom). In this example we yielded 99% pure $CD3^+$ T cells with an overall purity of 95% for CD62L and 99% for CD45RO and a remarkable 52% recovery. The bottom row of **Fig. 5.34a** provides additional data showing the phenotype of all cells without any pre-gating. We conclude from this that we have minimal risk emanating from a small potential contaminant with a $CD3^+/CD62L^-/CD45RO^+$ phenotype which is most likely an effector memory phenotype. Those cells have previously been characterized as short-lived cells with no evidence of mediating harmful side effects concerning their in vivo behavior upon adoptive transfer. We tested Fab dissociation by re-staining with an anti-IgG light chain antibody to detect any residual Fab fragments. In three-step serial T_{CM} purifications we yielded average purities of 93.5% ± 3.1 from PBMCs derived from human *buffycoats*. To be able to compare the outcome, we have used a starting population of 5×10^8 PBMCs from each donor. The cell numbers were determined after Ficoll separation of the blood. The average recovery rate was 32.9% ± 11.2, which corresponded to an absolute cell number average of 1.4×10^7 T_{CM} from a starting number of cells which is usually obtained from 300-500 mL of donor blood (**Fig. 5.34b**). Similar results were obtained from apheresis products, which provide much bigger cell numbers and are commonly used for example as a source of donor stem cells in the clinic. Our largest scale experiment was performed on 2×10^9 PBMCs. We show a summary of all T_{CM} purification experiments from apheresis products as the starting material in **Fig. 5.34c.** Noteworthy, in one case a low CD62L purity was observed indicating that shedding of CD62L might have occurred to some extent. In a separate experiment in the interest of CD62L shedding under given experimental conditions we did not observe any reduction in CD62L expression over time on PBMCs obtained from *buffycoat* und incubated with staining probes for 6 hours on ice (spans the experimental procedure).

Furthermore, being able to perform T_{CM} selections with a CD3-specific reagent allowed us to track if CD4 T cells are also preferentially enriched opposed to CD8 T cells when the same marker is used (cf. chapter 5.4.5). When we selected T cells with *Strep*tamers of mixed specificity for CD4 and CD8 at the same ratio we preferentially enriched $CD4^+$ cells over $CD8^+$ cells. CD4 frequencies were 4 times as high as CD8 frequencies or higher depending on the initial ratio (**Fig. 5.32a+b**). To test if this effect depends on the markers used or if it is of a more general cell-intrinsic nature, we analyzed the CD4: CD8 ratio of positively selected $CD3^+$ cells. We were not able to detect a shift in CD4: CD8 T cell ratios after a single step of CD3 positive enrichment (cf. **Fig. 5.34** first and second row). The CD4: CD8 ration before selection (first row) is 2 and the CD4: CD8 ratio after CD3 selection is 2.2 and therefore not in the range of selection bias we saw with mixed *Strep*tamers. However, combinatorial

expression of CD62L and CD45RO markers differs vastly between CD4 and CD8 subsets making the natural pattern of co-expression of the selection markers responsible for the high content of CD4$^+$ T$_{CM}$ upon CD3$^+$/CD62L$^+$/CD45RA$^-$ purification in most donors. Taken together the generated data convey evidence that T$_{CM}$ selections from very high starting cell numbers (2x10^9 cells) are possible with outstanding overall purities and very good target cell recovery rates in a closed system that can be directly reproduced in a clean room facility for the GMP production of clinical cell products. The total procedure required approximately 6 hours processing time.

.

TCM selection out of 5×10^8 BPBMCs

a — gating strategy; viability; purity CD3+; purity CD62L+; purity CD45RA−; removal

before selection anti-kappa + control

CD3+ fraction

CD3+/CD62L+ fraction

CD3+/CD62L+/CD45RA− fraction
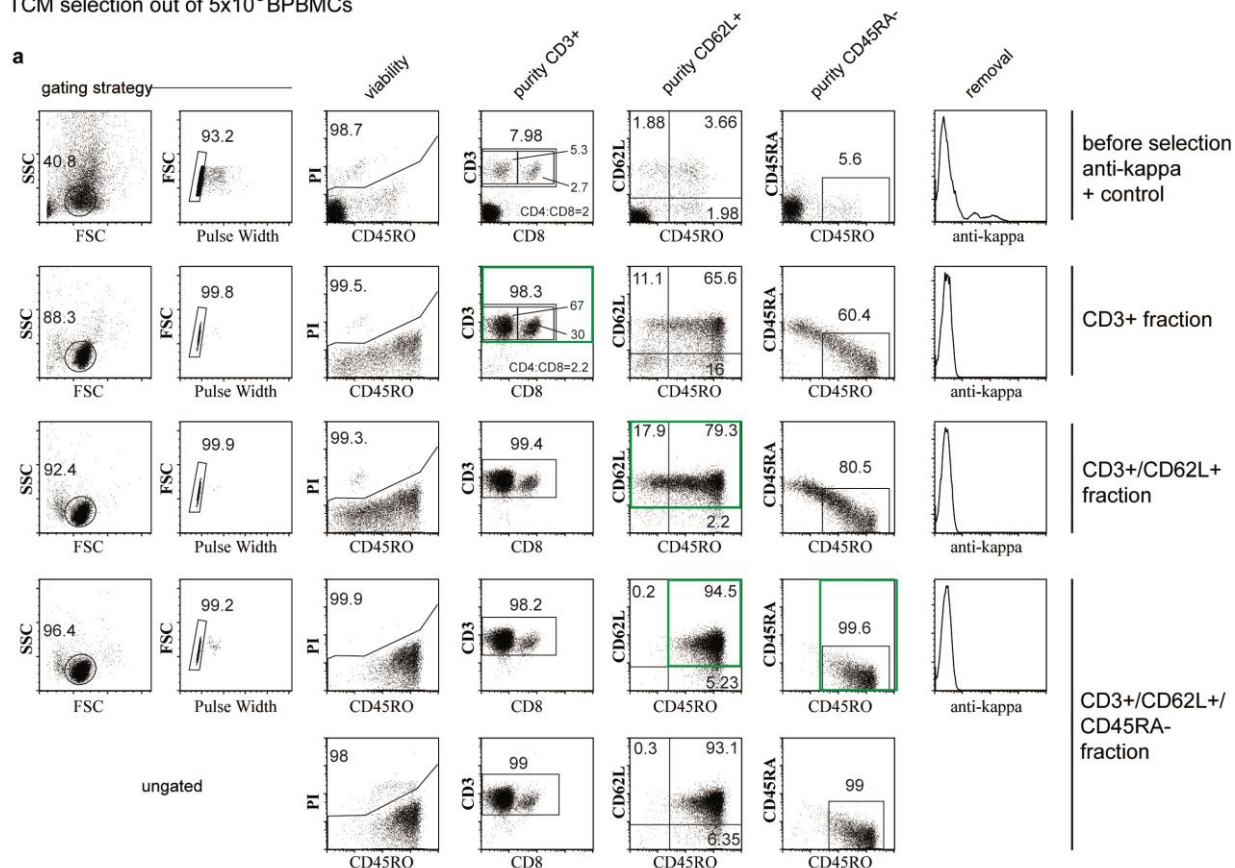
b

Buffycoat 5×10^8 PBMC

c
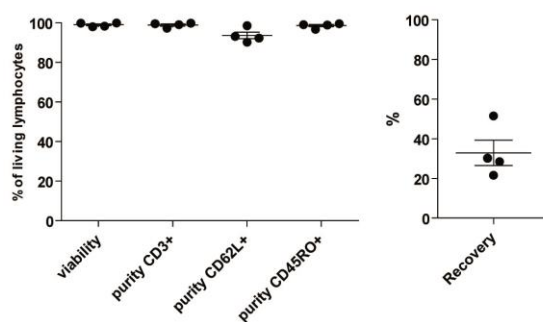
Apheresis $10^8 - 10^9$ PBMC
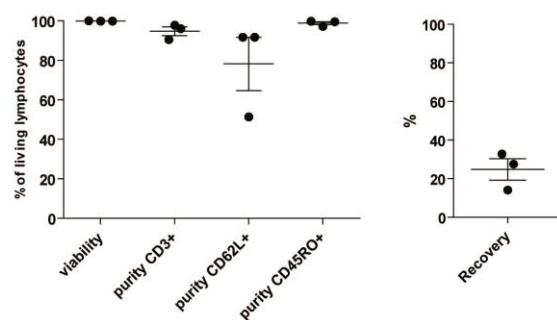
Fig. 0.34: Sequential positive enrichment of human central memory T cells using CD3, CD62L, and CD45RA Fab-*Strep*tamers in closed GMP-conform system

5x10^8 fresh human PBMCs were incubated with anti-CD3 Fab-*Strep*tamers conjugated with Strep-Tactin-functionalized magnetic microbeads. The CD3 positive fraction was collected and treated with 1 mM D-biotin and washed twice to remove remaining reagents. In a subsequent second selection step, CD62L positive T cells were enriched from the CD3$^+$ fraction as described for the first step. Finally, CD45RA$^+$ cells were depleted using a CD45RA specific Fab-*Strep*tamer conjugated to *Strep*-Tactin-coated beads. Living lymphocytes obtained before and after each selection step are shown for one representative experiment of 4 independent experiments from different donor material (**a**). Positive fractions and their respective gating are highlighted in green for each step. **b**. 4 independent experiments were performed using the CD3-based protocol for T$_{CM}$ enrichment. Purities for each selection step are given as well as cell recovery rates. All steps within one selection step including D-biotin treatment and removal of the magnetic beads were performed in a closed system of plastic bags and tubes designed for single use. **c**. Set of 3 experiments performed on apharesis material with PBMC contents of 10^8-2x10^9.

5.6 Further developments in T$_{CM}$ purification

A major improvement in advanced GMP production of cell therapeutics is the reduction of manufacturing time during cell processing procedures. To harness the full power of the *Strep*tamer technology, we intended to test novel, simplified protocols in order to be able to process a maximal number of cells in a minimal amount of time and effort. Ficoll separation and centrifugation steps during washing are a major time-consuming component, especially when they are conducted in a clean room in large scales.

5.6.1 Centrifugation-free purification of central memory T cells out of PBMCs

Removal of *Strep*-Tactin, monomeric Fab proteins and excess D-biotin after a positive selection step are crucial for subsequent selection steps. We could show that Strep-Tactin-coated magnetic microbeads can be safely removed by magnetic attraction in the field of a strong permanent magnet. However, removal of the soluble components Fab and excess D-biotin requires repeated cycles of centrifugation and subsequent removal of the supernatant containing those components. We hypothesize that Fab monomers, if not removed, will interfere with the following selection step in such a way, that monomeric Fab will partly couple with Strep-Tactin from the second *Strep*tamer forming new, unwanted *Strep*tamers of the previous specificity by Fab fragment exchange. To prove this hypothesis, we have stained PBMCs with CD4-specific *Strep*tamers in the presence or absence of CD8 Fab monomers. The *Strep*tamer specificity is clearly lost when CD8 Fab monomers were mixed with the cells prior to staining with CD4 *Strep*tamers. Both, CD4$^+$ and CD8$^+$ cells appear *Strep*tamer$^+$. Remarkably, the full staining intensity of the CD8 control *Strep*tamer staining (with 0.5 μg Fab/10^6 cells) was already reached when only 10% of the CD8 Fab monomers (0.05 μg Fab/10^6 cells) were used compared to a regular staining of 10^6 cells. This supports our hypothesis that Fab monomers

interfere with *Strep*tamer staining reagents. Our results clearly show *de novo* formation of CD8 specific *Strep*tamers (**Fig. 5.35a**). Next, we hypothesized that a clear, specific CD4 *Strep*tamer staining can be re-established when unbound CD8 Fab proteins are neutralized in the Fab/cell mix in advance of the *Strep*tamer incubation. For neutralization, we used a previously determined amount of 50 µg of soluble unconjugated *Strep*-Tactin per 10^6 cells. 10^6 fresh PBMCs together with 0.2µg CD8 Fab monomer were stained with a CD4-specific Fab-*Strep*tamer in the presence (**Fig. 5.35b** left panel) or absence (**Fig. 5.35b** right panel) of 50 µg Strep-Tactin as a neutralization reagent. CD4 Fab *Strep*tamer staining resulted in staining of $CD4^+$ and $CD8^+$ PBMCs when *Strep*-Tactin is omitted but retained specificity of the staining in the sample treated with *Strep*-Tactin. We conclude that addition of soluble *Strep*-Tactin before staining rescues the original specificity by neutralization of Fab monomers. All stainings were performed in a D-biotin free system. Neutralization of D-biotin supposedly requires larger amounts of reagents. We first tested avidin as a candidate reagent for D-biotin neutralization and calculated the necessary amount for neutralization of a 500µL D-biotin (100µM) solution and performed titrations to prove this (data not shown). Then, we performed simultaneous neutralization of CD8 Fab monomers and 100 µM D-biotin. According to our expectations, addition of *Strep*-Tactin alone was not sufficient to neutralize 500 µL of 100 µM D-biotin (**Fig. 5.35c** left panel). D-biotin was finally neutralized by addition of 100 µg avidin and *Strep*tamer staining was enabled. Avidin alone could not rescue the specificity of the CD4 Fab-*Strep*tamer because avidin is not able to neutralize Fab monomers due to its low affinity towards the *Strep*-tag (**Fig. 5.35c** middle). D-biotin and CD8 Fab monomers were neutralized when both neutralization reagents were added (**Fig. 5.35c** right panel). We conclude that it should be possible to neutralize soluble selection reagents after a positive selection step and removal of magnetic beads. We tested the neutralizing reagents avidin and *Strep*-Tactin in a serial positive magnetic selection. As shown in **Fig. 5.35d**, a CD62L *Strep*tamer selection could successfully be performed after a positive CD8 enrichment step and subsequent removal of beads and neutralization of Fab and excess D-biotin. The removal step in between selections involved neither additional washing buffer, nor centrifugation. This is the first evidence that a serial positive magnetic enrichment can in principle be performed without centrifugation and therefore a substantial amount of time can be saved.
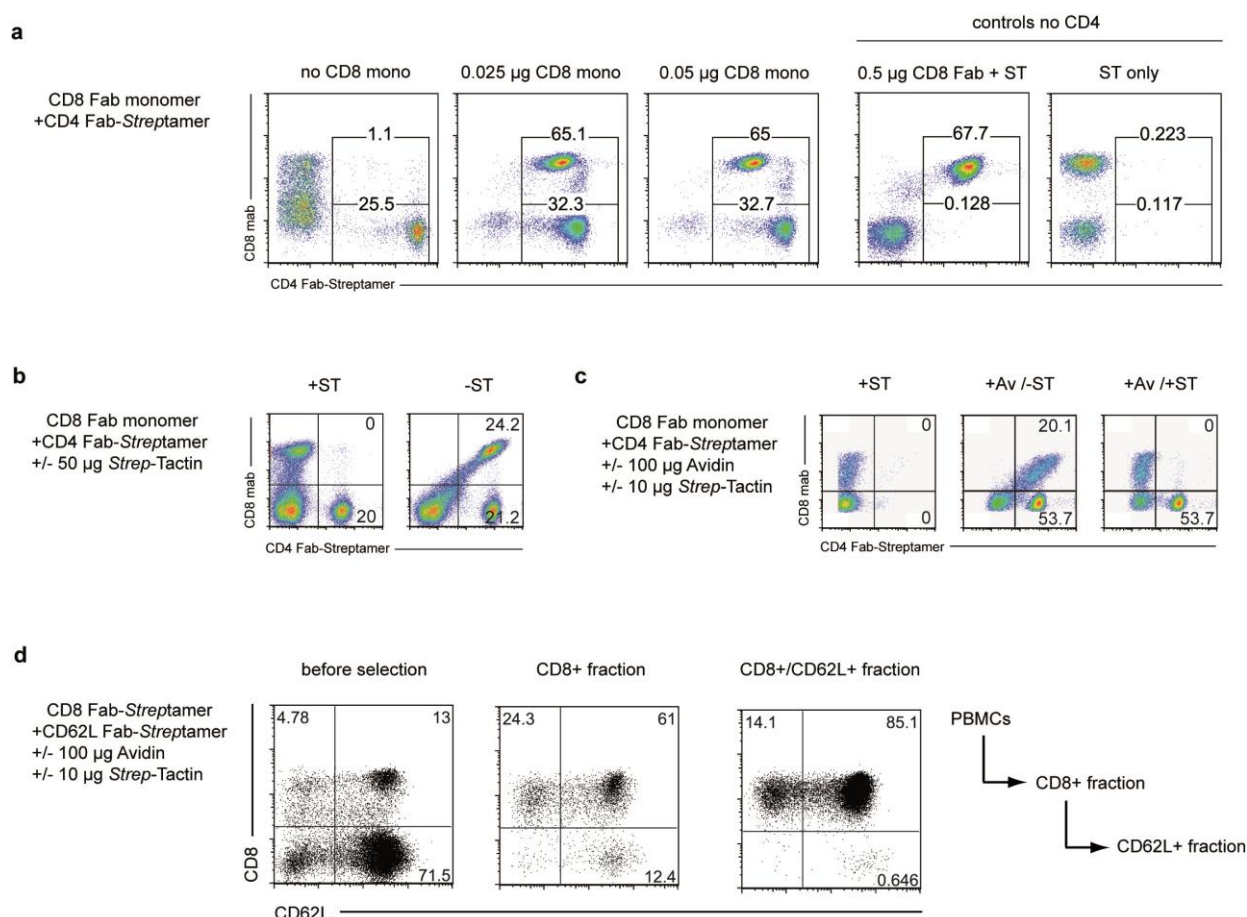
Fig. 0.35: Soluble Avidin and *Strep*-Tactin can neutralize Fab monomers and D-biotin.

a. 10^6 fresh PBMCs were stained with a CD4-specific Fab-*Strep*tamer in the absence or presence of 0.025 or 0.05µg CD8 Fab monomer. Controls stainings include 0.05 CD8 Fab with unbound *Strep*-Tactin (no CD4) and *Strep*-Tactin alone (background). **b**. 10^6 fresh PBMCs and 0.05µg CD8 Fab monomer were stained with a CD4-specific Fab-*Strep*tamer in the presence (left panel) or absence (right panel) of 50 µg *Strep*-Tactin (ST) as a neutralization reagent. CD4 Fab *Strep*tamers staining results in staining of CD4+ and CD8+ PBMCs when *Strep*-Tactin is omitted. The addition of soluble *Strep*-Tactin before staining rescues the CD4 specificity by neutralization of Fab monomers. **c**. Simultaneous neutralization of CD8 Fab monomers and 100 µM D-biotin by addition of *Strep*-Tactin (ST) and avidin (Av). Left: 10 µg of *Strep*-Tactin alone was not sufficient to neutralize 500 µL of 100 µM D-biotin. Middle: D-biotin neutralization by 100 µg avidin enables staining, but specificity is not kept because avidin alone is not able to neutralize Fab monomers. Right: D-biotin and CD8 Fab monomers are neutralized. **d**. Serial positive enrichment of CD8/CD62L positive cells out of 2×10^7 PBMCs. CD8 selection was performed as previously described. Positive fraction was treated with 1 mL 100 µM D-biotin and 100 µg avidin and 10 µg Strep-Tactin was added per 10^6 cells respectively. A CD62L-specific *Strep*tamer beads were added after 20 minutes for the second positive selection.

These results further encouraged us to test an easy-to-use system for efficient removal of D-biotin and monomeric residual Fab for the use in a closed system. Preliminary experiments confirmed that *Strep*-Tactin alone is capable of neutralizing Fab fragments and D-biotin if the concentration is high enough. A special removal column with high contents of *Strep*-Tactin was provided by Stage cell therapeutics. We hypothesized that the extremely high binding capacity of cross-linked biopolymer-particles can allow the fast and complete removal of soluble reagents. A high amount of *Strep*-Tactin is covalently bound to matrix biopolymers of 100 µm in diameter on average. The matrix can be employed in a cell suspension flow without any trapping or hindering of cells in a continuous flow. Therefore, a

cylindrical plastic syringe was modified with 20 μm filters to hold the matrix biopolymers in a section of the cylinder volume. The design allows cells to pass the filters while all matrix beads are held back (**Fig. 5.36a**). The matrix is characterized by its structural properties allowing the immobilization of huge amounts of *Strep*-Tactin on the inside of the particles. Experiments have shown that *Strep*-Tactin immobilization only on the surface of the biopolymers could not provide a sufficient amount of *Strep*-Tactin for neutralization of both Fab monomers and D-biotin. Thus, under flow conditions a continuous stable binding of dissociated Fab-monomers and excess D-biotin mainly on the inside of the particles is necessary. Compared to the molar equivalent of *Strep*-Tactin needed for D-biotin neutralization, residual free Fab monomers only account for about 1% of the necessary *Strep*-Tactin and can therefore be neglected in calculations. We have confirmed the location of *Strep*-Tactin by staining with the high affinity ligand D-biotin. Co-incubation of the matrix beads with biotinylated, PE-conjugated MHC-molecules resulted in bright staining of the matrix material (**Fig. 5.36b**). This system in principle now allows elimination of soluble selection reagents without centrifugation. Monomeric Fabs and excess D-biotin should be completely removed from the cell suspension after each step without accumulation of *Strep*-Tactin-bound or unbound residual reagents after a single step which could be carried over to the next step in the selection cycle. The general setup and operating principle of the removal column are shown in **Fig 5.37**. After D-biotin treatment of the positive fraction, cells and soluble selection reagents are separated from magnetic particles in a magnetic field. The extremely high content of Strep-Tactin within the polymeric matrix stably binds Fab monomers and excess D-biotin while cells can flow through the matrix unimpeded. At this point it is critical to use as little D-biotin for removal of *Strep*tamers as possible. We have shown earlier that 100 μM solutions of D-biotin were sufficient for reversing *Strep*tamer stainings in all experiments. All calculations are therefore based on a D-biotin concentration of 100 μM.
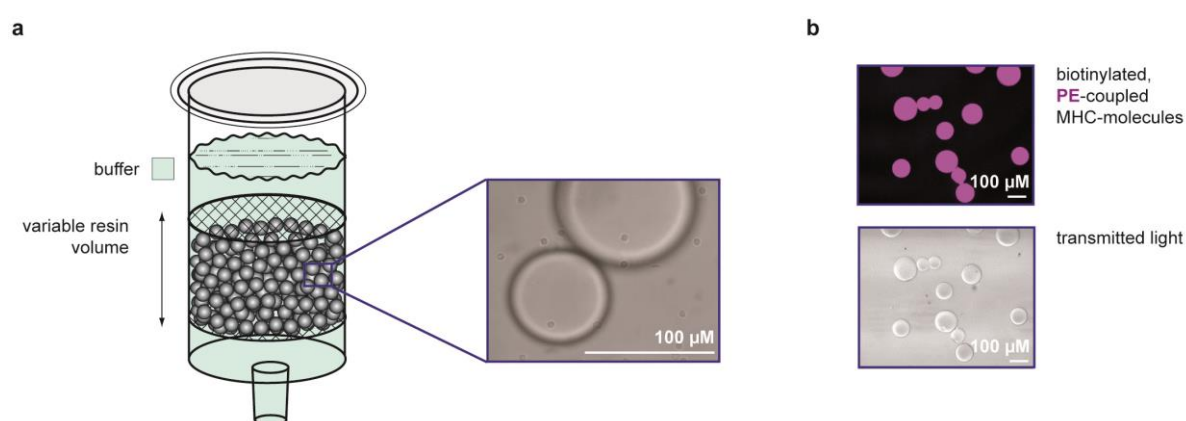
Fig. 0.36: Removal column: centrifugation-free elimination of soluble selection reagents

Setup of a plastic column of packaged cross-linked biopolymer-particles that allows the fast and complete removal of soluble reagents in a cell suspension flow without any trapping of cells or hindering of the continuous flow. **a**. Column is set up by a cylindric plastic tube comprising a chamber that holds the matrix resin within a 20μm pore size mesh. Polymer particles are

100 μm in diameter on average and are shown in a microscopic image with T cells as a size reference. **b**. Microscopic image of fluorescence labeled *Strep*-Tactin.(provided by Herbert Stadler).
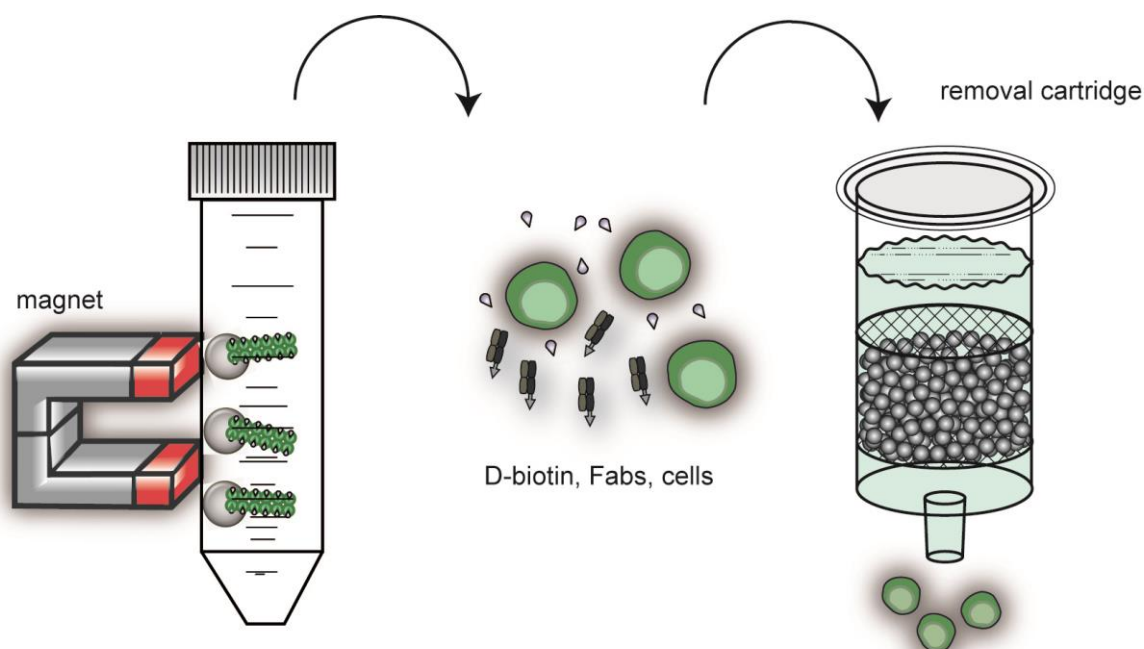
Fig. 0.37: Principle of the complete removal of selection reagents with the novel removal column

After D-biotin treatment, cells and soluble selection reagents are separated from magnetic particles in a magnetic field. The extremely high content of *Strep*-Tactin within the polymeric matrix stably binds Fab monomers and excess D-biotin while cells can flow through the matrix unimpeded.

Next, we evaluated parameters linked to the experimental implementation of the removal column prototype. To determine the D-biotin binding capacity of removal columns, we tested different columns and loaded them with a total of 7 mL of a 100 μM D-biotin solution (PBS/0.5% BSA/100 μM D-biotin) each. Given the small size of the columns, based on our calculations 7 mL D-biotin is sufficient to reach the level of D-biotin saturation in the column leading to a leak of D-biotin from the matrix at some point, which is detected by the drop in MFI when *Strep*tamer stained cells are co-incubated with aliquots taken from the flowthrough of the column. Aliqouts of 0.5 mL are continuously collected from the flow through from the columns and each aliquot is co-incubated with CD3-*Strep*tamer$^+$ cells. The MFI is determined by flow cytometry. A 0.5 mL column for example can securely hold back at least 2 mL of 100 mM D-biotin and a 1 mL column can absorb at least 3.5 mL before leaking biotin into the flow as shown in detail in **Fig. 5.38**. We have tested three different column sizes and determined the respective D-biotin binding capacities by comparison with CD3-*Strep*tamer$^+$ cells co-incubated with D-biotin-free buffer as a control. Below the lower limit of MFIs measured without D-biotin, drops in MFIs are considered to be D-biotin mediated. The flow rate of a liquid through the matrix in a removal column was previously measured as a function of column height and revealed a linear relationship. We therefore expected a linear relationship between the column height which equals the column volume in this case and the D-biotin binding capacity. We found almost equal disparity between the three column sizes (vertical dashed lines). When comparing

the measured binding capacities, a linear relationship is revealed by these results. In other words, the flow rate is bisected when the column height is doubled.
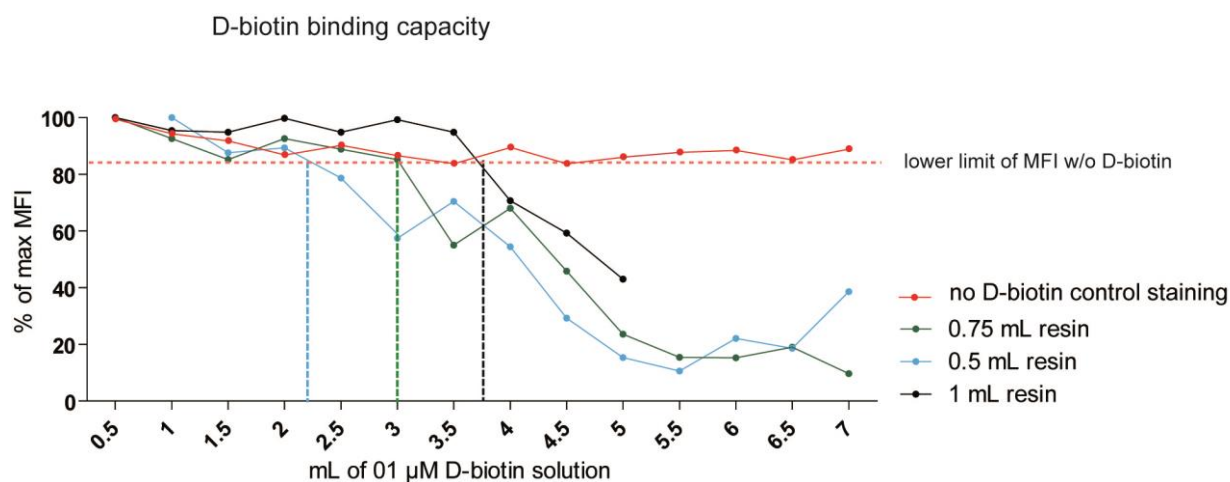

Fig. 0.38: Estimation of the D-biotin binding capacity by virtue of column size

For each column size (represented by black, blue and green graphs), *Strep*tamer stained PBMCs were distributed to 14 identical reaction tubes at 1x10^6 cells per sample. 7 mL of a 100 μM D-biotin solution (PBS/0.5%BSA/100 μM D-biotin) were continuously run over each column. Portions of 0.5 mL of the flow through were collected at the end of each column and incubated with the prepared *Strep*tamer stained PBMCs. FACS analysis was performed after a 20-minute incubation period to determine the mean fluorescence intensity (MFI).

To test the performance of D-biotin and Fab monomer binding, the removal column was first implemented in the removal of a *Strep*tamer staining. Reversibility testing was now performed under the previously defined standard conditions comprising 3 wash steps and in a side-by-side assay with implementation of the removal column without centrifugation. The following experiment includes two different Fab proteins with slightly different Fab dissociation behavior. The CD4 Fab as a reference is perfectly reversible under standard conditions while a small amount of residual CD45RO Fab for the selected clone was detectable by *Strep*-Tactin restaining under the given conditions. We found identical results for the CD4 Fab comparing removal column and standard protocol. We conclude that the same removal efficiency is achieved for both strategies while the application of the removal cartridge yields good results in a much shorter time (ca. 40 min saving). Further, the implementation of the removal column with its extremely high binding capacity by virtue of large amounts of *Strep*-Tactin clearly enhanced Fab dissociation from the cells as seen in direct comparison of *Strep*-Tactin re-stainings upon both strategies in the case of CD45RO (**Fig. 5.39**).
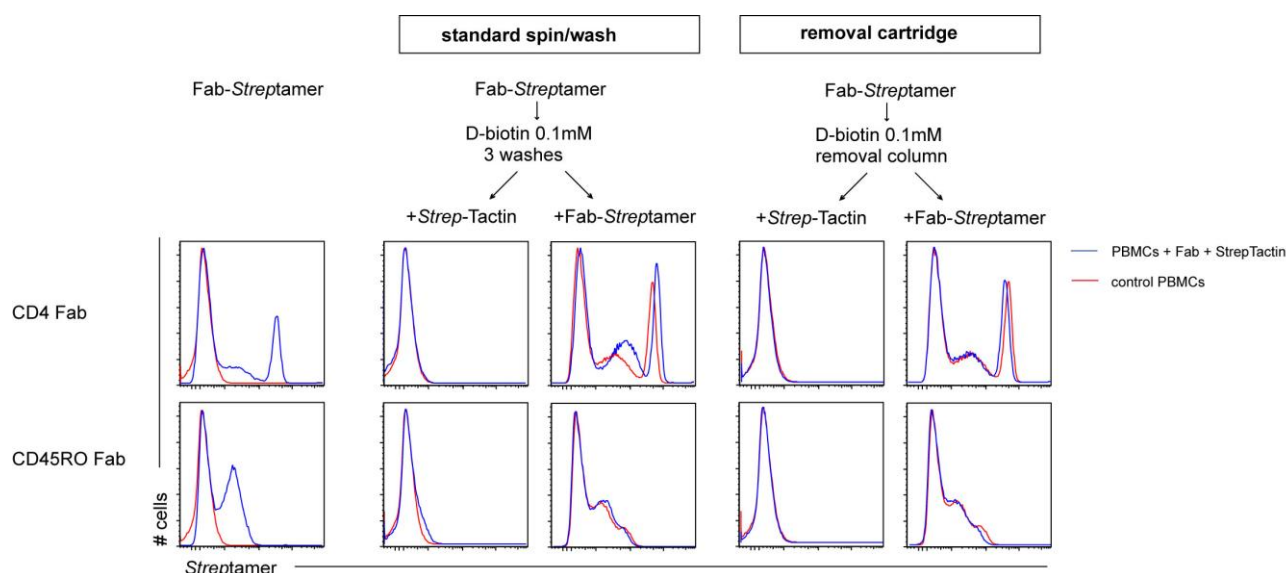
Fig. 0.39:Implementation of a removal column enhances Fab dissociation in a FACS-based reversibility assay

$2x10^7$ fresh PBMCs were stained with a CD45RO or CD4 Streptamer were split into two groups after they have been exposed to a 0.1 mM D-biotin solution (PBS/0.5%BSA/0.1 mM D-biotin) 20 minutes. One group underwent the standard wash protocol for Fab dissociation and D-biotin removal while the other group was run over a removal column. Cells of both groups were re-stained with fresh PE-conjugated *Strep*-Tactin or fresh Fab-*Strep*tamer. Red graphs represent control samples which were treated with PBS in place of Fab protein in the initial staining.

Subsequently, we have performed two-step serial magnetic enrichments implementing the removal cartridge between the first and the second selection step to collect evidence that the novel matrix can help improve multi-parameter cell purification. A representative experiment is shown in **Fig. 5.40**. In a first selection step, CD4+ cells were separated from a mixture of fresh PBMCs. The positive fraction was treated with 0.1 μM D-biotin for 20 minutes and was run over a removal column of 4 mL *Strep*-Tactin resin in size. The fraction was counted and aliquots were re-stained with phenotypic antibodies and *Strep*-Tactin-PE as a control for reversibility. We show two-step serial enrichments from 4 independent experiments including 8 positive selection steps. Purities of second step selections are clearly as good as purities from untouched cells that have never undergone a selection and reversibility cycle before indicating that no remaining selection markers interfere with subsequent selections. The recovery rates differed between the first and the second selection but this effect is marker-dependent. According to this, the measured recovery rates were not different from the usual recovery rates obtained from single positive selection with the same markers. Good purities and substantial cell counts in the second selection indicate the absence of excess D-biotin and Fab monomers (**Fig. 5.40b**). This is the first evidence that the removal column can be successfully implemented in reversible multi-parameter cell selections ensuring the complete removal of selection reagents without the need for centrifugation.
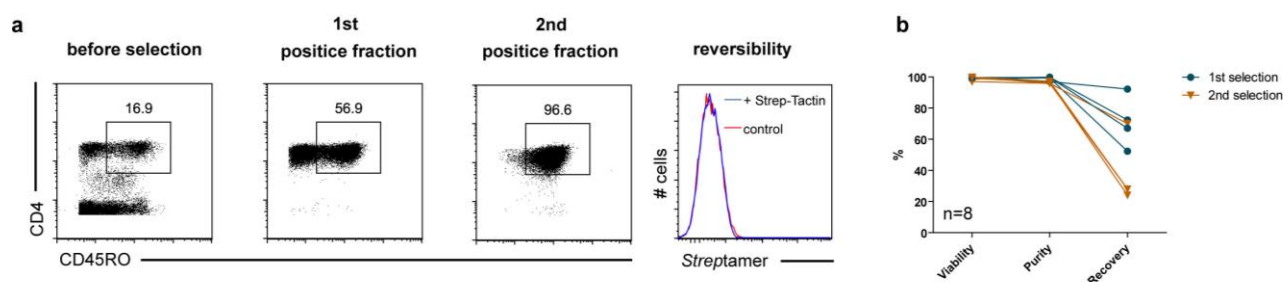
Fig. 0.40: Two-parameter selections using a high capacity *Strep*-Tactin removal column for reagent removal

$5x10^7$ or 10^8 fresh PBMCs were prepared for positive magnetic selection as previously described. After the first selection step, positive fractions were run on a 4 mL removal column. **a**. Dot plots show aliquots from before selection and positive fractions from the first and second positive selection. Cells from the 1st positive fraction were re-stained with fresh PE-conjugated *Strep*-Tactin for detection of any residual Fab-monomers. **b**. Summary of all two-parameter positive selections performed with implementation of the removal column.

Centrifugation steps in between selection cycles not only enable separation of soluble components from cellular components but also allow adjustment of the volume. The use of removal columns in a centrifugation-free system does not provide a means of reducing the volume in the positive fraction once D-biotin was added. We have compared the cell recovery rates from second selection steps with those from untouched cells that have never undergone a previous selection and reagent removal cycle and did not find any evidence for a substantial cell loss during removal with the removal column. However, to ensure maximal recovery rates in subsequent selections we wanted to dilute the target cell fraction as little as possible. We have experimentally determined the necessary wash volume as a multiple of the respective column size to recover at least 90% of all cells that were loaded on the columns. Therefore, cells were counted before and after flow through a removal cartridge and after each wash. Cell numbers varied slightly between experiments. Starting material was 10^8 cells respectively. In three independ experiments with different column sizes we determined that washing with a 2.5- or 3-fold of the matrix volume recovered 90% or more of the cells from the removal column. We did not observe any cell loss due to adhesion to the matrix material and were able to recover basically 100% of cells in all cases (**Fig. 5.41**).
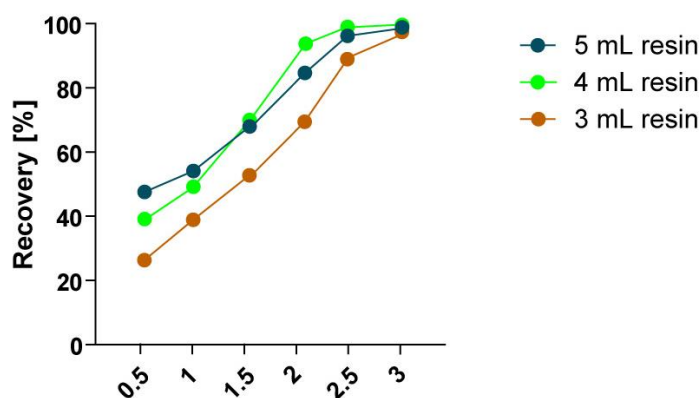
Fig. 0.401: Cell recovery from removal columns during reagent removal

10^8 fresh PBMCs were run over different removal columns. Columns were washed with six aliquots of 0.5 mL wash buffer (PBS/0.5% BSA) and counted after each step.

Next, we performed a three-parameter TCM enrichment as previously described with three different removal columns after each step as a proof-of-principle for the implementation of multiple removal columns into the sequential selection process. We have performed sequential CD8$^+$/CD62L$^+$/CD45RA$^-$ selection as previously described in more detail. After each individual enrichment step, the positive fraction was treated with D-biotin and subsequently run over a 4 mL removal column to remove Fab fragments from the previous selection and excess D-biotin. The magnet to remove magnetic particles was employed simultaneously in close proximity to the removal column. This centrifugation-free CD8$^+$ T$_{CM}$ purification yielded a CD8 purity of 99.2% and an overall purity of 96% for all three markers (CD8/CD62L/CD45RO, **Fig. 5.42**).
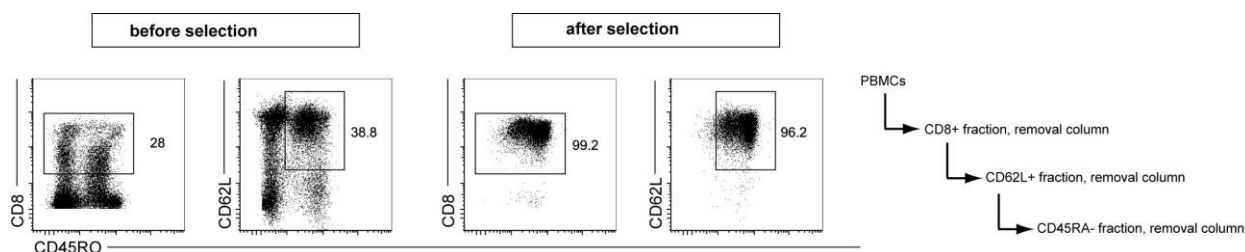

Fig. 0.412: Implementation of multiple removal columns in a three-parameter T$_{CM}$ purification

5×10^8 fresh human PBMCs were incubated with anti-CD8 Fab-*Strep*tamers conjugated with Strep-Tactin-functionalized magnetic microbeads. The CD8 positive fraction was collected and treated with 0.1 mM D-biotin and loaded on a 4 mL resin size removal column to remove remaining reagents. The removal column was placed in close proximity to a strong permanent magnet. In a subsequent second selection step, CD62L positive T cells were enriched from the CD8$^+$ fraction as described for the first step. Finally, CD45RA$^+$ cells were depleted using a CD45RA specific Fab-*Strep*tamer conjugated to *Strep*-Tactin-coated beads. Living lymphocytes obtained before and after the selection procedure are shown. Numbers in dot plots indicate gate frequencies.

Finally, we sought to combine multiple removal columns with the previously established T$_{CM}$ selection protocol using the clinically approved CTS magnet for separation. With disposable tubing sets for each selection step that were connected to reservoir and collection bags prior to the experiment we were able to perform each step in a closed-system. We performed a three-parameter T$_{CM}$ enrichment using the markers CD3/CD62L/CD45RA sequentially with two different 5 mL removal columns after the CD3 and CD62L positive selection step respectively. A *buffycoat* from a healthy volunteer yielded 4×10^8 PBMCs upon Ficoll separation with a T$_{CM}$ content of 10%. To depict viability, phenotype, and purity of every single positive fraction and the final fraction in the purification process we show all relevant gates and our complete gating strategy in the first 4 rows (gated on lymphocyte singlets). Here, we yielded 97.6% purity in the first positive fraction (CD3$^+$ T cells). For CD62L, we obtained a purity of 98.6%. Finally, CD45RA depletion resulted in a 98.5% pure CD45RO$^+$ population. We were able to recover 24.5% of T$_{CM}$s throughout all three steps of the enrichment process. Remarkably, the

purities for each individual marker were almost identical when no pre-gating was applied (**Fig. 5.43**). We conclude that an uncontaminated T_{CM} subpopulation can be obtained by serial positive enrichment even without the time-consuming conventional protocol for reagent removal by implementation of removal columns. The high purities and recovery rates indicate that the implementation of removal columns in between selection steps allows a reduction of the process duration by 90-120 minutes without losses in cell purity and yield.

TCM selection out of 4×10^8 BPBMCs
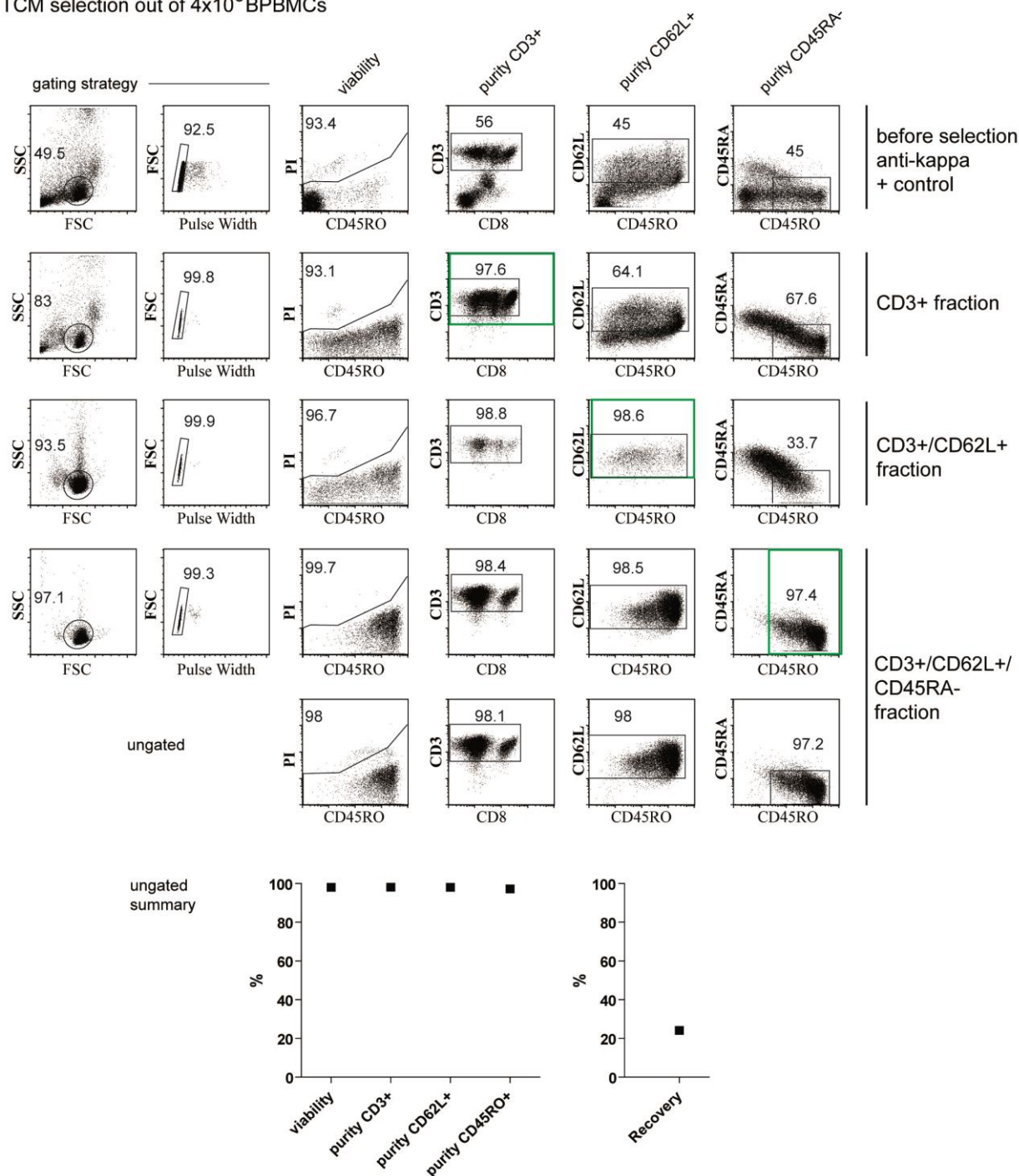
Fig. 0.423: Implementation of removal columns in a three-parameter T$_{CM}$ purification using

4×10^8 fresh human PBMCs from a *buffycoat* were incubated with anti-CD3 Fab-*Strep*tamers conjugated with Strep-Tactin-functionalized magnetic microbeads. The CD3 positive fraction was collected and treated with 0.1 mM D-biotin for 10 min prior to loading the fraction on a 5-mL high capacity ST bremoval column to remove remaining reagents. In a subsequent second selection step, CD62L positive T cells were enriched from the CD3$^+$ fraction as described for the first step. Finally, CD45RA$^+$ cells were depleted using a CD45RA specific Fab-*Strep*tamer conjugated to *Strep*-Tactin-coated beads. Living lymphocytes obtained before and after each selection step are shown. Positive fractions and their respective gating are highlighted in green for each step. Each row depicts cells which have undergone none, one, two, or three selection cycles (top to bottom).

5.6.2 Transfer of the *Strep*tamer-based TCM purification protocol to an affinity-based non-magnetic cell selection technology

To circumvent time intensive wash and centrifugation steps for isolation as well as for removal of monomeric *Strep*tamer components (D-biotin, MHC-/Fab-monomers) we implemented high capacity *Strep*-Tactin biopolymers into the removal process to capture residual selection reagents. We further aimed at a faster and easier magnet-free column-based selection technology using *Strep*-Tactin-coated biopolymer matrices for positive enrichment of cells through column affinity. Advantages of column-based cell selections include reduced handling complexity, more time saving during washing steps as well, incubation time on the magnet is no longer necessary, and beads can be functionalized prior to the cell selection process to omit pre-incubation time for reagents. *Strep*-Tactin-coated biopolymer-beads are at least 100 μm in diameter therefore allowing packaging in columns that enable the unhindered flow of cells in an identical way like removal columns. The non-magnetic technology is based on biopolymer beads that can be coated with multimerized Fab protein exclusively on the surface. The technology was originally invented and developed by Dr. Herbert Stadler (STAGE cell therapeutics). Although the cell selection columns consist of a very similar matrix material like the previously described removal columns, the *Strep*-Tactin coupling and location are distinctly different. Images of *Strep*-Tactin coated polymers stained with PE-coupled, biotinylated MHC-molecules clearly show, that *Strep*-Tactin is exclusively located on the surface of the beads in contrast to the removal beads which carry *Strep*-Tactin within the material (**Fig. 5.44**).

biotinylated, PE-coupled
MHC-molecules

transmitted light
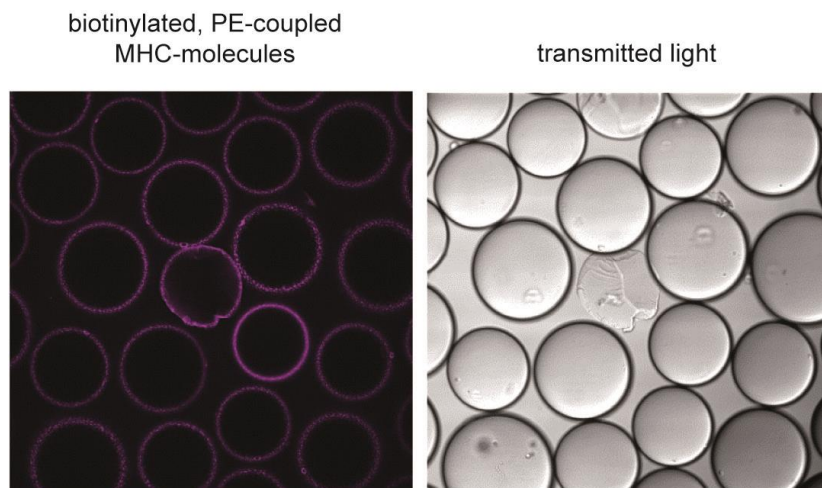
Fig. 0.434: Microscopic image of large non-magnetic polymer beads with *Strep*-Tactin conjugation

Strep-Tactin coated Polymer beads in a 1:1 suspension with PBS were stained with biotinylated,PE-conjugated MHC-multimers to visualize the local distribution of *Strep*-Tactin within beads. A transmitted-light bright-field microscopic image and a fluorescence microscopic image are shown with kind permission by Dr. Stadler.

Next, we showed that polymer beads with *Strep*-Tactin coating on the surface can specifically hold back cells on their surface which are stably bound throughout washing of the beads with PBS/BSA until disruption of the *Strep*-Tactin-Fab multimer by D-biotin treatment. We pre-loaded *Strep*-Tactin beads with 0.2 µg *Strep*-tagged CD4 specific Fab monomers to coat beads with Fab-*Strep*tamers which are formed through the *Strep*-Tactin on the bead surface. Thereby the polymer beads were functionalized for a positive CD4 enrichment step. Fresh PBMCs were incubated with the functionalized polymer beads for 20 minutes and the beads were washed carefully (**Fig. 5.45a**). Next, we demonstrated that the disruption of the *Strep*-Tactin-Fab complex with 1 mM D-biotin works well and might follow similar kinetics as the disruption of Fab-magnetic bead complexes (**Fig. 5.45b**). Our data indicate that a specific subpopulation of cells is successfully immobilized by previously functionalized biopolymers. The immobilization is likely to withstand a continuous flow since cells did not detach from the large beads through careful re-suspension of the mix during washing. D-biotin addition on the other hand caused instantaneous detachment of the cells from the beads. During the extended incubation time diffuse movement of detached cells became abundant.

Fig. 0.445: functionalized non-magnetic beads retain cells during washes and release cells upon D-biotin treatment

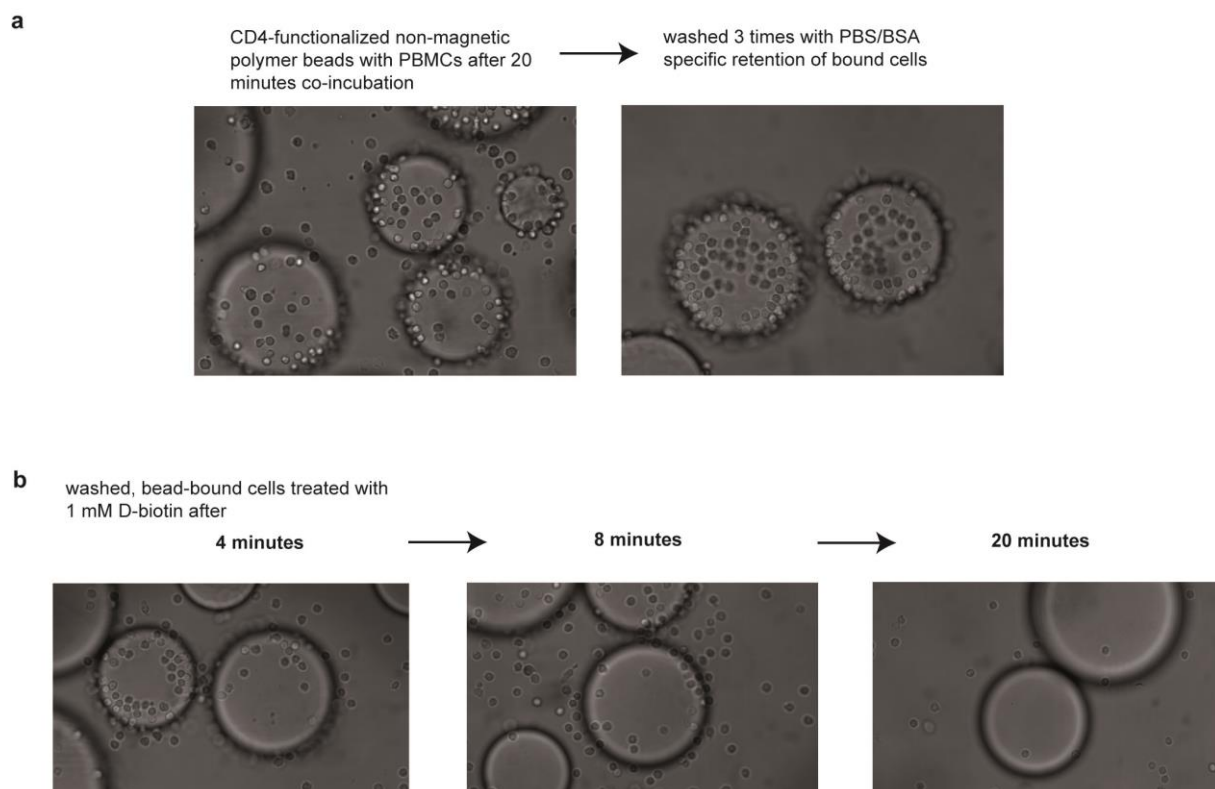Polymer beads were kept in a 1:1 dilution with PBS/BSA. 10 µl of the bead suspension was functionalized with 0.2 µg of CD4-specific Fab fragments for 5 minutes. **a**. After a 20-minute co-incubation with fresh PBMCs, unbound cells were washed away by repetitive dilution with 1 mL PBS/BSA and subsequent sedimentation and taking the supernatant (3 times). **b**. kinetics of the release after treatment with a 1 mM D-biotin solution.

In the previous experiment, the functionalized beads and cells were co-incubated in a reaction tube under constant gentle agitation. To be able to implement an affinity-based selection matrix into the process in a closed system, the beads must be packaged into columns with a unidirectional cell flow. We have evaluated three different strategies to implement selection columns into a cell flow and tested under which flow conditions (flow rate, constant flow or incubation stops) most cells were specifically retained by the affinity matrix. (i) gravity flow conditions, (ii) a tube leading from the column was inserted into a peristaltic electric pump which can keep a constant flowrate, (iii) manual application of suction through a syringe attached to a tube leading from the column. We have measured the retention indirectly by analysis of the flowthrough. Cells were stained and absolute cell numbers were determined. A high depletion of target cells and therefore a low detection of positive events in the flowthrough corresponds to a good retention of target specific cells. Specificity of retention was determined upon D-biotin treatment and subsequent release of the cells by re-staining and determination of the respective target cell purity. Gravity flow rates were too fast for stable retention of all cells and since the flow rate depends on the packaging of the matrix beads it was preferable to use a pump or manual suction at flow rates for a constant flow. We found flow rates of about 250 µL per minute for optimal cell retention. Next, we intended to determine the maximal retention capacity

of a bead matrix of 0.5 mL in size under optimized flow conditions. We have counted CD8$^+$ cells that have been retained by and subsequently released from 50 μL of functionalized biopolymer beads from a surplus of PBMCs. At the time when samples collected from the column flowthrough contained the same CD8 frequency as before the 50 μl column had retained 10^7 CD8$^+$ cells from the suspension. We were then interested in the number of cells in the positive fraction that can be held back by a 500 μL selection column while the target cell loss does not surpass 5%. We found that 2 mL of cell suspension containing a maximum of 5×10^8 cells can be securely loaded on a functionalized 500 μl selection column in order to achieve a depletion of target cells from the flowthrough of at least 95%. In summary, biopolymer-based selection columns can be conjugated with Fabs by simple loading of a diluted protein solution without the need for pre-incubation of Fab fragments and beads. To determine the necessary column length for selection, the number of cells as well as the concentration of the cell suspension are important parameters. The length and width of a column determine the flow rate under gravity conditions. Since this is subject to severe variation, a constant flow rate is striven for. Optimal loading conditions prevail at flow rates of up to 250μl/min while target cells are stably bound at flow rates up to 4 mL/min. A faster flow rate can cause detachment of target cells during wash steps. For columns ranging from 500μL to 5 mL resin volume wash steps require a 10-fold of the respective resin volume. For the elution with a 0.1 μM D-biotin solution the same parameters apply. Flow rates should never exceed 4mL/min to prevent cell damage due to spontaneous detachment from the resin.

5.6.3   Whole blood purification process without the need for prior density gradient centrifugation

For the following experiments, we took fresh whole blood from healthy volunteers for CD8 positive selections on Fab-functionalized biopolymer columns. The blood was layered onto the columns at once or in portions of ~3 mL depending on the blood volume applied. When overlaid with 1-2 mL of buffer, it is clearly visible that almost no red blood cells remain on the selection column in the flow through. Only a slight shade of red remains on the column after flow through before the wash with buffer (wash). The column right before elution of the positive fraction is perfectly white (**Fig. 5.46**). A potential source for contamination with red blood cells and other unwanted populations is the seam between two plastic parts (indicated by black arrow). In some experiments, contaminating cells have disengaged from rough seams during elution. In these cases, CD8 purities were comparably poorer probably because CD8$^+$ cells were outnumbered by contaminating red blood cells. For this reason, purities after a single positive selection step from whole blood were stated based on living T cells (pre-gated on CD3+ living lymphocytes). However, not every experiment suffered from contamination. We conclude that the underlying reasons are attributed to the quality of the plastic surface in welded areas. A representative CD8 positive selection from 10mL of whole blood is shown in **Fig. 5.46**. From a very small initial CD8 frequency of 0.35% of all blood cells a 96.1% pure CD8$^+$ fraction was purified in a

single step with no substantial contamination. In this example the CD8 purities raised to a comparable value of 97% indicating that the contamination with non-nucleated blood cells was neglectable (**Fig. 5.47a**). In conclusion, excellent purities and viability of CD8$^+$ cells can be achieved from whole blood in a direct positive selection using selection columns. Similar results were obtained regardless of the initial number of cells (either 1 mL or 10 mL of whole blood). In six independent experiments we yielded average recovery rates of 39.6%±9.2 exceeding those of single selection out of PBMCs by far when the recovery rate during Ficoll separation is also considered (**Fig. 5.47b**). As a rule of thumb, 50%-80% of PBMCs are lost during the density gradient centrifugation procedure. Recovery rates of a conventional single CD8$^+$ selection therefore averaged at 10-25% when taking into account these losses occurring during Ficoll separation. Separation from isolated PBMCs yielded even better recoveries.
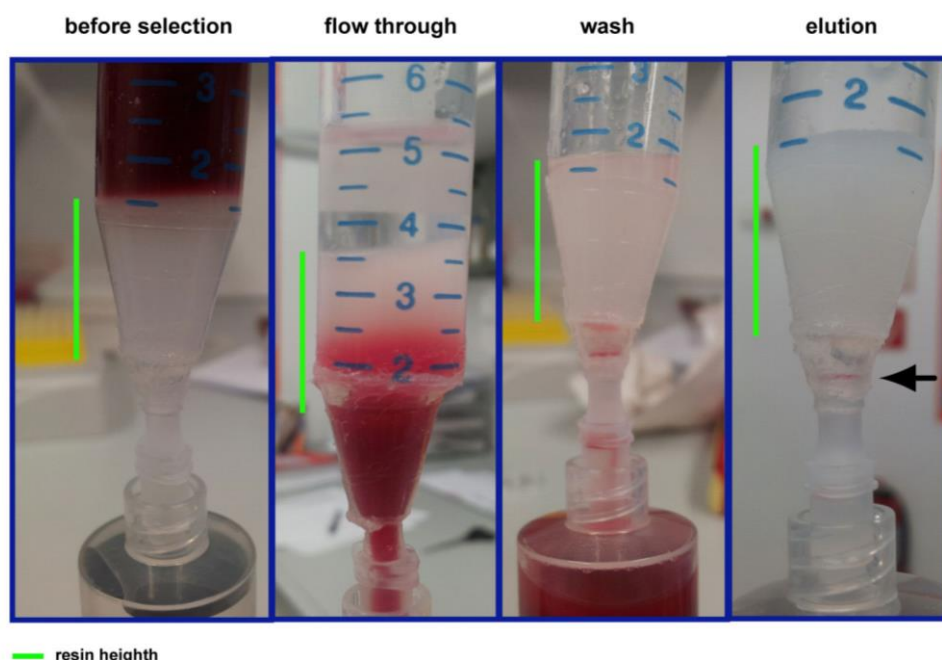
Fig. 0.456: Column-based positive selection process from undiluted whole blood

A 15 mL conical tube was modified using a mesh of 20 μm pore size to hold 1 mL of biopolymer resin. The column is then functionalized using 4 μg of CD8 Fab protein in 500μl of PBS/0.5% BSA. 10 mL of whole blood from a healthy volunteer were carefully layered on the previously functionalized CD8 selection column (first picture from the left). A semi-continuous flow of max. 500 μl/min was applied by manual suction through a conventional syringe. Wash buffer was applied in two steps à 5 mL each. During the first step the discoloration indicated that non-nucleated cells were not trapped within the selection matrix (second picture from the left). A completely washed column was free of contaminating red blood cells except for rough welding seams (third picture from the left). D-biotin treatment was applied to elute CD8$^+$ cells from the matrix (elution).
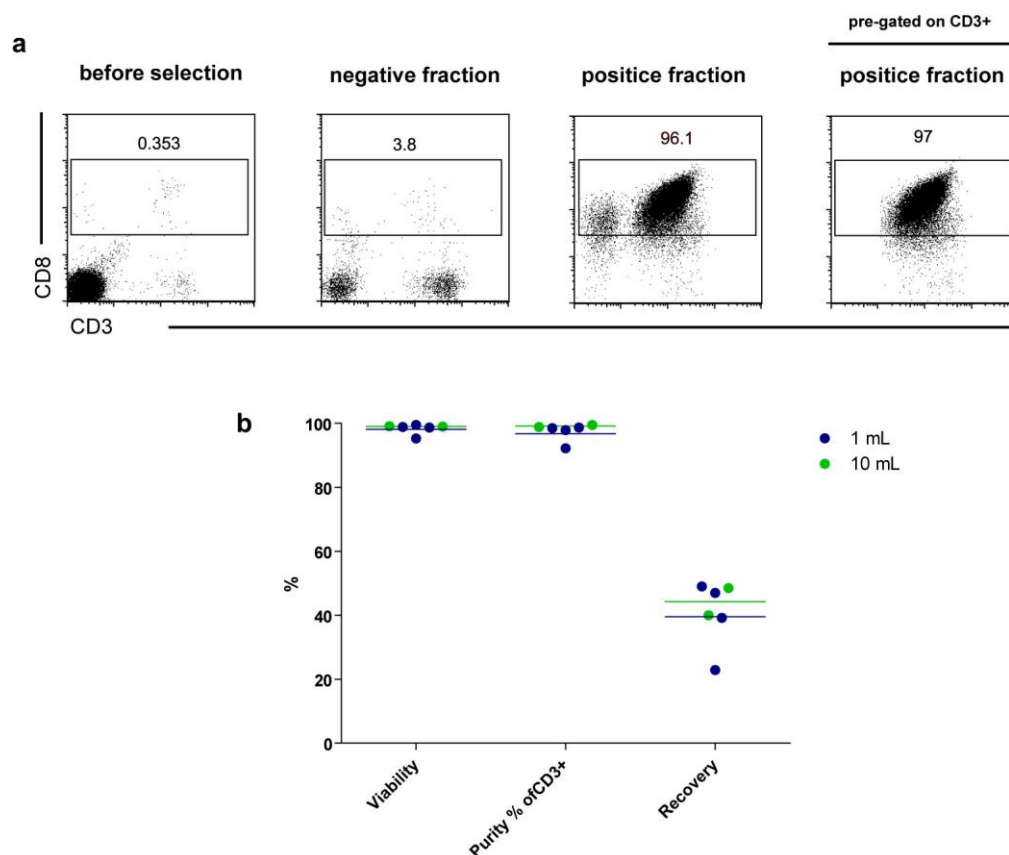
Fig. 0.47: Column-based positive CD8 *Strep*tamer selections from whole blood

Two different column sizes were used for the selection from 1 mL or 10 mL freshly drawn whole blood. For 10 mL whole blood, columns were prepared with 1 mL resin and loaded with 4 µg CD8 Fab. For 1 mL whole blood, columns were prepared with 400 µL resin and loaded with 2 µg CD8 Fab. **a**. A representative selection was performed, and samples from each fraction were taken (except 1st flowthrough), and re-stained with antibodies for flow cytometry. **b**. Summary of CD8 positve selections from whole blood performed on Fab-loaded *Strep*-Tactin columns (n=6).

6. Discussion

This thesis work is focused on the development of a pre-GMP protocol for the positive selection of human central memory T cells (T_{CM}) using the novel *Strep*tamer-based reversible cell isolation technology. The central memory T cell subset has previously been associated with several traits which can positively influence the clinical outcome of adoptive T cell transfer. Therefore, many experts in the field of cellular therapy have proposed that clinical purification not only of different cell lineages (e. g. T cells, B cells, NK cells) but also defined cell subsets (e.g. memory subsets like central memory T cells and/or naïve T cells) might be advantageous. Obtaining optimal purities in the enrichment process is believed to be crucial to enhance the efficacy of adoptive T cell therapy.

This challenge has been embraced by a number of research groups who developed novel cell purification techniques over the past years. Efforts in this area are complicated by fact that they have to get approved by regulatory authorities before they can be tested in clinical applications. If selection reagents (often conjugated paramagnetic beads or fluorochromes) stay on the purified cell population and get co-transferred into patients, laborious toxicity and immunogenicity studies have to be performed during the process of clinical approval. We present here a protocol for the selection of central memory T cells that can overcome some of these hurdles. We evaluated cell separation reagents that enable serial positive enrichment and demonstrated that serial magnetic enrichment works robustly over three parameters yielding very high purities and recovery rates. Thereby, the final cell product is free of any staining reagents. Based on this procedure, we established a GMP-compliant process and scaled the process up for the use in patients.

6.1   Advantages of central memory T cells for adoptiveT cell therapy

The role of distinct T cell subsets with respect to overall efficacy as well as safety of adoptively transferred T cells is still controversially discussed. In terms of adoptive T cell therapy against tumors, the memory compartment has been thoroughly investigated throughout the past years. The central memory T cell subset has been associated with stem cell-like characteristics, which might be important for the subsequent clinical outcome of adoptive T cell transfer including longevity, the ability to migrate to lymph nodes, the generation of different effector and memory T cell subsets, an excellent proliferative capacity and a good safety profile. T_{CM} are long-lived antigen experienced cells with a high differentiation plasticity. Indeed, it has been shown that a single central memory T cell can reconstitute all T cell compartments except the naïve compartment. In several studies in mice, non-

human primates and humans, preparing a therapeutic T cell product comprised of cells from the central memory phenotype was shown to provide high *in vivo* persistence and functionality of the transferred T cells [1-4].

In most published clinical adoptive immunotherapy studies in which T cells are used to treat cancer or viral infections, the subset composition of transferred cells was not determined when cells were administered to patients, despite the knowledge that the phenotypic composition of the T cell pool in individual donors is highly variable (interindividual differences between donors) and can similarly differ in therapeutic cell products. Nonetheless, phenotypic features were retrospectively analyzed in some cases in attempts to correlate clinical outcome with intrinsic cell attributes of the infused T cells.

In studies with tumor infiltrating lymphocytes for example, the retrospective analysis of phenotypic markers demonstrated that relative frequencies of $CD62L^+$ T cells correlated beneficially with the regression of late-stage cancers. Genetically modified naïve and central memory T cells (both $CD62L^+$) contributed especially well to an objective anti-tumor response in allogeneic transfers. For therapy of latent viral diseases, the central memory compartment is a defined subset that harbors specific T cells that are reactive towards viral antigens. T cells specific for antigens of latent viruses can confer direct protection against re-activation by the particular pathogen in the recipient upon adoptive transfer. Antigen specificity against a defined epitope can also be exploited by using the respective peptide vaccine as a booster to activate and expand them *in vivo* in the recipient (for example CMV or EBV antigens).

Selection of a pure central memory T cell subset can improve adoptive T cell therapy since the heterogeneous and often highly variable compositions of currently used clinical cell products very likely interferes with the efficacy of T cell therapies. This could for example be due to regulatory T cells that could dampen the effects of central memory T cells or the competition for cytokines from exhausted cell subsets (T_{EMRA}) cells that may act as a cytokine sink but be less able to mediate therapeutic activity [5]. Therefore it might be advantageous to eliminate some subsets from a therapeutic cell product while other cell intrinsic properties which determine the ability of self-renewal and long-term persistence should be positively selected.

Central memory T cells share some characteristic traits with naïve T cells. For instance, the naïve T cell subset also harbors broad differentiation plasticity and is considered a suitable subset candidate for immune reconstitution as well. It has been shown for the adoptive T cell therapy of cancer that engineered T cells recombinantly expressing tumor-reactive TCR or CARs mediated a more complete and durable tumor regression when derived from naïve than memory T cells [6-8]. The cells that were investigated in these studies underwent quite extensive *in vitro* manipulation. Therefore, it is possible that other transduction or expansion methods could give different results.

On the other hand, in contrast to central memory T cells, naïve T cells usually carry the greatest TCR diversity and the potential reactivity profile is very broad. In allogeneic transfer, naïve T cells have therefore a particularly high risk for allo-recognition of healthy tissue in the recipient (Graft-versus-

host-Disease) [9, 10]. Antigen-experienced T cells might have some advantages compared to naïve T cells. For instance, in allogeneic settings antigen-experienced memory cells are likely to possess a superior safety profile because they carry TCRs, which should mainly be directed against non-self antigens that were for example previously presented in the context of infection.

It has also been reported that aging and regimens of conventional cancer therapy (like chemotherapy and/or radiation) can impact the size and robustness of the pool of naïve T cells whilst memory T cell compartments are less affected [11].

In summary, central memory T cells might posses superior traits with respect to safety and furthermore posses the advantage of a relatively high differentiation plasticity among the memory subsets. Therefore we chose to develop reagents and procedures to isolate central memory T cells for clinical use, although by modifying the selection steps, we could in principle also obtain naïve or effector memory T cells with the reagents that we have developed. Whether ultimately a defined mixture of cells or a single purified subset are most beneficial for the treatment of patients remains to be answered in clinical trials. Clinical protocols supporting the selection of highly defined T cell subsets will provide the opportunity to address these questions in clinical settings.

6.2   Central memory T cell subset selection

Subpopulations, like central memory T cells, can only be detected by their complex combination of expression markers and require elaborate protocols for purification. Not all isolation techniques are suitable for targeting such complex subsets. Especially the isolation of T_{CM} is challenging, as this subpopulation occurs in the peripheral blood at a very low frequency of 1.5-2% of PBMCs [12]. The first clinical protocol to enrich T_{CM} using standard non-reversible reagents was developed by Wang et al. [13]. A vast cocktail of depleting monoclonal antibodies was applied to exclude cells that express the markers CD4, CD14, or CD45RA. To finally enrich T_{CM} from the remaining negative fraction, a positive selection step for CD62L expressing cells was conducted. The authors described their approach as a robust technique for the purification of central memory T cells that demonstrated enhanced in vivo persistence and safety in a clinical phase I/II trial. However, this protocol results in many contaminating CD62L$^+$ cells that are not depleted by even the large cocktail of antibodies and may have uncertain consequences in a therapeutic setting. Inspired by this work, we have developed an improved protocol using reversible markers for the serial enrichment of central memory T cells and compared our results with the previously described clinical protocol for the preparation of T_{CM}. While recovering about 25% of target cells in relation to the number of T_{CM} in the initial product, the final purities reached by the published protocol averaged 36%, which is unsatisfactory since contaminating cells might mediate unwanted toxicities like GvHD. For reasons discussed before (e.g. GvHD risk, regulatory cells, and cytokine sink), purities of at least 90% were aimed at when developing our

alternative approach. Mainly CD13$^+$ basophils were identified to contaminate the T cell product in the previously published protocol. To further improve the quality of selected cells according to this strategy, it would be necessary to include even more depleting antibodies in the first step of processing. Such an adaption of the selection protocol has quite some consequences, especially since all reagents have to be manufactured in compliance with GMP regulations. This is an expensive and also a time consuming process. We demonstrate with this thesis work how to overcome such hurdles by *Strep*tamer-based serial positive enrichment of T$_{CM}$. In contrast to the published method, the mean purity of recovered CD8$^+$ T$_{CM}$ was 97.8% with a 29.5% average recovery (Fig. 5.30). CD3$^+$ T$_{CM}$ selections yielded 93.5% purity (mean) and recovered on average 32.9% of the initial number of T$_{CM}$ (Fig. 5.34). CD13$^+$ basophils were never detected in our TCM products (data not shown). However, some observations could not be vastly improved by application of a *Strep*tamer-based isolation protocol for T$_{CM}$. An important issue is that the recovery rates differed between donors using both the recently published depletion- and the *Strep*tamer-based protocol. This could be due to interindividual differences in the expression of the markers used for selections. Since only CD62L was used for positive selection in the protocol from Wang et al., differences in CD62L expression are most likely involved to provoke scattering in recovery rates. However, we have detected variation in recovery rates to some extent for all markers (Fig. 5.31). This indicates that the detected differences in recovery are not restricted to the CD62L selection step but represent more the sum of combined variations during selection for all three surface markers. Possibly, the expression of target molecules per cell influences the selection efficacy. This interpretation is supported by the observation that we often preferentially purified cells expressing the target molecule at a higher level. Segregation by gates between high and low expressing CD8 T cells for example revealed that losses during the wash (incomplete depletion in the negative fraction) occurred mainly in the CD8 low expressing population. Taken together, our data show a vast improvement on the purities and a slight improvement on the recovery rates of T$_{CM}$ for clinical use of the Fab *Strep*tamer-based enrichment protocol compared to available alternatives.

6.3 Advantages of reversible reagents for positive selections

6.3.1 Reversible reagents improve multi-parameter positive selections

Multi-parameter positive magnetic selection was first enabled by the use of *Strep*tamer-based selection reagents [14]. In this thesis work, we focused on purification of the clinically relevant subset of central memory T cells. However, also effector memory and naïve T cells can in principle be easily selected

in parallel during the same clinical selection process using our set of reversible reagents. By performing the positive CD62L selection step at the end, central memory (CD3$^+$/CD45RO$^+$/CD62L$^+$) and effector memory T cells (CD3$^+$/CD45RO$^+$/CD62L$^-$) could be separated at high purities from the same donor in parallel. Similarly, naïve (CD3$^+$/CD62L$^+$/CD45RA$^+$) and central memory T cells (CD3$^+$/CD62L$^+$/CD45RA$^-$) could be isolated from the same donor material by applying CD45RA or CD45RO at the end. Compared to negative selection protocols or single parameter selection, the proposed strategy provides for cost-efficient isolation of highly pure subsets. This enables direct comparison of individual subsets from the same donor material in terms of efficacy in adoptive T cell therapy in future trials.

In the case of many subsets that require multi-parameter sorting, serial positive enrichment may become a cost-efficient way to achieve superior purities and recovery rates. The *Strep*tamer technology is very flexible and can be applied for a theoretically infinite number of combinations of different surface antigens. This strategy can be translated very rapidly into clinical processing facilities and can be combined with already approved cell processing devices, as shown here for the CTS platform.

During this thesis work, an alternative clinical-scale selection protocols over two positive parameters has been suggested for naïve and central memory T cells [15]. Here, the selection approach relies on the combination of two different non-reversible magnetic selection strategies. The first positive selection step is conducted with standard nano-sized magnetic 'microbeads' and the subsequent step is performed with larger (3.5 µm in diameter) beads with a standard permanent magnet, thus eliminating interference with the previously applied smaller beads through a stronger magnetic field. Limitations of this approach are costs that are related to the approval of GMP-grade non-reversible reagents and the limit to only two positive enrichment steps due to the size range of suitable magnetic particles. Combination of this technology with reversible *Strep*tamers is possible, since we have shown that CD3-, CD4-, CD8-, CD62L-, or CD45RA-specific Fab *Strep*tamers perform well with nano-sized particles (Fig. 5.20). Combining both strategies should improve the process duration because reagent removal is only necessary between positive steps that are conducted with same-sized magnetic particles.

Multi-parameter analysis and selection of cells are usually associated with flow cytometry. Indeed, FACS sorting is another potential clinical approach towards multi-parameter cell isolation. Its great advantage over magnetic sorting is the possibility of simultaneous sorting over multiple parameters. This can vastly reduce processing times for initial cell numbers roughly below 10^8. Great efforts are made in developing clinical cell sorters, but the complex technical equipment make it more difficult to develop a protocol that is generally approved by regulatory authorities. Highly advanced hardware and disposable tubing sets are necessary and currently it is still not possible to conduct a sterile selection process at low costs. The disadvantages of the open system in FACS sorters, like aerosol generation, are especially challenging. Aerosols are a potential hazard for personnel who work with human

material. The safety assessment of fluorescent labels, when applied together with the selected cells into patients, is another unsolved issue (see below). Becton Dickinson´s Influx is an example for a first cell sorter that can be implemented into GMP cell processing platforms. Novel technologies, like cell sorters based on microfluidics, promise to circumvent aerosol production and are more likely to ensure occupational safety. FACS sorting in general can also vastly benefit from the Fab-*Strep*tamer technology. We have shown that Fab *Strep*tamers specific for CD4, CD8, CD3, CD62L or CD45RA and CD45RO multimerized with a fluorescent *Strep*-Tactin backbone perform identical to the conventional fluorescent monoclonal antibodies (Fig. 5.1, 5.2, 5.4, 5.6 and 5.7). Therefore, our marker set for the positive selection of central memory T cells can easily be combined with FACS-based cell isolation techniques. This was recently successfully tested in our group (Stemberger et al., unpublished data). The use of fully reversible fluorochrome-conjugated Fab-*Strep*tamers for clinical FACS sorting could especially overcome toxicity concern regarding the use of fluorochromes during the selection process.

6.3.2   Circumventing problems caused by remaining sort markers

For clinical applications it is important that uncompromised biological function of transferred cells is ensured. It is known for a long time that remaining sort markers, such as antibody conjugates, can cause cell damage and even unwanted side effects upon infusion. The co-infusion of selection markers such as monoclonal antibodies is a potential source for toxic side effects.

Positive enrichment of cell populations leaves the purified cells usually with a non-reversibly bound selection marker. Depending on the target and its functions, there are several mechanisms how the cell function might be impaired. First, cell selection markers can cause premature activation or receptor blockade in some cases leading to alterations of the cell's effector functions. Direct comparison of conventionally labeled cells with Streptamer-labeled cells that are subsequently reversed and untouched control cells in the case of CD3 have convincingly shown that CD3 binding caused activation in vitro only in the group with the conventional irreversible marker (unpublished data).

Further, remaining surface markers can hinder successful engraftment or clinical effects when the cells are directly transferred or compromise cell expansion *ex vivo*. In the case of murine CD62L, the irreversible antibody used for sorting vastly compromised engraftment of T cells [16]. If sorted cells are expanded *in vitro* prior to adoptive transfer, the positive selection marker should get diluted in cell culture and therefore should not interfere with engraftment.

Finally, receptor blockade might occur if targets are associated with receptor functions. This is relevant for selection of regulatory T cell, which are a defined candidate subset of T cells that have therapeutic potential for GVHD and autoimmunity, and are defined as CD4$^+$, CD25$^+$ and CD127$^-$. For regulatory T cells, it is almost impossible to envision a protocol for effective purification by negative selection and the CD25 (IL2 receptor alpha) marker is necessary for the positive selection of the

regulatory T cell subset. Blocking CD25 with non-reversible selection reagents can interfere with IL-2 binding to the receptor resulting in a lack of proliferation and survival of these cells.

Potential immunogenicity of antibody reagents used for cell selection is in principle independent of the target and its functions. To circumvent potential complications, it is essential to use humanized monoclonal antibodies to prevent immunogenicity. Nevertheless, non-reversible selection markers that are co-transferred with the cell product into patients have to undergo cost-intensive testing before receiving approval from the authorities. The reversible *Strep*tamer technology is a versatile tool to circumvent the need for toxicity and immunogenicity testing, provided it can be demonstrated that these reagents can be fully removed from the selected cells and therefore, are not co-transferred into patients. Indeed, first Fab-based *Strep*tamers recently received the legal approval for clinical use and were classified as minimally manipulative to the sorted cell population.

6.4   Generation of Fab *Strep*tamer reversibility

We have demonstrated full reversibility for a complete set of Fab *Strep*tamers, which was used for the separation of central memory T cells. We found that reagent reversibility depended mainly on the wash procedure and the temperature. In some cases it was necessary to shift the temperature to room temperature during the removal phase to facilitate rapid dissociation of the Fab monomers (Fig. 5.16 and Fig. 5.18). According to our hypothesis, receptor internalization might occur at higher temperature (e.g. room temperature). Our results demonstrate that Fab reversibility needs to be determined for each new Fab individually. Our laboratory is currently developing a flow-based k_{off}-rate assay for tracking of monomer dissociation on a population level. This technology allows to accurately measure the dissociation of monomeric ligands from the surface of living cells and should be broadly applicable to measure reliable values for the dissociation kinetics of Fab proteins from the cell surface [17].

A limitation of the Fab *Strep*tamer technology is the generation of reversible Fab monomers. If the parental Fab fragment isn't of low enough affinity to begin with, its binding affinity has to be reduced by the introduction of amino acid exchanges within the framework or variable region. We have faced examples where it was very difficult to sufficiently reduce binding affinity by mutation. In some cases we observed a 'non-reversible' compound within the Fab preparations, although the majority of Fab dissociated rapidly from the cell surface (Fig. 5.14). Biochemical analyses demonstrated that heavy and light chains were not represented at a 1:1 ratio in all Fab preparations. We are currently improving vectors and protein purification to eliminate a surplus of one antibody chain. Furthermore, we have gathered data indicative of better Fab quality when two different tags are fused to the heavy and light chain respectively for protein enrichment.

To speed up the general process of reagent removal, we tested a biopolymer-based column that works under simplest gravity flow conditions and which it is able to capture excess D-biotin and Fab

monomers through its high Strep-Tactin content by affinity (Figs. 5.36-5.42). We further demonstrated that it is possible to implement such removal columns into a fully closed system for one positive enrichment step (Fig. 5.43). The subsequent enrichment step still required an opening of the sterile system. The implementation of removal columns into the CTS DynaMag-based sterile system was out of the scope of this thesis and will be continued in pre-clinical and clinical work in the future.

6.5 Optimization of positive magnetic selection with larger magnetic microbeads

Current clinical cell isolations usually rely on magnetic beads of sizes in the nanometer range (50-100 nm in diameter). These technologies all depend on specialized equipment like microcolumns for retention of the cell-bead complexes. We have demonstrated that nano-sized magnetic beads are not fully reversible under the given experimental conditions. Further, our experiments suggest that some nano-sized beads remain on the cell surface or inside the cells in a Fab-independent manner. It is known that depending on the size, particles of up to 200 nm can be rapidly internalized by mammalian cells even at very low temperatures (4°C) [18-20]. Besides that, very small particles might get trapped on the cell surface, which is not smooth but consists of folds and grooves resulting from membrane evaginations. Furthermore, small changes in the cell membrane due to its semi-fluidity might cause trapping of magnetic particles, thus interfering with potential reversibility.

As a solution to this problem, we combined the reversible *Strep*tamer technology with larger magnetic microbeads (micrometer range). Using this approach, we were even able to show that the duration of the purification process can be reduced due to faster immobilization in the field of a strong permanent magnet. Most of our experiments were conducted with microbeads in the micrometer range of 1-1.5 µm in diameter, which sediment in a magnetic field in less than 1 minute. They also showed outstanding purities in positive cell selections compared to other bead sizes in positive selections (Fig. 5.20, Fig. 5.23, Fig. 5.24 and Fig. 5.26). Processing time and costs are still one of the major hurdles in broader availability of cell therapy for a wide range of applications. Reducing duration and the need for specialized equipment are likely to be valuable steps towards affordable and effective T cell therapies.

As an alternative, intermediate size beads (in the nanometer range, 200-300 nm in diameter) have been introduced to the field which can be retained in close proximity to a magnet without the need for separation columns [21]. These beads combine the advantage of bigger beads with the advantages of nano-sized beads which can be separated by centrifugation and do not pellet like cells and debris. In the future, different bead sizes might contribute distinctly to individual applications.

In the case of direct transfusion of a cell product upon selection, the co-infusion of larger magnetic beads into patients is not approved by regulatory authorities. Therefore, so far only negatively sorted cell products have been used for clinical cell processing with larger beads. Reversible *Strep*tamers for the first time allow the use of larger microbeads for clinical positive enrichment, since the bead can be fully removed after the selection process.

6.6   Clinical applications for *Strep*tamer-based T_{CM} purification

Clinical approaches to isolate central memory T cells so far either rely on negative selection techniques or on *in vitro*-stimulation and subsequent phenotyping before selection. An example is a recent study from a group that identified and expanded human T cell clones for infusion based on secretion of cytokines. T cells with a high IL-2: IFN- γ ratio were identified and expanded as central memory-like T cells for the transfer to patients [22]. Laborious cell culture steps that consume weeks of cell preparation in a GMP facility could be eliminated by application of the *Strep*tamer-based selection of central memory T cells.

Similarly, for the treatment of virus infections upon allogeneic hematopoietic stem cell transplantation (HSCT), e.g. CMV, the recently approved MHC *Strep*tamer technology successfully eliminated the need for *in vitro* re-stimulation with peptides by direct isolation of CMV-specific T cells [23-26]. MHC-based *Strep*tamers have received approval for clinical use recently. Previously it was necessary to use antigen stimulation to grow out high numbers of cloned T cells with a defined specificity from polyclonal T cell populations.

Other potentially interesting target cell populations for clinical use are naïve T cells or regulatory T cells, which can be obtained in a very similar way as here described for central memory cells. Even protocols that require *ex vivo* gene manipulation can be modified in a way that *Strep*tamer selection and subsequent viral transduction of T cells can be completed, perhaps this all can be accomplished in less than 24 hours (Dr. Michael Jensen, personal communication).

In this thesis, we have made some effort to reduce the time consumption of the T_{CM} isolation process as it would be carried out in a GMP facility. We have estimated that the process currently requiring 6-8 hours (depending on the starting number of cells) can be vastly shortened by eliminating centrifugation steps during reagent removal (see above). We could show that the implementation of a removal column after each positive selection step resulted in at least 90 minutes of saved time. It is very likely that the biopolymer-based removal columns will receive clinical approval by the national authorities soon; this could help to further reduce the overall processing time.

We were interested in purification of central memory cells, for example also as a basis for the introduction of a transgene as well as for direct primary transfer. The idea that T_{CM} might also be a suitable subpopulation for *in vitro* gene manipulation was assessed in animal studies in mice and non-

human primates [2, 3]. Even when gene-modification requires an expansion step *in vitro,* cells derived from central memory precursors persisted long term *in vivo*. It has been demonstrated by Berger et al. that cell clones expanded from central memory T cells were detectable in vivo after many months while clones generated from effector memory T cells disappeared after only two weeks. These data have been gathered from adoptive transfer experiments in macaques, an animal model very close to the human organism.

A common misconception in adoptive T cell therapy concerns the missing strict dose-response relationship as known for non-living biologicals. A very low number of T cells can already be enough to mediate efficient cell engraftment and subsequent *in vivo* expansion. Pre-selection of a defined cell subset with superior *in vivo* engraftment and survival characteristics could help to make subsequent clinical responses more effective, predictable and perhaps also safer. Since antigen-induced activation can lead to excessive proliferation, cell numbers can expand very quickly upon transfer. A recent report from our lab showed that lowest numbers of *Strep*tamer-enriched cells led to strong expansion of functional T cells in patients upon allogeneic HSCT [27].

6.7 Clinical trial using *Strep*tamer-enriched T_{CM} for immune reconstitution of post HPCT patients

Immune recovery from deficiencies in B- and T- cell reconstitution after hematopoietic progenitor cell transplantation (HPCT) is a process that can take up to over one year. During this time patients have to undergo prolonged administration of antiviral medications to prevent life-threatening infections, with significant side effects. It was shown that adoptive T cell transfer is a therapeutic approach that can effectively treat reactivations with latent viruses upon HPCT [28, 29].

Our pre-GMP selection protocol of CD3$^+$ central memory T cells was recently tested in the clean room GMP-facility TUMcells to initiate the application process for production approval. The first results from GMP-purifications demonstrate that central memory T cells can be purified to very high purities and with high yields under conditions following the good manufacturing practice (GMP) guidelines. These efforts initiated already the launch of a clinical phase I/IIa study where purified central memory T cells are given in escalating doses to assess their safety and persistence in patients upon allogeneic stem cell transplantation. The study runs under the name *prophylactic application of escalating doses of donor-derived central memory T lymphocytes (TCM) after allogeneic hematopoetic progenitor cell transplantation (HPCT) to prevent infectious complications (PACT): A Prospective, first in man, open Phase I/IIa Clinical Trial.* Aim is the prophylactic administration of escalating doses of *Strep*tamer selected central memory T cells to patients following hematopoietic progenitor cell transplantation (HPCT). This is the first-in-man trial of clinical grade-purified CD3$^+$CD62L$^+$CD45RA$^-$CD45RO$^+$ central memory T cells by means of serial positive enrichment. The goal of this trial is to administer

the first T cell dose 30 days post HPCT from the donor and assess potentially occurring Graft-versus-host disease and any other side-effects related to T cell administration. In detail, the first dose received 30 days post HPCT is 5×10^3 T_{CM}/kg, on day 60 10^4 T_{CM} /kg and on day 90 5×10^4 T_{CM} /kg. The transferred population contains $CD4^+$ and $CD8^+$ T_{CM} representing the whole repertoire of long-lived antigen-experienced T cells in the donor. Depending on the prevalence in the population, donor-derived T_{CM} might contain CMV-, EBV-, or Adenovirus-specific T cells. Even anti-fungal T cells specific for aspergillus have been described. These cells can work as a prophylactic strategy to protect HPCT patients from secondary infections with opportunistic pathogens, superinfections, or reactivations with latent viruses by means of immune reconstitution. Further, the persistence and expansion of transferred T cells will be monitored. Our working hypothesis is that the prophylactic application of low numbers of TCMs can significantly reduce the occurrence of infections with opportunistic pathogens upon allogeneic HSCT.

This direct clinical translation of the generated data from animal models or *in vitro* assays will shed light on the proliferative capacity and safety profile of the T_{CM} subpopulation.

7. Material and Methods

7.1 Material

7.1.1 Equipment

Equipment	Supplier
Centrifuges	Centrifuge Biofuge fresc, Heraeus, Hanau, Germany
	Sorvall® RC 26 Plus, Heraeus, Hanau, Germany
	Multifuge 3 SR, Heraeus, Hanau, Germany
Cell isolation systems	MiniMACS, Miltenyi, Bergisch Gladbach, Germany
	MidiMACS, Miltenyi, Bergisch Gladbach, Germany
	Fab *Strep*tamer magnetic isolation, IBA, Göttingen, Germany
Flow cytometer	Cyan ADP, Dako Cytomation, Fort Collins, USA
	FACSAria cell sorter, Becton Dickinson, Heidelberg, Germany
HE33 agarose gel casting system	Hoefer, San Francisco, USA
Heating block Thermomixer compact	Eppendorf, Hamburg, Germany
Incubator Cytoperm 2	Heraeus, Hanau, Germany
Laminar flow hood HERA safe	Heraeus, Hanau, Germany
Microscopes	Axiovert S100, Carl Zeiss, Jena, Germany
	Carl Zeiss, Jena, Germany
	Confocal microscope Leica SP 5, Leica, Bensheim, Germany
MightySmall SE245 gel casting system	Hoefer, San Francisco, USA
NanoDrop spectrophotometer	NanoDrop, Baltimore, USA
Neubauer counting chamber	Schubert, München, Germany
Shaker Multitron Version 2	INFORS AG, Bottmingen, Germany

Equipment	Supplier
Superflow *Strep*-Tactin columns	IBA, Göttingen, Germany
Thermocycler TProfessional Thermocycler	Biometra, Göttingen, Germany
Vacuum filtering system Stericup 0.22 μm	Millipore, Bedfore, USA
Waterbath LAUDA ecoline 019	Lauda, Lauda-Königshofen, Germany

7.1.2 Chemicals and reagents

Reagent	Supplier
Acrylamide/Bis 30%	Biorad, München
Ammoniumchloride (NH_4Cl)	Sigma, Taufkirchen, Germany
Ampicillin	Sigma, Taufkirchen, Germany
Biocoll Ficoll solution	Biochrom, Berlin, Germany
Bovine serum albumin (BSA)	Sigma, Taufkirchen, Germany
Cytofix/Cytoperm	BD Biosciences, Heidelberg, Germany
d-Biotin	Sigma, Taufkirchen, Germany
Desthiobiotin	Sigma, Taufkirchen, Germany
Dimethyl sulfoxid (DMSO)	Sigma, Taufkirchen, Germany
Dynabeads® Human T-Activator CD3/CD28	GibcoBRL, Karlsruhe, Germany
dNTP	Roche, Mannheim, Germany
EDTA	Sigma, Taufkirchen, Germany
Ethanol	Klinikum rechts der Isar, Munich, Germany
Ethidium-monazide-bromide (EMA)	Molecular Probes, Leiden, The Netherlands
Fetal calf serum (FCS)	Biochrom, Berlin, Germany
Gentamycin	GibcoBRL, Karlsruhe, Germany
Golgi-Plug	BD Biosciences, Heidelberg, Germany
HCl	Roth, Karlsruhe, Germany
HEPES	GibcoBRL, Karlsruhe, Germany
Interleukin-2, human	Novatis, Basel, Switzerland
Isopropanol	Roth, Karlsruhe, Germany
L-Glutamine	GibcoBRL, Karlsruhe, Germany
Magnesiumsulfate ($MgSO_4$)	Sigma, Taufkirchen, Germany
$MgCl_2$	Sigma, Taufkirchen, Germany
NaOH	Roth, Karlsruhe, Germany
PageRuler Protein Ladder	Fermentas, St. Leon-Rot

Reagent	Supplier
Penicillin	Roth, Karlsruhe, Germany
PermWash 10x	BD Biosciences, Heidelberg, Germany
pET expression vectors	Novagen, Darmstadt, Germany
Phosphate buffered saline (PBS)	Biochrom, Berlin, Germany
Polybrene (Hexadimethrine bromide)	Sigma, Taufkirchen, Germany
Potassiumphosphate (K_2PO_4)	Sigma, Taufkirchen, Germany
Propidiumjodide (PI)	Molecular Probes, Invitrogen,
RPMI 1640	GibcoBRL, Karlsruhe, Germany
Sodiumchloride (NaCl)	Roth, Karlsruhe, Germany
Strep-Tactin-APC	IBA, Göttingen, Germany
*Strep*tactin-bead conjugate	IBA, Göttingen, Germany
Strep-Tactin-PE	IBA,Göttingen, Germany
Streptavidin PE	BD Pharmingen, San Diego, USA
Sucrose	Sigma, Taufkirchen, Germany
Tris-hydrochloride (Tris-HCl)	Roth, Karlsruhe, Germany
Triton X-100	Biorad, Munich, Germany
Trypan Blue	Sigma, Taufkirchen, Germany
β-Mercaptoethanol	Sigma, Taufkirchen, Germany

7.1.3 Media and buffers

Buffer /Medium	Composition
Ammoniumchloride-Tris (ACT)	0.17 M NH_4Cl
	0.3 M Tris-HCl, pH 7.5
Cell culture medium	1x RPMI 1640
	10% (w/v) FCS
	0.025% (w/v) L-Glutamine
	0.1% (w/v) HEPES
	0.001% (w/v) Gentamycin
	0.002% (w/v) Streptomycin
Complete freezing medium (CFM)	FCS
	10% DMSO

Buffer /Medium	Composition
D-biotin 100 mM stock solution	2.4431 g d-biotin
FACS buffer	1x PBS
	0.5% (w/v) BSA
	pH 7,45
Human T cell culture medium	1x RPMI 1640
	10% (w/v) human serum
	0.025% (w/v) L-Glutamine
	0.1% (w/v) HEPES
	0.001% (w/v) Gentamycin
	0.002% (w/v) Streptomycin
	0.002% (w/v) Penicillin
Periplasmic lysis buffer (P)	100 mM Tris/HCl, pH 8
	500 mM sucrose
	1 mM EDTA
Protein purification elution buffer (E)	100 mM Tris/HCl
	150 mM NaCl
	1 mM EDTA
	2.5 mM desthiobiotin, pH 8
Protein purification washing (W)	100 mM Tris/HCl, pH 8
	150 mM NaCl
	1 mM EDTA

7.1.4 antibodies and conjugates

Reagent	Clone	Supplier
Human CD127 PE-Cy7	R34.34	Beckman Coulter, Brea, USA
Human CD14 PE-Cy7	61D3	eBioscience, San Diego, USA

Human CD19 ECD	J3-119	Beckman Coulter, Brea, USA
Reagent	Clone	Supplier
Human CD28	28.2	BD Pharmingen, San Diego, USA
Human CD3 APC	UCHT1	Beckman Coulter, Brea, USA
Human CD3 eF450	OKT3	eBioscience, San Diego, USA
Human CD3 Orthoclone	OKT3	Janssen-Cilag, Neuss, Germany
Human CD3 Pacific Blue	UCHT1	BD Pharmingen, San Diego, USA
Human CD3 PE	UCHT1	Beckman Coulter, Brea, USA
Human CD3 PE-Cy7	UCHT1	eBioscience, San Diego, USA
Human CD4 eF450	OKT4	eBioscience, San Diego, USA
Human CD4 FITC	X35	Beckman Coulter, Brea, USA
Human CD4 Pacific Orange	S3.5	Life technologies, Carlsbad, USA
Human CD45RA	4KB5	Dako, Fort Collins, USA
Human CD45RA APC	HI100	BD Pharmingen, San Diego, USA
Human CD45RA PE-Cy7	L48	BD Pharmingen, San Diego, USA
Human CD45RO FITC	UCHL1	Beckman Coulter, Brea, USA
Human CD45RO PE	UCHL1	eBioscience, San Diego, USA
Human CD49d	9F10	BD Pharmingen, San Diego, USA
Human CD62L FITC	HI100	BD Pharmingen, San Diego, USA
Human CD62L PE	LT-TD180	Exbio, Prague, Czech Republik
Human CD8 eF450	OKT8	eBioscience, San Diego, USA
Human CD8 Pacific Blue	B9.11	Beckman Coulter, Brea, USA
Human CD8 PE	RPA-T8	BD Pharmingen, San Diego, USA
Human IFN-γ FITC	45.15	Beckman Coulter, Brea, USA
Human IFN-γ PE-Cy7	B27	BD Pharmingen, San Diego, USA
Human IL-2 APC	MQ1-17H12	eBioscience, San Diego, USA
Human Ki-67 PE	B56	BD Pharmingen, San Diego, USA
Human TNF-α PE-Cy7	Mab11	eBioscience, San Diego, USA

7.1.5 Cells

PBMCs from human blood were obtained from volunteer healthy donors upon written informed consent. Usage of the blood samples was approved according to the national law by the local Institutional Review Board (Ethikkommission der Medizinischen Fakultät der Technischen Universität München).

7.1.6 Software

Software	Company
Adobe Illustrator	Adobe Systems, San Jose, USA
End Note Programm	Microsoft, Redmond, USA
FlowJo	Treestar, Ashland, USA
Graph Pad Prism	Graph Pad Software, La Jolla, USA
Microsoft Office	Microsoft, Redmond, USA
Summit	Dako, Fort Collins, USA

7.2   Methods

7.2.1   Ficoll density centrifugation and determination of cell numbers

Healthy donor blood was diluted 1:1 with sterile PBS. The mix was carefully pipetted on top of 10 mL of Biocoll® Ficoll solution in a 15 mL conical plastic tube for centrifugation at 2000 rpm for 20 min at 22°C. For washing, PBMC layer was harvested and diluted in 45 mL sterile PBS and pelleted by centrifugation at 1500 rpm for 10 min.

The PBMC pellet was re-suspended in 20 mL PBS/0.5%BSA/1mM EDTA for cell counting. Cell counts were determined in a 1:10 dilution with a 0.15% Trypan Blue in PBS solution for live/dead discrimination using a Neubauer counting chamber.

At least two squares were counted: $count/square * 10^5 = \frac{cells}{ml}$

The PBMC suspension was pelleted again at 1500 rpm for 10 min and taken up in 100 µl of PBS/0.5%BSA1mM EDTA per 1x10^7 PBMCs.

7.2.2   Cryopreservation of human lymphocytes and cell lines

Cell numbers were determined using a Neubauer counting chamber in a 1:10 solution of 0.15% Trypan Blue in PBS. Cells and complete freezing medium (FCS/10% DMSO) were cooled to 4 °C before the cells ware pelleted by centrifugation at 1500 rpm for 8 min at 4°C. The pelleted cells were taken up in complete freezing medium to a final concentration of 2x10^7 per mL. The suspension was quickly transferred to 1 mL cryopreservation tubes and rested on wet ice. After 30 min. the tubes were frozen in a –80°C freezer. After 48 hrs, the tubes were frozen in liquid nitrogen for long-term storage. For thawing, the tubes were immersed in a 38°C water bath under gentle agitation for 1 min. After 1 min, the content was quickly diluted in 10 mL of full RPMI medium, centrifuged at 1500 rpm for 8

min and this step was repeated once using fresh RPMI medium. According to the specific experimental requirements, the cells can be rested in supplemented RPMI (T cell medium) at a concentration of 1x10^6 cells per well in a 48-well tissue culture plate overnight.

7.2.3   Activation of T lymphocytes

Cells and Dynabeads® Human T-Activator CD3/CD28 Beads were prepared as described in the product directions. 750 000 cells per well were distributed in a 48-well tissue culture plate. 1.5x10^6 T-Activator beads were added to achieve the desired bead-to-cell ratio of 3:1. The plates were stored in the incubator ($37°C/95\% H_2O/5\% CO^2$). It is recommended to check the distributed cells and beads under the microscope. To remove the Beads, the content of individual wells was transferred to a tube, placed on a magnet and washed with PBS/5% BSA.

7.2.4   *In vitro* cultivation and expansion of T lymphocytes

First, T lymphocytes were washed and counted or taken from an over-night culture after resting. Autologous (recommended) or non-autologuos feeder PBMCs were thawed and the cell counts were determined. 5x10^6 PBMCs were needed for 1 T_{25} tissue culture flask which yields 1-2x10^7 T cells after 14 days of cultivation. The PBMCs were washed in full RPMI and have received irradiation at 35 Gy. Further, 2.5x10^7 B-LCL cells are washed and irradiated at 50 Gy. All irradiated cells are mixed together in human T cell medium and 600 ng of OKT-3 antibody was added to the mix. The mix was topped off with 19 mL of human T cell medium and transferred sterilely to a T_{25} tissue culture flask. 1 mL of human T cell medium was used to dilute and transfer 50 000 T lymphocytes to the flask. The flasks were stored in the incubator ($37°C/95\% H_2O/5\% CO^2$). After 24 hrs, 20 μL of a 50U/μL (in PBS) pre-diluted solution of IL-2 was added to each flask followed by gentle shaking. On day 4 after stimulation, the content of each flask was pelleted and the cells were taken up in 20 mL of fresh T cell medium supplemented with 20 μL of a 50U/μL solution of IL-2. Every 72 hrs after that, a half medium change with supplemented medium was performed and the cells were counted and split if the counts exceeded 1x10^6 cells/mL. The protocol for rapid expansion of T lymphocytes was published by Riddell et al. [159].

7.2.5   Fab expression and purification

The wildtype Fab fragments were generated by gene synthesis (GeneArt) based on published sequences of the heavy and light variable regions (V_H and V_L) of the respective mAb clones. Variable

sequences were linked to the constant Fab regions and the heavy chain was fused to a OneSTrEPtag affinity tag (IBA). In a final cloning step, the Fab-*Strep*tag fusion gene sequences were introduced into the Acceptor vector pASG-IBAwt2, adapted for periplasmatic expression of the Fab protein. Combinatorial cloning was performed using the StarGate cloning system, following the manufacturer's recommendations (IBA). After each cloning step, sequences were verified by Sanger sequencing at the commercial provider GATC using own primers.

For Fab protein expression, the *E.coli* strain JM83 was transformed with the plasmid DNA by electroporation. After growing bacteria to an optical density at 600nm (OD_{600}) of 0.5-0.6 in 1L cultures, periplasmatic expression of the Fab-*Strep*tag fusion protein was induced by adding anhydrotetracycline (AHT, 1:10,000) that activated the *tet*-promoter in the final expression vector. After three hours of protein expression, bacteria were harvested by centrifuging at 5000g at 4°C for 12 minutes. Pelleted bacteria can be stored at -80°C.

For extracting the Fab protein from the periplasma, bacteria were resuspended in buffer P and incubated at 4°C for 30 minutes. Extracted proteins were separated from solid components of the bacteria by centrifugation at 15,000rpm at 4°C for 15 minutes. To digest the DNA, the supernatant was incubated with Benzonase (1:2000-1:6000) in the presence of 100μL/10-30mL supernatant of 1M $MgCl_2$ at 4°C for 30 minutes. The digested Fab protein solution was filtered through a sterile 0.2μm filter.

For affinity purification, filtered Fab fragments were applied onto a *Strep*-Tactin superflow column (IBA) that had been equilibrated with 2.5mL buffer W twice. After washing the Fab proteins on the column with 1mL buffer W 5 times, the Fab fragments were eluted from the column by adding 0.8mL, 1.5mL and 1mL buffer E. Using the middle elution fraction, the buffer E is exchanged for PBS (pH 7.5) by dialysis. The protein concentration was measured at 280nm using a NanoDrop spectrometer. Additionally, the size, quantity and purity of Fab fragments were examined by using the Agilent 2100 Bioanalyzer system.

7.2.6   T lymphocyte-mediated kill assay (Chromium release assay)

96-well tissue culture plates were set up and run in triplicates with controls for minimum and maximum release. To determine cytolytic activity 10^3 target cells were labeled with 51Cr for 90 min. Excess 51Cr was removed from the supernatant by centrifugation (2washes). Co-cultures with 51Cr-labeled target cells and effectot T cells were set up and incubated for 4h at different effector/target ratios (E/T ratios). Spontaneous release was determined using target cells incubated alone and maximum release was determined by direct lysis of target cells using the detergent Triton-X. After incubation, 30 μL of the supernatant was transferred to solid scintillator-coated lumaplates and dried over night before analysis. The specific lysis was calculated as follows: % specific cytotoxicity =

[mean sample release (cpm) - mean spontaneous release (cpm)]/[mean maximal release (cpm) - mean spontaneous release (cpm)] $\times$ 100.

7.2.7 Antibody and *Strep*tamer staining with subsequent FACS analysis

For phenotypic characterization of cells, a master mix of the respective monoclonal antibody-conjugates was prepared, and was added to the cell samples. During the labeling cells were kept on ice, in the dark for 20 min. *Strep*tamer staining was conducted in the same way. After the incubation period, cells were centrifuged in a 96-well tissue culture plate and underwent two additional washes. All samples were analyzed with a CyanLx 9 color flow cytometer.

7.2.8 MACS sorting

MACS cell isolation was performed on Miltenyi LS-columns according to the manufacturers recommendations. In brief, paramagnetic beads-based *Strep*tamers were co-incubated with freshly isolated cells for 20 min at 4°C. Cell suspension was washed once and centrifuged at 300g. MACS columns were placed on a magnet and were equilibrated with buffer (PBS/0.5% BSA/1mM EDTA). The *Strep*tamer-labeled cells were transferred to the column and washed three times. Positive cells were eluted by displacement of the column from the magnet. Cells were eluted off the column under pressure.

7.2.9 Magnetic microbead sorting

Fab-*Strep*tamers were prepared first by co-incubation of Fab fusion proteins with *Strep*-Tactin-coated magnetic microbeads. For 1×10^8 cells, 20 µg Fab was thawed and diluted in 250 µL PBS/0.5%BSA/1mM EDTA. Dilution ensures a more equal distribution of Fabs on the backbone. Diluted Fabs were mixed with 300 µL microbead suspension (pre-diluted 1:1 with 150 µL buffer). Up to 5×10^8 cells were placed in a 50 ml sort tube and the volume was adjusted to 1mL per 1×10^8 cells. The prepared reagent was added after at least 45 min pre-incubation and the mix was incubated rolling at 4°C for 30 min. Tubes were filled up to approx. 10 ml per 1×10^8 cells and placed on the magnet for at least 1 min. The supernatant was taken with a serological 10 ml pipette and collected in a 50 ml Falcon tube. Washing was repeated 4 more times. Pellets were re-suspended in 5 ml FACS buffer containing 0.1 or 1 mM D-biotin and re-suspended well, then incubated for 10 min on ice. Beads were separated from the suspension on the magnet. After 1 minute, the supernatant containing the positive cell fraction was collected in a fresh tube. The step was repeated one more time to flush any remaining cells off the magnetic beads. Cells are re-suspended in buffer without D-biotin and washed two

additional times. The positive fraction was spun down at 1500 rpm for 8 min at 4°C and the supernatant is taken off with a pump. The pellet is re-suspended pellet in the desired volume and washed on the magnet to get rid of remaining beads. The supernatant is collected and washed. It can then be used for additional selection steps.

8. Acknowledgements

I could never forget Paula Kosasih and all the other great people from the FHCRC in Seattle who taught me so much and whom I miss deeply.

Many thanks go to my lectors Dr. Georg Dössinger, Dr. Christian Stemberger, and Katrin Molter for their infinite support.

My infinite love to all my friends to whom I owe my greatest gratitude for their time and moral support at crazy times. Sabine Neumeier, Christina Daschkin, Ines Vogler, Katrin Molter, and Daniel Wiegand, you are the best friends I could wish for.

I am extremely grateful for the sublime friendship with Tobias Göpel and Alex Scherer. Words are not enough to express my feelings for you.

Finally, my dear family was unexceptionally supportive of me throughout my life. At this point I want to thank my grandparents for their loving support and for understanding my needs.

Infinite thanks to my parents for the strongest support I could possibly receive. I have spent the best times with you. Your unconditional love and encouragement are never taken for granted.

Thank You!

9. Bibliographie

[1]   Stemberger C, Dreher S, Tschulik C, Piossek C, Bet J, Yamamoto TN, Schiemann M, Neuenhahn M, Martin K, Schlapschy M, Skerra A, Schmidt T, Edinger M, Riddell SR, Germeroth L and Busch DH. Novel serial positive enrichment technology enables clinical multiparameter cell sorting. PloS one. 2012;7(4):e35798. PubMed PMID: 22545138. Pubmed Central PMCID: 3335788.

[2]   Nauerth M, Weissbrich B, Knall R, Franz T, Dossinger G, Bet J, Paszkiewicz PJ, Pfeifer L, Bunse M, Uckert W, Holtappels R, Gillert-Marien D, Neuenhahn M, Krackhardt A, Reddehase MJ, Riddell SR and Busch DH. TCR-Ligand koff Rate Correlates with the Protective Capacity of Antigen-Specific CD8+ T Cells for Adoptive Transfer. Science translational medicine. 2013 Jul 3;5(192):192ra87. PubMed PMID: 23825303.

[3]   Dossinger G, Bunse M, Bet J, Albrecht J, Paszkiewicz PJ, Weissbrich B, Schiedewitz I, Henkel L, Schiemann M, Neuenhahn M, Uckert W and Busch DH. MHC multimer-guided and cell culture-independent isolation of functional T cell receptors from single cells facilitates TCR identification for immunotherapy. PloS one. 2013;8(4):e61384. PubMed PMID: 23637823. Pubmed Central PMCID: 3637308.

[4]   Janeway CA, Jr. and Jason JM. How T lymphocytes recognize antigen. Critical reviews in immunology. 1980 May;1(2):133-64. PubMed PMID: 6174271.

[5]   Black FL and Rosen L. Patterns of measles antibodies in residents of Tahiti and their stability in the absence of re-exposure. Journal of immunology. 1962 Jun;88:725-31. PubMed PMID: 13869650.

[6]   Hammarlund E, Lewis MW, Hansen SG, Strelow LI, Nelson JA, Sexton GJ, Hanifin JM and Slifka MK. Duration of antiviral immunity after smallpox vaccination. Nature medicine. 2003 Sep;9(9):1131-7. PubMed PMID: 12925846.

[7]   Fugmann SD, Lee AI, Shockett PE, Villey IJ and Schatz DG. The RAG proteins and V(D)J recombination: complexes, ends, and transposition. Annual review of immunology. 2000;18:495-527. PubMed PMID: 10837067.

[8]   Garcia KC, Teyton L and Wilson IA. Structural basis of T cell recognition. Annual review of immunology. 1999;17:369-97. PubMed PMID: 10358763.

[9]   Germain RN. MHC-dependent antigen processing and peptide presentation: providing ligands for T lymphocyte activation. Cell. 1994 Jan 28;76(2):287-99. PubMed PMID: 8293464.

[10]   Quezada SA, Simpson TR, Peggs KS, Merghoub T, Vider J, Fan X, Blasberg R, Yagita H, Muranski P, Antony PA, Restifo NP and Allison JP. Tumor-reactive CD4(+) T cells develop cytotoxic activity and eradicate large established melanoma after transfer into lymphopenic hosts. The Journal of experimental medicine. 2010 Mar 15;207(3):637-50. PubMed PMID: 20156971. Pubmed Central PMCID: 2839156.

[11]   Ince TA, Richardson AL, Bell GW, Saitoh M, Godar S, Karnoub AE, Iglehart JD and Weinberg RA. Transformation of different human breast epithelial cell types leads to distinct tumor phenotypes. Cancer cell. 2007 Aug;12(2):160-70. PubMed PMID: 17692807.

[12]   Zinkernagel RM. Differentiation of T cells: thymic selection of specificity for self. Progress in clinical and biological research. 1982;85 Pt A:427-34. PubMed PMID: 6981116.

[13]   London CA, Lodge MP and Abbas AK. Functional responses and costimulator dependence of memory CD4+ T cells. Journal of immunology. 2000 Jan 1;164(1):265-72. PubMed PMID: 10605020.

[14]   Schweitzer AN and Sharpe AH. Studies using antigen-presenting cells lacking expression of both B7-1 (CD80) and B7-2 (CD86) show distinct requirements for B7 molecules during priming versus restimulation of Th2 but not Th1 cytokine production. Journal of immunology. 1998 Sep 15;161(6):2762-71. PubMed PMID: 9743334.

[15]   Borrow P, Tough DF, Eto D, Tishon A, Grewal IS, Sprent J, Flavell RA and Oldstone MB. CD40 ligand-mediated interactions are involved in the generation of memory CD8(+) cytotoxic T lymphocytes (CTL) but are not required for the maintenance of CTL memory following virus infection. Journal of virology. 1998 Sep;72(9):7440-9. PubMed PMID: 9696840. Pubmed Central PMCID: 109974.

[16]   Jenkins MR and Griffiths GM. The synapse and cytolytic machinery of cytotoxic T cells. Current opinion in immunology. 2010 Jun;22(3):308-13. PubMed PMID: 20226643.

[17]   Dustin ML. Coordination of T cell activation and migration through formation of the immunological synapse. Annals of the New York Academy of Sciences. 2003 Apr;987:51-9. PubMed PMID: 12727623.

[18]   Kaspar AA, Okada S, Kumar J, Poulain FR, Drouvalakis KA, Kelekar A, Hanson DA, Kluck RM, Hitoshi Y, Johnson DE, Froelich CJ, Thompson CB, Newmeyer DD, Anel A, Clayberger C and Krensky AM. A distinct pathway of cell-mediated apoptosis initiated by granulysin. Journal of immunology. 2001 Jul 1;167(1):350-6. PubMed PMID: 11418670.

[19]   Sen GC. Viruses and interferons. Annual review of microbiology. 2001;55:255-81. PubMed PMID: 11544356.

[20]   Lucifora J, Xia Y, Reisinger F, Zhang K, Stadler D, Cheng X, Sprinzl MF, Koppensteiner H, Makowska Z, Volz T, Remouchamps C, Chou WM, Thasler WE, Huser N, Durantel D, Liang TJ, Munk C, Heim MH, Browning JL, Dejardin E, Dandri M, Schindler M, Heikenwalder M and Protzer U. Specific and Nonhepatotoxic Degradation of Nuclear Hepatitis B Virus cccDNA. Science. 2014 Feb 20. PubMed PMID: 24557838.

[21]   Rock KL and Shen L. Cross-presentation: underlying mechanisms and role in immune surveillance. Immunological reviews. 2005 Oct;207:166-83. PubMed PMID: 16181335.

[22]   Gasteiger G, Kastenmuller W, Ljapoci R, Sutter G and Drexler I. Cross-priming of cytotoxic T cells dictates antigen requisites for modified vaccinia virus Ankara vector vaccines. Journal of virology. 2007 Nov;81(21):11925-36. PubMed PMID: 17699574. Pubmed Central PMCID: 2168793.

[23]   Hansen SG, Sacha JB, Hughes CM, Ford JC, Burwitz BJ, Scholz I, Gilbride RM, Lewis MS, Gilliam AN, Ventura AB, Malouli D, Xu G, Richards R, Whizin N, Reed JS, Hammond KB, Fischer M, Turner JM, Legasse AW, Axthelm MK, Edlefsen PT, Nelson JA, Lifson JD, Fruh K and Picker LJ. Cytomegalovirus vectors violate CD8+ T cell epitope recognition paradigms. Science. 2013 May 24;340(6135):1237874. PubMed PMID: 23704576. Pubmed Central PMCID: 3816976.

[24]   Boshoff C and Weiss R. AIDS-related malignancies. Nature reviews Cancer. 2002 May;2(5):373-82. PubMed PMID: 12044013.

[25]   Aloj G, Giardino G, Valentino L, Maio F, Gallo V, Esposito T, Naddei R, Cirillo E and Pignata C. Severe combined immunodeficiences: new and old scenarios. International reviews of immunology. 2012 Feb;31(1):43-65. PubMed PMID: 22251007.

[26]   Boeckh M, Leisenring W, Riddell SR, Bowden RA, Huang ML, Myerson D, Stevens-Ayers T, Flowers ME, Cunningham T and Corey L. Late cytomegalovirus disease and mortality in recipients of allogeneic hematopoietic stem cell transplants: importance of viral load and T-cell immunity. Blood. 2003 Jan 15;101(2):407-14. PubMed PMID: 12393659.

[27]   Brunstein CG, Weisdorf DJ, DeFor T, Barker JN, Tolar J, van Burik JA and Wagner JE. Marked increased risk of Epstein-Barr virus-related complications with the addition of antithymocyte globulin to a nonmyeloablative conditioning prior to unrelated umbilical cord blood transplantation. Blood. 2006 Oct 15;108(8):2874-80. PubMed PMID: 16804113. Pubmed Central PMCID: 1895580.

[28]   Myers GD, Krance RA, Weiss H, Kuehnle I, Demmler G, Heslop HE and Bollard CM. Adenovirus infection rates in pediatric recipients of alternate donor allogeneic bone marrow transplants receiving either antithymocyte globulin (ATG) or alemtuzumab (Campath). Bone marrow transplantation. 2005 Dec;36(11):1001-8. PubMed PMID: 16184180.

[29]   Marcen R, Pascual J, Tato AM, Teruel JL, Villafruela JJ, Fernandez M, Tenorio M, Burgos FJ and Ortuno J. Influence of immunosuppression on the prevalence of cancer after kidney transplantation. Transplantation proceedings. 2003 Aug;35(5):1714-6. PubMed PMID: 12962768.

[30]   Stemberger C, Huster KM, Koffler M, Anderl F, Schiemann M, Wagner H and Busch DH. A single naive CD8+ T cell precursor can develop into diverse effector and memory subsets. Immunity. 2007 Dec;27(6):985-97. PubMed PMID: 18082432.

[31]   Tubo NJ, Pagan AJ, Taylor JJ, Nelson RW, Linehan JL, Ertelt JM, Huseby ES, Way SS and Jenkins MK. Single Naive CD4(+) T Cells from a Diverse Repertoire Produce Different Effector Cell Types during Infection. Cell. 2013 May 9;153(4):785-96. PubMed PMID: 23663778.

[32]   Stemberger C, Neuenhahn M, Buchholz VR and Busch DH. Origin of CD8+ effector and memory T cell subsets. Cellular & molecular immunology. 2007 Dec;4(6):399-405. PubMed PMID: 18163951.

[33]   Arsenio J, Kakaradov B, Metz PJ, Kim SH, Yeo GW and Chang JT. Early specification of CD8+ T lymphocyte fates during adaptive immunity revealed by single-cell gene-expression analyses. Nature immunology. 2014 Apr;15(4):365-72. PubMed PMID: 24584088. Pubmed Central PMCID: 3968536.

[34]   Huster KM, Busch V, Schiemann M, Linkemann K, Kerksiek KM, Wagner H and Busch DH. Selective expression of IL-7 receptor on memory T cells identifies early CD40L-dependent generation of distinct CD8+ memory T cell subsets. Proceedings of the National Academy of Sciences of the United States of America. 2004 Apr 13;101(15):5610-5. PubMed PMID: 15044705. Pubmed Central PMCID: 397444.

[35]   Obar JJ and Lefrancois L. Early signals during CD8 T cell priming regulate the generation of central memory cells. Journal of immunology. 2010 Jul 1;185(1):263-72. PubMed PMID: 20519649. Pubmed Central PMCID: 2997352.

[36]   Appay V, Dunbar PR, Callan M, Klenerman P, Gillespie GM, Papagno L, Ogg GS, King A, Lechner F, Spina CA, Little S, Havlir DV, Richman DD, Gruener N, Pape G, Waters A, Easterbrook P, Salio M, Cerundolo V, McMichael AJ and Rowland-Jones SL. Memory CD8+ T cells vary in differentiation phenotype in different persistent virus infections. Nature medicine. 2002 Apr;8(4):379-85. PubMed PMID: 11927944.

[37]   Dykstra B, Kent D, Bowie M, McCaffrey L, Hamilton M, Lyons K, Lee SJ, Brinkman R and Eaves C. Long-term propagation of distinct hematopoietic differentiation programs in vivo. Cell stem cell. 2007 Aug 16;1(2):218-29. PubMed PMID: 18371352.

[38]   Buchholz VR, Flossdorf M, Hensel I, Kretschmer L, Weissbrich B, Graf P, Verschoor A, Schiemann M, Hofer T and Busch DH. Disparate Individual Fates Compose Robust CD8+ T Cell Immunity. Science. 2013 Mar 14. PubMed PMID: 23493420.

[39]   Gerlach C, Rohr JC, Perie L, van Rooij N, van Heijst JW, Velds A, Urbanus J, Naik SH, Jacobs H, Beltman JB, de Boer RJ and Schumacher TN. Heterogeneous differentiation patterns of individual CD8+ T cells. Science. 2013 May 3;340(6132):635-9. PubMed PMID: 23493421.

[40]   Zhang Y, Joe G, Hexner E, Zhu J and Emerson SG. Host-reactive CD8+ memory stem cells in graft-versus-host disease. Nature medicine. 2005 Dec;11(12):1299-305. PubMed PMID: 16288282.

[41]   Gattinoni L, Lugli E, Ji Y, Pos Z, Paulos CM, Quigley MF, Almeida JR, Gostick E, Yu Z, Carpenito C, Wang E, Douek DC, Price DA, June CH, Marincola FM, Roederer M and Restifo NP. A human memory T cell subset with stem cell-like properties. Nature medicine. 2011 Oct;17(10):1290-7. PubMed PMID: 21926977. Pubmed Central PMCID: 3192229.

[42]   Gattinoni L, Zhong XS, Palmer DC, Ji Y, Hinrichs CS, Yu Z, Wrzesinski C, Boni A, Cassard L, Garvin LM, Paulos CM, Muranski P and Restifo NP. Wnt signaling arrests effector T cell differentiation and generates CD8+ memory stem cells. Nature medicine. 2009 Jul;15(7):808-13. PubMed PMID: 19525962. Pubmed Central PMCID: 2707501.

[43]   Graef P BV, Stemberger C, Flossdorf M, Henkel L, Schiemann M. Serial transfer of single-derived immunocompetence reveals stemness of CD8+ central memory T cells. Immunity ;accepted. 2014.

[44]   Stemberger C, Neuenhahn M, Gebhardt FE, Schiemann M, Buchholz VR and Busch DH. Stem cell-like plasticity of naive and distinct memory CD8+ T cell subsets. Seminars in immunology. 2009 Apr;21(2):62-8. PubMed PMID: 19269852.

[45]   Hinrichs CS, Borman ZA, Gattinoni L, Yu Z, Burns WR, Huang J, Klebanoff CA, Johnson LA, Kerkar SP, Yang S, Muranski P, Palmer DC, Scott CD, Morgan RA, Robbins PF, Rosenberg SA and Restifo NP. Human effector CD8+ T cells derived from naive rather than memory subsets possess superior traits for adoptive immunotherapy. Blood. 2011 Jan 20;117(3):808-14. PubMed PMID: 20971955. Pubmed Central PMCID: 3035075.

[46]   Buchholz VR, Flossdorf M, Hensel I, Kretschmer L, Weissbrich B, Graf P, Verschoor A, Schiemann M, Hofer T and Busch DH. Disparate individual fates compose robust CD8+ T cell immunity. Science. 2013 May 3;340(6132):630-5. PubMed PMID: 23493420.

[47]   Berger C, Jensen MC, Lansdorp PM, Gough M, Elliott C and Riddell SR. Adoptive transfer of effector CD8+ T cells derived from central memory cells establishes persistent T cell memory in primates. The Journal of clinical investigation. 2008 Jan;118(1):294-305. PubMed PMID: 18060041. Pubmed Central PMCID: 2104476.

[48]   Huster KM, Koffler M, Stemberger C, Schiemann M, Wagner H and Busch DH. Unidirectional development of CD8+ central memory T cells into protective Listeria-specific effector memory T cells. European journal of immunology. 2006 Jun;36(6):1453-64. PubMed PMID: 16637009.

[49]   Wang A, Chandran S, Shah SA, Chiu Y, Paria BC, Aghamolla T, Alvarez-Downing MM, Lee CC, Singh S, Li T, Dudley ME, Restifo NP, Rosenberg SA and Kammula US. The stoichiometric production of IL-2 and IFN-gamma mRNA defines memory T cells that can self-renew after adoptive transfer in humans. Science translational medicine. 2012 Aug 29;4(149):149ra20. PubMed PMID: 22932225.

[50]   Wang X, Berger C, Wong CW, Forman SJ, Riddell SR and Jensen MC. Engraftment of human central memory-derived effector CD8+ T cells in immunodeficient mice. Blood. 2011 Feb 10;117(6):1888-98. PubMed PMID: 21123821. Pubmed Central PMCID: 3056638.

[51]   Michie CA, McLean A, Alcock C and Beverley PC. Lifespan of human lymphocyte subsets defined by CD45 isoforms. Nature. 1992 Nov 19;360(6401):264-5. PubMed PMID: 1436108.

[52]   Sallusto F, Lenig D, Forster R, Lipp M and Lanzavecchia A. Two subsets of memory T lymphocytes with distinct homing potentials and effector functions. Nature. 1999 Oct 14;401(6754):708-12. PubMed PMID: 10537110.

[53]   Kaech SM, Tan JT, Wherry EJ, Konieczny BT, Surh CD and Ahmed R. Selective expression of the interleukin 7 receptor identifies effector CD8 T cells that give rise to long-lived memory cells. Nature immunology. 2003 Dec;4(12):1191-8. PubMed PMID: 14625547.

[54]   Akbar AN, Terry L, Timms A, Beverley PC and Janossy G. Loss of CD45R and gain of UCHL1 reactivity is a feature of primed T cells. Journal of immunology. 1988 Apr 1;140(7):2171-8. PubMed PMID: 2965180.

[55]   Busch DH, Pilip IM, Vijh S and Pamer EG. Coordinate regulation of complex T cell populations responding to bacterial infection. Immunity. 1998 Mar;8(3):353-62. PubMed PMID: 9529152.

[56]   Merkenschlager M, Terry L, Edwards R and Beverley PC. Limiting dilution analysis of proliferative responses in human lymphocyte populations defined by the monoclonal antibody UCHL1: implications for differential CD45 expression in T cell memory formation. European journal of immunology. 1988 Nov;18(11):1653-61. PubMed PMID: 2974420.

[57]   Galon J, Costes A, Sanchez-Cabo F, Kirilovsky A, Mlecnik B, Lagorce-Pages C, Tosolini M, Camus M, Berger A, Wind P, Zinzindohoue F, Bruneval P, Cugnenc PH, Trajanoski Z, Fridman WH and Pages F. Type, density, and location of immune cells within

human colorectal tumors predict clinical outcome. Science. 2006 Sep 29;313(5795):1960-4. PubMed PMID: 17008531.

[58]   Matsushita H, Vesely MD, Koboldt DC, Rickert CG, Uppaluri R, Magrini VJ, Arthur CD, White JM, Chen YS, Shea LK, Hundal J, Wendl MC, Demeter R, Wylie T, Allison JP, Smyth MJ, Old LJ, Mardis ER and Schreiber RD. Cancer exome analysis reveals a T-cell-dependent mechanism of cancer immunoediting. Nature. 2012 Feb 16;482(7385):400-4. PubMed PMID: 22318521.

[59]   Delorme EJ and Alexander P. Treatment of Primary Fibrosarcoma in the Rat with Immune Lymphocytes. Lancet. 1964 Jul 18;2(7351):117-20. PubMed PMID: 14160543.

[60]   Koebel CM, Vermi W, Swann JB, Zerafa N, Rodig SJ, Old LJ, Smyth MJ and Schreiber RD. Adaptive immunity maintains occult cancer in an equilibrium state. Nature. 2007 Dec 6;450(7171):903-7. PubMed PMID: 18026089.

[61]   Dranoff G, Jaffee E, Lazenby A, Golumbek P, Levitsky H, Brose K, Jackson V, Hamada H, Pardoll D and Mulligan RC. Vaccination with irradiated tumor cells engineered to secrete murine granulocyte-macrophage colony-stimulating factor stimulates potent, specific, and long-lasting anti-tumor immunity. Proceedings of the National Academy of Sciences of the United States of America. 1993 Apr 15;90(8):3539-43. PubMed PMID: 8097319. Pubmed Central PMCID: 46336.

[62]   Shankaran V, Ikeda H, Bruce AT, White JM, Swanson PE, Old LJ and Schreiber RD. IFNgamma and lymphocytes prevent primary tumour development and shape tumour immunogenicity. Nature. 2001 Apr 26;410(6832):1107-11. PubMed PMID: 11323675.

[63]   Sato E, Olson SH, Ahn J, Bundy B, Nishikawa H, Qian F, Jungbluth AA, Frosina D, Gnjatic S, Ambrosone C, Kepner J, Odunsi T, Ritter G, Lele S, Chen YT, Ohtani H, Old LJ and Odunsi K. Intraepithelial CD8+ tumor-infiltrating lymphocytes and a high CD8+/regulatory T cell ratio are associated with favorable prognosis in ovarian cancer. Proceedings of the National Academy of Sciences of the United States of America. 2005 Dec 20;102(51):18538-43. PubMed PMID: 16344461. Pubmed Central PMCID: 1311741.

[64]   Sharma P, Shen Y, Wen S, Yamada S, Jungbluth AA, Gnjatic S, Bajorin DF, Reuter VE, Herr H, Old LJ and Sato E. CD8 tumor-infiltrating lymphocytes are predictive of survival in muscle-invasive urothelial carcinoma. Proceedings of the National Academy of Sciences of the United States of America. 2007 Mar 6;104(10):3967-72. PubMed PMID: 17360461. Pubmed Central PMCID: 1820692.

[65]   Lee HE, Chae SW, Lee YJ, Kim MA, Lee HS, Lee BL and Kim WH. Prognostic implications of type and density of tumour-infiltrating lymphocytes in gastric cancer. British journal of cancer. 2008 Nov 18;99(10):1704-11. PubMed PMID: 18941457. Pubmed Central PMCID: 2584941.

[66]   Xu W, Liu H, Song J, Fu HX, Qiu L, Zhang BF, Li HZ, Bai J and Zheng JN. The appearance of Tregs in cancer nest is a promising independent risk factor in colon cancer. Journal of cancer research and clinical oncology. 2013 Nov;139(11):1845-52. PubMed PMID: 24005418.

[67]   Chiba T, Ohtani H, Mizoi T, Naito Y, Sato E, Nagura H, Ohuchi A, Ohuchi K, Shiiba K, Kurokawa Y and Satomi S. Intraepithelial CD8+ T-cell-count becomes a prognostic factor after a longer follow-up period in human colorectal carcinoma: possible association with suppression of micrometastasis. British journal of cancer. 2004 Nov 1;91(9):1711-7. PubMed PMID: 15494715. Pubmed Central PMCID: 2410024.

[68]   Wakabayashi O, Yamazaki K, Oizumi S, Hommura F, Kinoshita I, Ogura S, Dosaka-Akita H and Nishimura M. CD4+ T cells in cancer stroma, not CD8+ T cells in cancer cell nests, are associated with favorable prognosis in human non-small cell lung cancers. Cancer science. 2003 Nov;94(11):1003-9. PubMed PMID: 14611679.

[69]   Dudley ME, Gross CA, Langhan MM, Garcia MR, Sherry RM, Yang JC, Phan GQ, Kammula US, Hughes MS, Citrin DE, Restifo NP, Wunderlich JR, Prieto PA, Hong JJ, Langan RC, Zlott DA, Morton KE, White DE, Laurencot CM and Rosenberg SA. CD8+ enriched "young" tumor infiltrating lymphocytes can mediate regression of metastatic melanoma. Clinical cancer research : an official journal of the American Association for Cancer Research. 2010 Dec 15;16(24):6122-31. PubMed PMID: 20668005. Pubmed Central PMCID: 2978753.

[70]   Di Ianni M, Falzetti F, Carotti A, Terenzi A, Castellino F, Bonifacio E, Del Papa B, Zei T, Ostini RI, Cecchini D, Aloisi T, Perruccio K, Ruggeri L, Balucani C, Pierini A, Sportoletti P, Aristei C, Falini B, Reisner Y, Velardi A, Aversa F and Martelli MF. Tregs prevent GVHD and promote immune reconstitution in HLA-haploidentical transplantation. Blood. 2011 Apr 7;117(14):3921-8. PubMed PMID: 21292771.

[71]   Brunstein CG, Miller JS, Cao Q, McKenna DH, Hippen KL, Curtsinger J, Defor T, Levine BL, June CH, Rubinstein P, McGlave PB, Blazar BR and Wagner JE. Infusion of ex vivo expanded T regulatory cells in adults transplanted with umbilical cord blood: safety profile and detection kinetics. Blood. 2011 Jan 20;117(3):1061-70. PubMed PMID: 20952687. Pubmed Central PMCID: 3035067.

[72]   Thomas ED, Lochte HL, Jr., Cannon JH, Sahler OD and Ferrebee JW. Supralethal whole body irradiation and isologous marrow transplantation in man. The Journal of clinical investigation. 1959 Oct;38:1709-16. PubMed PMID: 13837954. Pubmed Central PMCID: 444138.

[73]   Horowitz MM, Gale RP, Sondel PM, Goldman JM, Kersey J, Kolb HJ, Rimm AA, Ringden O, Rozman C, Speck B and et al. Graft-versus-leukemia reactions after bone marrow transplantation. Blood. 1990 Feb 1;75(3):555-62. PubMed PMID: 2297567.

[74]   Weiden PL, Flournoy N, Thomas ED, Prentice R, Fefer A, Buckner CD and Storb R. Antileukemic effect of graft-versus-host disease in human recipients of allogeneic-marrow grafts. The New England journal of medicine. 1979 May 10;300(19):1068-73. PubMed PMID: 34792.

[75]   Goldman JM, Gale RP, Horowitz MM, Biggs JC, Champlin RE, Gluckman E, Hoffmann RG, Jacobsen SJ, Marmont AM, McGlave PB and et al. Bone marrow transplantation for chronic myelogenous leukemia in chronic phase. Increased risk for relapse associated with T-cell depletion. Annals of internal medicine. 1988 Jun;108(6):806-14. PubMed PMID: 3285744.

[76]   Chen BJ, Deoliveira D, Cui X, Le NT, Son J, Whitesides JF and Chao NJ. Inability of memory T cells to induce graft-versus-host disease is a result of an abortive alloresponse. Blood. 2007 Apr 1;109(7):3115-23. PubMed PMID: 17148592. Pubmed Central PMCID: 1852216.

[77]   Kolb HJ. Graft-versus-leukemia effects of transplantation and donor lymphocytes. Blood. 2008 Dec 1;112(12):4371-83. PubMed PMID: 19029455.

[78]   Hudecek M, Bartsch K, Tschiedel S and Niederwieser D. [Minor antigens - major impact. The role of minor histocompatibility antigens in allogeneic hematopoietic stem cell transplantation]. Deutsche medizinische Wochenschrift. 2008 Jul;133(28-29):1511-6. PubMed PMID: 18597211. Kleine Antigene - grosse Wirkung. Die Rolle von Minor-Histokompatibilitatsantigenen bei der allogenen Blutstammzelltransplantation.

[79]   Rosenberg SA, Spiess P and Lafreniere R. A new approach to the adoptive immunotherapy of cancer with tumor-infiltrating lymphocytes. Science. 1986 Sep 19;233(4770):1318-21. PubMed PMID: 3489291.

[80]   Rosenberg SA, Packard BS, Aebersold PM, Solomon D, Topalian SL, Toy ST, Simon P, Lotze MT, Yang JC, Seipp CA and et al. Use of tumor-infiltrating lymphocytes and interleukin-2 in the immunotherapy of patients with metastatic melanoma. A preliminary report. The New England journal of medicine. 1988 Dec 22;319(25):1676-80. PubMed PMID: 3264384.

[81]   Dudley ME, Wunderlich JR, Yang JC, Hwu P, Schwartzentruber DJ, Topalian SL, Sherry RM, Marincola FM, Leitman SF, Seipp CA, Rogers-Freezer L, Morton KE, Nahvi A, Mavroukakis SA, White DE and Rosenberg SA. A phase I study of nonmyeloablative chemotherapy and adoptive transfer of autologous tumor antigen-specific T lymphocytes in patients with metastatic melanoma. Journal of immunotherapy. 2002 May-Jun;25(3):243-51. PubMed PMID: 12000866. Pubmed Central PMCID: 2413438.

[82]   Dudley ME, Wunderlich JR, Shelton TE, Even J and Rosenberg SA. Generation of tumor-infiltrating lymphocyte cultures for use in adoptive transfer therapy for melanoma

patients. Journal of immunotherapy. 2003 Jul-Aug;26(4):332-42. PubMed PMID: 12843795. Pubmed Central PMCID: 2305721.

[83]   Gattinoni L, Powell DJ, Jr., Rosenberg SA and Restifo NP. Adoptive immunotherapy for cancer: building on success. Nature reviews Immunology. 2006 May;6(5):383-93. PubMed PMID: 16622476. Pubmed Central PMCID: 1473162.

[84]   Dudley ME, Wunderlich JR, Yang JC, Sherry RM, Topalian SL, Restifo NP, Royal RE, Kammula U, White DE, Mavroukakis SA, Rogers LJ, Gracia GJ, Jones SA, Mangiameli DP, Pelletier MM, Gea-Banacloche J, Robinson MR, Berman DM, Filie AC, Abati A and Rosenberg SA. Adoptive cell transfer therapy following non-myeloablative but lymphodepleting chemotherapy for the treatment of patients with refractory metastatic melanoma. Journal of clinical oncology : official journal of the American Society of Clinical Oncology. 2005 Apr 1;23(10):2346-57. PubMed PMID: 15800326. Pubmed Central PMCID: 1475951.

[85]   Baitsch L, Baumgaertner P, Devevre E, Raghav SK, Legat A, Barba L, Wieckowski S, Bouzourene H, Deplancke B, Romero P, Rufer N and Speiser DE. Exhaustion of tumor-specific CD8(+) T cells in metastases from melanoma patients. The Journal of clinical investigation. 2011 Jun;121(6):2350-60. PubMed PMID: 21555851. Pubmed Central PMCID: 3104769.

[86]   Gattinoni L, Klebanoff CA and Restifo NP. Paths to stemness: building the ultimate antitumour T cell. Nature reviews Cancer. 2012 Oct;12(10):671-84. PubMed PMID: 22996603.

[87]   Choi D, Kim TG and Sung YC. The past, present, and future of adoptive T cell therapy. Immune network. 2012 Aug;12(4):139-47. PubMed PMID: 23091437. Pubmed Central PMCID: 3467412.

[88]   Yee C, Thompson JA, Byrd D, Riddell SR, Roche P, Celis E and Greenberg PD. Adoptive T cell therapy using antigen-specific CD8+ T cell clones for the treatment of patients with metastatic melanoma: in vivo persistence, migration, and antitumor effect of transferred T cells. Proceedings of the National Academy of Sciences of the United States of America. 2002 Dec 10;99(25):16168-73. PubMed PMID: 12427970. Pubmed Central PMCID: 138583.

[89]   Riddell RH. Flat adenomas and carcinomas: seeking the invisible? Gastrointestinal endoscopy. 1992 Nov-Dec;38(6):721-3. PubMed PMID: 1473681.

[90]   Roskrow MA, Suzuki N, Gan Y, Sixbey JW, Ng CY, Kimbrough S, Hudson M, Brenner MK, Heslop HE and Rooney CM. Epstein-Barr virus (EBV)-specific cytotoxic T lymphocytes for the treatment of patients with EBV-positive relapsed Hodgkin's disease. Blood. 1998 Apr 15;91(8):2925-34. PubMed PMID: 9531603.

[91]   Brodie SJ, Lewinsohn DA, Patterson BK, Jiyamapa D, Krieger J, Corey L, Greenberg PD and Riddell SR. In vivo migration and function of transferred HIV-1-specific cytotoxic T cells. Nature medicine. 1999 Jan;5(1):34-41. PubMed PMID: 9883837.

[92]   Schmitt A, Tonn T, Busch DH, Grigoleit GU, Einsele H, Odendahl M, Germeroth L, Ringhoffer M, Ringhoffer S, Wiesneth M, Greiner J, Michel D, Mertens T, Rojewski M, Marx M, von Harsdorf S, Dohner H, Seifried E, Bunjes D and Schmitt M. Adoptive transfer and selective reconstitution of streptamer-selected cytomegalovirus-specific CD8+ T cells leads to virus clearance in patients after allogeneic peripheral blood stem cell transplantation. Transfusion. 2011 Mar;51(3):591-9. PubMed PMID: 21133926.

[93]   Stemberger C, Graef P, Odendahl M, Albrecht J, Dossinger G, Anderl F, Buchholz VR, Gasteiger G, Schiemann M, Grigoleit GU, Schuster FR, Borkhardt A, Versluys B, Tonn T, Seifried E, Einsele H, Germeroth L, Busch DH and Neuenhahn M. Lowest numbers of primary CD8+ T cells can reconstitute protective immunity upon adoptive immunotherapy. Blood. 2014 May 22. PubMed PMID: 24855206.

[94]   Berger C, Turtle CJ, Jensen MC and Riddell SR. Adoptive transfer of virus-specific and tumor-specific T cell immunity. Current opinion in immunology. 2009 Apr;21(2):224-32. PubMed PMID: 19304470. Pubmed Central PMCID: 2720155.

[95]   Schietinger A, Delrow JJ, Basom RS, Blattman JN and Greenberg PD. Rescued tolerant CD8 T cells are preprogrammed to reestablish the tolerant state. Science. 2012 Feb 10;335(6069):723-7. PubMed PMID: 22267581. Pubmed Central PMCID: 3754789.

[96]   Morgan RA, Dudley ME, Wunderlich JR, Hughes MS, Yang JC, Sherry RM, Royal RE, Topalian SL, Kammula US, Restifo NP, Zheng Z, Nahvi A, de Vries CR, Rogers-Freezer LJ, Mavroukakis SA and Rosenberg SA. Cancer regression in patients after transfer of genetically engineered lymphocytes. Science. 2006 Oct 6;314(5796):126-9. PubMed PMID: 16946036. Pubmed Central PMCID: 2267026.

[97]   Shao H, Zhang W, Hu Q, Wu F, Shen H and Huang S. TCR mispairing in genetically modified T cells was detected by fluorescence resonance energy transfer. Molecular biology reports. 2010 Dec;37(8):3951-6. PubMed PMID: 20373027.

[98]   Brenner MK and Heslop HE. Adoptive T cell therapy of cancer. Current opinion in immunology. 2010 Apr;22(2):251-7. PubMed PMID: 20171074. Pubmed Central PMCID: 3093371.

[99]   Drake CG, Jaffee E and Pardoll DM. Mechanisms of immune evasion by tumors. Advances in immunology. 2006;90:51-81. PubMed PMID: 16730261.

[100] Shen L and Rock KL. Priming of T cells by exogenous antigen cross-presented on MHC class I molecules. Current opinion in immunology. 2006 Feb;18(1):85-91. PubMed PMID: 16326087.

[101] Morgan RA, Chinnasamy N, Abate-Daga D, Gros A, Robbins PF, Zheng Z, Dudley ME, Feldman SA, Yang JC, Sherry RM, Phan GQ, Hughes MS, Kammula US, Miller AD, Hessman CJ, Stewart AA, Restifo NP, Quezado MM, Alimchandani M, Rosenberg AZ, Nath A, Wang T, Bielekova B, Wuest SC, Akula N, McMahon FJ, Wilde S, Mosetter B, Schendel DJ, Laurencot CM and Rosenberg SA. Cancer regression and neurological toxicity following anti-MAGE-A3 TCR gene therapy. Journal of immunotherapy. 2013 Feb;36(2):133-51. PubMed PMID: 23377668. Pubmed Central PMCID: 3581823.

[102] Johnson LA, Morgan RA, Dudley ME, Cassard L, Yang JC, Hughes MS, Kammula US, Royal RE, Sherry RM, Wunderlich JR, Lee CC, Restifo NP, Schwarz SL, Cogdill AP, Bishop RJ, Kim H, Brewer CC, Rudy SF, VanWaes C, Davis JL, Mathur A, Ripley RT, Nathan DA, Laurencot CM and Rosenberg SA. Gene therapy with human and mouse T-cell receptors mediates cancer regression and targets normal tissues expressing cognate antigen. Blood. 2009 Jul 16;114(3):535-46. PubMed PMID: 19451549. Pubmed Central PMCID: 2929689.

[103] Robbins PF, Morgan RA, Feldman SA, Yang JC, Sherry RM, Dudley ME, Wunderlich JR, Nahvi AV, Helman LJ, Mackall CL, Kammula US, Hughes MS, Restifo NP, Raffeld M, Lee CC, Levy CL, Li YF, El-Gamil M, Schwarz SL, Laurencot C and Rosenberg SA. Tumor regression in patients with metastatic synovial cell sarcoma and melanoma using genetically engineered lymphocytes reactive with NY-ESO-1. Journal of clinical oncology : official journal of the American Society of Clinical Oncology. 2011 Mar 1;29(7):917-24. PubMed PMID: 21282551. Pubmed Central PMCID: 3068063.

[104] Eshhar Z, Waks T, Gross G and Schindler DG. Specific activation and targeting of cytotoxic lymphocytes through chimeric single chains consisting of antibody-binding domains and the gamma or zeta subunits of the immunoglobulin and T-cell receptors. Proceedings of the National Academy of Sciences of the United States of America. 1993 Jan 15;90(2):720-4. PubMed PMID: 8421711. Pubmed Central PMCID: 45737.

[105] Kowolik CM, Topp MS, Gonzalez S, Pfeiffer T, Olivares S, Gonzalez N, Smith DD, Forman SJ, Jensen MC and Cooper LJ. CD28 costimulation provided through a CD19-specific chimeric antigen receptor enhances in vivo persistence and antitumor efficacy of adoptively transferred T cells. Cancer research. 2006 Nov 15;66(22):10995-1004. PubMed PMID: 17108138.

[106] Song DG, Ye Q, Poussin M, Harms GM, Figini M and Powell DJ, Jr. CD27 costimulation augments the survival and antitumor activity of redirected human T cells in vivo. Blood. 2012 Jan 19;119(3):696-706. PubMed PMID: 22117050.

[107] Stephan MT, Ponomarev V, Brentjens RJ, Chang AH, Dobrenkov KV, Heller G and Sadelain M. T cell-encoded CD80 and 4-1BBL induce auto- and transcostimulation, resulting in potent tumor rejection. Nature medicine. 2007 Dec;13(12):1440-9. PubMed PMID: 18026115.

[108]   Kalos M, Levine BL, Porter DL, Katz S, Grupp SA, Bagg A and June CH. T cells with chimeric antigen receptors have potent antitumor effects and can establish memory in patients with advanced leukemia. Science translational medicine. 2011 Aug 10;3(95):95ra73. PubMed PMID: 21832238. Pubmed Central PMCID: 3393096.

[109]   Till BG, Jensen MC, Wang J, Qian X, Gopal AK, Maloney DG, Lindgren CG, Lin Y, Pagel JM, Budde LE, Raubitschek A, Forman SJ, Greenberg PD, Riddell SR and Press OW. CD20-specific adoptive immunotherapy for lymphoma using a chimeric antigen receptor with both CD28 and 4-1BB domains: pilot clinical trial results. Blood. 2012 Apr 26;119(17):3940-50. PubMed PMID: 22308288. Pubmed Central PMCID: 3350361.

[110]   Park JR, Digiusto DL, Slovak M, Wright C, Naranjo A, Wagner J, Meechoovet HB, Bautista C, Chang WC, Ostberg JR and Jensen MC. Adoptive transfer of chimeric antigen receptor re-directed cytolytic T lymphocyte clones in patients with neuroblastoma. Molecular therapy : the journal of the American Society of Gene Therapy. 2007 Apr;15(4):825-33. PubMed PMID: 17299405.

[111]   Pule MA, Savoldo B, Myers GD, Rossig C, Russell HV, Dotti G, Huls MH, Liu E, Gee AP, Mei Z, Yvon E, Weiss HL, Liu H, Rooney CM, Heslop HE and Brenner MK. Virus-specific T cells engineered to coexpress tumor-specific receptors: persistence and antitumor activity in individuals with neuroblastoma. Nature medicine. 2008 Nov;14(11):1264-70. PubMed PMID: 18978797. Pubmed Central PMCID: 2749734.

[112]   Chapuis AG, Thompson JA, Margolin KA, Rodmyre R, Lai IP, Dowdy K, Farrar EA, Bhatia S, Sabath DE, Cao J, Li Y and Yee C. Transferred melanoma-specific CD8+ T cells persist, mediate tumor regression, and acquire central memory phenotype. Proceedings of the National Academy of Sciences of the United States of America. 2012 Mar 20;109(12):4592-7. PubMed PMID: 22393002. Pubmed Central PMCID: 3311364.

[113]   Chapuis AG, Ragnarsson GB, Nguyen HN, Chaney CN, Pufnock JS, Schmitt TM, Duerkopp N, Roberts IM, Pogosov GL, Ho WY, Ochsenreither S, Wolfl M, Bar M, Radich JP, Yee C and Greenberg PD. Transferred WT1-reactive CD8+ T cells can mediate antileukemic activity and persist in post-transplant patients. Science translational medicine. 2013 Feb 27;5(174):174ra27. PubMed PMID: 23447018.

[114]   Riddell SR, Jensen MC and June CH. Chimeric Antigen Receptor Modified T Cells - Clinical Translation in Stem Cell Transplantation and Beyond. Biology of blood and marrow transplantation : journal of the American Society for Blood and Marrow Transplantation. 2012 Oct 17. PubMed PMID: 23085599.

[115]   Louis CU, Savoldo B, Dotti G, Pule M, Yvon E, Myers GD, Rossig C, Russell HV, Diouf O, Liu E, Liu H, Wu MF, Gee AP, Mei Z, Rooney CM, Heslop HE and Brenner MK. Antitumor activity and long-term fate of chimeric antigen receptor-positive T cells in patients with neuroblastoma. Blood. 2011 Dec 1;118(23):6050-6. PubMed PMID: 21984804. Pubmed Central PMCID: 3234664.

[116] Gattinoni L, Klebanoff CA, Palmer DC, Wrzesinski C, Kerstann K, Yu Z, Finkelstein SE, Theoret MR, Rosenberg SA and Restifo NP. Acquisition of full effector function in vitro paradoxically impairs the in vivo antitumor efficacy of adoptively transferred CD8+ T cells. The Journal of clinical investigation. 2005 Jun;115(6):1616-26. PubMed PMID: 15931392. Pubmed Central PMCID: 1137001.

[117] <Restifo NP_Human effector CD8+ T cells derived from naive rather than memory subsets possess superior _Blood_2011.pdf>.

[118] Bleakley M, Turtle CJ and Riddell SR. Augmentation of anti-tumor immunity by adoptive T-cell transfer after allogeneic hematopoietic stem cell transplantation. Expert review of hematology. 2012 Aug;5(4):409-25. PubMed PMID: 22992235.

[119] Terakura S, Yamamoto TN, Gardner RA, Turtle CJ, Jensen MC and Riddell SR. Generation of CD19-chimeric antigen receptor modified CD8+ T cells derived from virus-specific central memory T cells. Blood. 2012 Jan 5;119(1):72-82. PubMed PMID: 22031866. Pubmed Central PMCID: 3251238.

[120] Dudley ME, Gross CA, Somerville RP, Hong Y, Schaub NP, Rosati SF, White DE, Nathan D, Restifo NP, Steinberg SM, Wunderlich JR, Kammula US, Sherry RM, Yang JC, Phan GQ, Hughes MS, Laurencot CM and Rosenberg SA. Randomized selection design trial evaluating CD8+-enriched versus unselected tumor-infiltrating lymphocytes for adoptive cell therapy for patients with melanoma. Journal of clinical oncology : official journal of the American Society of Clinical Oncology. 2013 Jun 10;31(17):2152-9. PubMed PMID: 23650429. Pubmed Central PMCID: 3731980.

[121] Nakanishi Y, Lu B, Gerard C and Iwasaki A. CD8(+) T lymphocyte mobilization to virus-infected tissue requires CD4(+) T-cell help. Nature. 2009 Nov 26;462(7272):510-3. PubMed PMID: 19898495. Pubmed Central PMCID: 2789415.

[122] Hunder NN, Wallen H, Cao J, Hendricks DW, Reilly JZ, Rodmyre R, Jungbluth A, Gnjatic S, Thompson JA and Yee C. Treatment of metastatic melanoma with autologous CD4+ T cells against NY-ESO-1. The New England journal of medicine. 2008 Jun 19;358(25):2698-703. PubMed PMID: 18565862. Pubmed Central PMCID: 3277288.

[123] Riddell SR, Sommermeyer D, Berger C, Liu LS, Balakrishnan A, Salter A, Hudecek M, Maloney DG and Turtle CJ. Adoptive therapy with chimeric antigen receptor-modified T cells of defined subset composition. Cancer journal. 2014 Mar-Apr;20(2):141-4. PubMed PMID: 24667960.

[124] Miltenyi S, Muller W, Weichel W and Radbruch A. High gradient magnetic cell separation with MACS. Cytometry. 1990;11(2):231-8. PubMed PMID: 1690625.

[125]   Battye FL and Shortman K. Flow-Cytometry and Cell-Separation Procedures. Current opinion in immunology. 1991 Apr;3(2):238-41. PubMed PMID: WOS:A1991FK59300014. English.

[126]   Gutierrez C, Bernabe RR, Vega J and Kreisler M. Purification of human T and B cells by a discontinuous density gradient of percoll. Journal of immunological methods. 1979;29(1):57-63. PubMed PMID: 226632.

[127]   Pellegrino MA, Ferrone S and Theofilopoulos AN. Rosette formation of human lymphoid cells with monkey red blood cells. Journal of immunology. 1975 Oct;115(4):1065-71. PubMed PMID: 809506.

[128]   Altman JD, Moss PA, Goulder PJ, Barouch DH, McHeyzer-Williams MG, Bell JI, McMichael AJ and Davis MM. Phenotypic analysis of antigen-specific T lymphocytes. Science. 1996 Oct 4;274(5284):94-6. PubMed PMID: 8810254.

[129]   Casati A, Varghaei-Nahvi A, Feldman SA, Assenmacher M, Rosenberg SA, Dudley ME and Scheffold A. Clinical-scale selection and viral transduction of human naive and central memory CD8 T cells for adoptive cell therapy of cancer patients. Cancer immunology, immunotherapy : CII. 2013 Aug 1. PubMed PMID: 23903715.

[130]   Knabel M, Franz TJ, Schiemann M, Wulf A, Villmow B, Schmidt B, Bernhard H, Wagner H and Busch DH. Reversible MHC multimer staining for functional isolation of T-cell populations and effective adoptive transfer. Nature medicine. 2002 Jun;8(6):631-7. PubMed PMID: 12042816.

[131]   Schmidt TG and Skerra A. One-step affinity purification of bacterially produced proteins by means of the "Strep tag" and immobilized recombinant core streptavidin. Journal of chromatography A. 1994 Aug 5;676(2):337-45. PubMed PMID: 7921186.

[132]   Schmidt TG and Skerra A. The Strep-tag system for one-step purification and high-affinity detection or capturing of proteins. Nat Protoc. 2007;2(6):1528-35. PubMed PMID: 17571060.

[133]   Korndorfer IP and Skerra A. Improved affinity of engineered streptavidin for the Strep-tag II peptide is due to a fixed open conformation of the lid-like loop at the binding site. Protein science : a publication of the Protein Society. 2002 Apr;11(4):883-93. PubMed PMID: 11910031. Pubmed Central PMCID: 2373521.

[134]   McNiece IK, Stoney GB, Kern BP and Briddell RA. CD34+ cell selection from frozen cord blood products using the Isolex 300i and CliniMACS CD34 selection devices. Journal of hematotherapy. 1998 Oct;7(5):457-61. PubMed PMID: 9829320.

[135]   Abts H, Emmerich M, Miltenyi S, Radbruch A and Tesch H. CD20 positive human B lymphocytes separated with the magnetic cell sorter (MACS) can be induced to proliferation and antibody secretion in vitro. Journal of immunological methods. 1989 Dec 20;125(1-2):19-28. PubMed PMID: 2481694.

[136]   Kammula US, Lee KH, Riker AI, Wang E, Ohnmacht GA, Rosenberg SA and Marincola FM. Functional analysis of antigen-specific T lymphocytes by serial measurement of gene expression in peripheral blood mononuclear cells and tumor specimens. Journal of immunology. 1999 Dec 15;163(12):6867-75. PubMed PMID: 10586088.

[137]   Trzonkowski P, Bieniaszewska M, Juscinska J, Dobyszuk A, Krzystyniak A, Marek N, Mysliwska J and Hellmann A. First-in-man clinical results of the treatment of patients with graft versus host disease with human ex vivo expanded CD4+CD25+CD127- T regulatory cells. Clinical immunology. 2009 Oct;133(1):22-6. PubMed PMID: 19559653.

[138]   Levine BL, Bernstein WB, Aronson NE, Schlienger K, Cotte J, Perfetto S, Humphries MJ, Ratto-Kim S, Birx DL, Steffens C, Landay A, Carroll RG and June CH. Adoptive transfer of costimulated CD4+ T cells induces expansion of peripheral T cells and decreased CCR5 expression in HIV infection. Nature medicine. 2002 Jan;8(1):47-53. PubMed PMID: 11786906.

[139]   Cobbold M, Khan N, Pourgheysari B, Tauro S, McDonald D, Osman H, Assenmacher M, Billingham L, Steward C, Crawley C, Olavarria E, Goldman J, Chakraverty R, Mahendra P, Craddock C and Moss PA. Adoptive transfer of cytomegalovirus-specific CTL to stem cell transplant patients after selection by HLA-peptide tetramers. The Journal of experimental medicine. 2005 Aug 1;202(3):379-86. PubMed PMID: 16061727. Pubmed Central PMCID: 2213070.

[140]   Nadali G, de Wynter EA and Testa NG. CD34 cell separation: from basic research to clinical applications. International journal of clinical & laboratory research. 1995;25(3):121-7. PubMed PMID: 8562973.

[141]   Schumm M, Lang P, Taylor G, Kuci S, Klingebiel T, Buhring HJ, Geiselhart A, Niethammer D and Handgretinger R. Isolation of highly purified autologous and allogeneic peripheral CD34+ cells using the CliniMACS device. Journal of hematotherapy. 1999 Apr;8(2):209-18. PubMed PMID: 10349915.

[142]   Wang X, Naranjo A, Brown CE, Bautista C, Wong CW, Chang WC, Aguilar B, Ostberg JR, Riddell SR, Forman SJ and Jensen MC. Phenotypic and functional attributes of lentivirus-modified CD19-specific human CD8+ central memory T cells manufactured at clinical scale. Journal of immunotherapy. 2012 Nov-Dec;35(9):689-701. PubMed PMID: 23090078. Pubmed Central PMCID: 3525345.

[143]   Klebanoff CA, Gattinoni L, Palmer DC, Muranski P, Ji Y, Hinrichs CS, Borman ZA, Kerkar SP, Scott CD, Finkelstein SE, Rosenberg SA and Restifo NP. Determinants of

successful CD8+ T-cell adoptive immunotherapy for large established tumors in mice. Clinical cancer research : an official journal of the American Association for Cancer Research. 2011 Aug 15;17(16):5343-52. PubMed PMID: 21737507. Pubmed Central PMCID: 3176721.

[144] Guest RD, Kirillova N, Mowbray S, Gornall H, Rothwell DG, Cheadle EJ, Austin E, Smith K, Watt SM, Kuhlcke K, Westwood N, Thistlethwaite F, Hawkins RE and Gilham DE. Definition and application of good manufacturing process-compliant production of CEA-specific chimeric antigen receptor expressing T-cells for phase I/II clinical trial. Cancer immunology, immunotherapy : CII. 2013 Nov 5. PubMed PMID: 24190544.

[145] Klebanoff CA, Gattinoni L, Torabi-Parizi P, Kerstann K, Cardones AR, Finkelstein SE, Palmer DC, Antony PA, Hwang ST, Rosenberg SA, Waldmann TA and Restifo NP. Central memory self/tumor-reactive CD8+ T cells confer superior antitumor immunity compared with effector memory T cells. Proceedings of the National Academy of Sciences of the United States of America. 2005 Jul 5;102(27):9571-6. PubMed PMID: 15980149. Pubmed Central PMCID: 1172264.

[146] Gattinoni L, Finkelstein SE, Klebanoff CA, Antony PA, Palmer DC, Spiess PJ, Hwang LN, Yu Z, Wrzesinski C, Heimann DM, Surh CD, Rosenberg SA and Restifo NP. Removal of homeostatic cytokine sinks by lymphodepletion enhances the efficacy of adoptively transferred tumor-specific CD8+ T cells. The Journal of experimental medicine. 2005 Oct 3;202(7):907-12. PubMed PMID: 16203864. Pubmed Central PMCID: 1397916.

[147] Hinrichs CS, Borman ZA, Cassard L, Gattinoni L, Spolski R, Yu Z, Sanchez-Perez L, Muranski P, Kern SJ, Logun C, Palmer DC, Ji Y, Reger RN, Leonard WJ, Danner RL, Rosenberg SA and Restifo NP. Adoptively transferred effector cells derived from naive rather than central memory CD8+ T cells mediate superior antitumor immunity. Proceedings of the National Academy of Sciences of the United States of America. 2009 Oct 13;106(41):17469-74. PubMed PMID: 19805141. Pubmed Central PMCID: 2762661.

[148] Teschner D, Distler E, Wehler D, Frey M, Marandiuc D, Langeveld K, Theobald M, Thomas S and Herr W. Depletion of naive T cells using clinical grade magnetic CD45RA beads: a new approach for GVHD prophylaxis. Bone marrow transplantation. 2014 Jan;49(1):138-44. PubMed PMID: 23933765.

[149] Choufi B, Thiant S, Trauet J, Cliquennois M, Cherrel M, Boulanger F, Coiteux V, Magro L, Labalette M and Yakoub-Agha I. [The impact of donor naive and memory T cell subsets on patient outcome following allogeneic stem cell transplantation: Relationship between infused donor CD4(+)/CCR7(+) T cell subsets and acute graft-versus-host disease]. Pathologie-biologie. 2014 Jun;62(3):123-8. PubMed PMID: 24906571. Impact de la composition du greffon sur le devenir des patients apres une allogreffe de cellules souches hematopoietiques : correlation entre proportion des lymphocytes T CD4(+) du greffon exprimant le CCR7 et la survenue d'une GVH aigue.

[150] Mackall CL and Gress RE. Thymic aging and T-cell regeneration. Immunological reviews. 1997 Dec;160:91-102. PubMed PMID: 9476668.

[151] Sathaliyawala T, Kubota M, Yudanin N, Turner D, Camp P, Thome JJ, Bickham KL, Lerner H, Goldstein M, Sykes M, Kato T and Farber DL. Distribution and compartmentalization of human circulating and tissue-resident memory T cell subsets. Immunity. 2013 Jan 24;38(1):187-97. PubMed PMID: 23260195. Pubmed Central PMCID: 3557604.

[152] Jiang W, Kim BY, Rutka JT and Chan WC. Nanoparticle-mediated cellular response is size-dependent. Nature nanotechnology. 2008 Mar;3(3):145-50. PubMed PMID: 18654486.

[153] Chithrani BD, Ghazani AA and Chan WC. Determining the size and shape dependence of gold nanoparticle uptake into mammalian cells. Nano letters. 2006 Apr;6(4):662-8. PubMed PMID: 16608261.

[154] Gao H, Shi W and Freund LB. Mechanics of receptor-mediated endocytosis. Proceedings of the National Academy of Sciences of the United States of America. 2005 Jul 5;102(27):9469-74. PubMed PMID: 15972807. Pubmed Central PMCID: 1172266.

[155] Bergemann C. Funktionalisierte magnetische Nano- und Mikropartikel fur Anwendungen im Life Science Bereich. Biomedizinische Technik Biomedical engineering. 2012 Sep 4. PubMed PMID: 22947749.

[156] Li Pira G, Ivaldi F, Tripodi G, Martinengo M and Manca F. Positive selection and expansion of cytomegalovirus-specific CD4 and CD8 T cells in sealed systems: potential applications for adoptive cellular immunoreconstitution. Journal of immunotherapy. 2008 Oct;31(8):762-70. PubMed PMID: 18779743.

[157] Geddes M and Storek J. Immune reconstitution following hematopoietic stem-cell transplantation. Best practice & research Clinical haematology. 2007 Jun;20(2):329-48. PubMed PMID: 17448965.

[158] Zakrzewski JL, Goldberg GL, Smith OM and van den Brink MR. Enhancing T cell reconstitution after hematopoietic stem cell transplantation: a brief update of the latest trends. Blood cells, molecules & diseases. 2008 Jan-Feb;40(1):44-7. PubMed PMID: 17905611. Pubmed Central PMCID: 2684110.

[159] Riddell SR and Greenberg PD. The use of anti-CD3 and anti-CD28 monoclonal antibodies to clone and expand human antigen-specific T cells. Journal of immunological methods. 1990 Apr 17;128(2):189-201. PubMed PMID: 1691237.